

Li, H, Xing, W, Jiao, H, Yuen, KF, Gao, R, Li, Y, Matthews, C and Yang, Z

Bi-directional information fusion-driven deep network for ship trajectory prediction in intelligent transportation systems

<https://researchonline.ljmu.ac.uk/id/eprint/25043/>

Article

Citation (please note it is advisable to refer to the publisher's version if you intend to cite from this work)

Li, H ORCID logoORCID: <https://orcid.org/0000-0002-4293-4763>, Xing, W, Jiao, H, Yuen, KF, Gao, R, Li, Y, Matthews, C ORCID logoORCID: <https://orcid.org/0000-0002-4126-6484> and Yang, Z ORCID logoORCID: <https://orcid.org/0000-0003-1385-493X> (2024) Bi-directional information

LJMU has developed **LJMU Research Online** for users to access the research output of the University more effectively. Copyright © and Moral Rights for the papers on this site are retained by the individual authors and/or other copyright owners. Users may download and/or print one copy of any article(s) in LJMU Research Online to facilitate their private study or for non-commercial research. You may not engage in further distribution of the material or use it for any profit-making activities or any commercial gain.

The version presented here may differ from the published version or from the version of the record. Please see the repository URL above for details on accessing the published version and note that access may require a subscription.

For more information please contact researchonline@ljmu.ac.uk



Bi-directional information fusion-driven deep network for ship trajectory prediction in intelligent transportation systems

Huanhuan Li^a, Wenbin Xing^b, Hang Jiao^c, Kum Fai Yuen^d, Ruobin Gao^d, Yan Li^e, Christian Matthews^f, Zaili Yang^{a,*}

^a Liverpool Logistics, Offshore and Marine (LOOM) Research Institute, Faculty of Engineering and Technology, Liverpool John Moores University, Liverpool, UK

^b School of Intelligent Systems Engineering, Sun Yat-sen University, Guangdong, China

^c School of Electronic Information and Communications, Huazhong University of Science and Technology, Wuhan, China

^d School of Civil and Environmental Engineering, Nanyang Technological University, Singapore

^e State Key Laboratory of Information Engineering in Surveying, Mapping and Remote Sensing, Wuhan University, Wuhan, China

^f Department of Maritime and Mechanical Engineering, Liverpool John Moores University, Liverpool, UK

ARTICLE INFO

Keywords:

Ship trajectory prediction
Deep learning
Cascading network
Maritime safety
AIS data

ABSTRACT

Accurate ship trajectory prediction (STP) is crucial to realise the early warning of ship collision and ensure maritime safety. Driven by advancements in artificial intelligence technology, deep learning-based STP has become a predominant approach in the research field of ship collision avoidance. This paper, based on a state-of-the-art survey of the existing STP research progress, aims to develop a new bi-directional information fusion-driven prediction model that enables the achievement of more accurate STP results by addressing the drawbacks of the classical methods in the field. In this context, a cascading network model is developed by combining two bi-directional networks in a specific order. It incorporates the Bi-directional Long Short-Term Memory (BiLSTM) and the Bi-directional Gated Recurrent Unit (BiGRU) neural network into a single three-layer, information-enhanced network. It takes advantage of both networks to realise more accurate prediction of ship trajectories. Furthermore, the performance of the proposed model is comprehensively evaluated using Automatic Identification System (AIS) data from three water areas representing traffic scenarios of different safety concerns. The superiority of the proposed model is verified through comparative analysis with twenty other methods, including the state-of-the-art STP in the literature. The finding reveals that the new model is better than all the benchmarked ones, and thus, the new STP solution in this paper makes new contributions to improving autonomous navigation and maritime safety.

1. Introduction

The shipping industry is undergoing rapid growth (Bai et al., 2021; Deng et al., 2022) towards more efficient, secure, and sustainable transportation methods (Wong et al., 2022; Yang and Lam, 2023) thanks to the Industry 4.0 concept development (de la Peña Zarzuelo et al., 2020), including the Artificial Intelligence (AI) technology evolution. The integration of advanced sensors enables real-time monitoring and data collection of the maritime environment and ship movement status (Li and Yang, 2023). Concurrently,

* Corresponding author.

E-mail address: Z.Yang@ljmu.ac.uk (Z. Yang).

Nomenclature

Roman letters

Variable	Definition
ACDE	Adaptive Chaos Differential Evolution
ANN	Artificial Neural Network
AM	Attention Mechanisms
AI	Artificial Intelligence
AIS	Automatic Identification System
AR	AutoRegressive
ARIMA	Autoregressive Integrated Moving Average
AED	Average Euclidean distance
BPNN	Backpropagation Neural Network
BiGRU	Bi-directional Gated Recurrent Unit
BiLSTM	Bi-directional Long Short-Term Memory
BiRNN	Bi-directional Recurrent Neural Networks
CNN	Convolutional Neural Network
CNN	Convolutional Neural Networks
COG	Course Over Ground
Course-w	Course over water
DBSCAN	Density-Based Spatial Clustering of Applications with Noise
EM	Expectation-Maximisation
EKF	Extended Kalman Filter
ELM	Extreme Learning Machines
XGBoost	Extreme Gradient Boosting
FD	Fréchet distance
GAN	Generative Adversarial Network
GAT	Graph Attention Network
GRU	Gate Recurrent Unit
GMM	Gaussian Mixture Model
GP	Gaussian Process
GAN	Generative Adversarial Networks
GA	Genetic Algorithm
GCN	Graph Convolutional Network
GNN	Graph Neural Networks
G-STGAN	Gated Spatio-Temporal Graph Aggregation Network
Variable	Definition
HDBSCAN	Hierarchical Density-Based Spatial Clustering of Applications with Noise
KF	Kalman Filter
KNN	k-Nearest Neighbors
k-MC	k-order Markov Chain
LE-SOM	Laplacian Eigenmaps Self-Organizing Maps
LSTM	Long Short-Term Memory
MASS	Maritime Autonomous Surface Ships
MAE	Mean Absolute Error
MAPE	Mean Absolute Percentage Error
MCHN	Multi-graph Convolutional Hybrid Network
MSE	Mean Squared Error
MDN	Mixture Density Networks
MCM	Monte Carlo Method
MHA	Multi-Head Attention mechanism
MSCNN	Multi-Scale Convolutional Neural Network
STMGCN	Multi-Spatial-Temporal Graph Convolutional Neural network
MP-LSTM	Multi-step Prediction LSTM
NPC	Next-Point Connection
RF	Random Forests
RNN	Recurrent Neural Networks
SCI-EXPANDED	Science Citation Index Expanded
Seq2Seq	Sequence to Sequence
SSCI	Social Sciences Citation Index

SOG	Speed Over Ground
Speed-w	Speed over water
SVR	Support Vector Regression
SMAPE	Symmetric Mean Absolute Percentage Error
TripleConvTransformer	Transformer with a Convolutional neural network and a multihead attention mechanism
TBENet	Triple Bidirectional Enhanced Network
TTCN	Tiered Temporal Convolutional Network
VHF	Very High Frequency
WOS	Web of Science

diverse communication technologies facilitate the swift transmission and sharing of maritime information. Among these technologies, the Automatic Identification System (AIS) stands out as a critical tool for vessel identification and tracking, playing a vital role in ensuring the safety of maritime navigation (Fuentes, 2021; Li et al., 2022b; Xin et al., 2024). Leveraging Very High Frequency (VHF) radio waves, the AIS equipment assists in the exchange of critical vessel data, including ship name, ship type, navigation status, position (longitude and latitude), speed, and heading, between vessels and shore stations (Li et al., 2022a, 2024; Yang et al., 2019). Consequently, the utilisation of extensive maritime traffic data for Ship Trajectory Prediction (STP) has emerged as a crucial research area for maritime safety and navigation management. Specifically, it entails employing data analysis techniques to examine historical ship trajectory data and current ship status information to predict the possible future position of the ship accurately (Alizadeh et al., 2021a; Li et al., 2024).

Accurate and stable prediction plays a vital role in assisting ship crews to make proper decisions, thereby preventing collisions and avoiding deviations from the intended course (Li et al., 2023a). This contributes significantly to the sustainable development and prosperity of the shipping industry. The emergence of Maritime Autonomous Surface Ships (MASS) offers the potential for unmanned ships, mitigating the risks associated with human casualties and marking a key direction for future watercraft development (Chae et al., 2020; Filom et al., 2022; Li et al., 2023b; Negenborn et al., 2023; Wang et al., 2019b). It is essential to achieve the precise prediction of the surrounding ship trajectories for enabling collision avoidance based on deep learning methods in fully autonomous traffic (Negenborn et al., 2023). Furthermore, reliable prediction of ship movements can aid shipping companies in route planning, port operations, and traffic management, ultimately leading to cost reduction and increased transport efficiency (Zhang et al., 2022c). However, the complexity and variability of ship movements, along with the impact of external environmental factors on navigation, pose significant challenges in achieving accurate and reliable trajectory prediction (Xiao et al., 2017, 2020a). Therefore, it is imperative to explore advanced technological approaches to enhancing the accuracy and stability of STP, especially in light of the increasing industrial attention on MASS.

Currently, STP approaches are categorised into three groups, including traditional, machine learning-based, and deep learning-based methods. The traditional methods solely relying on kinematic equations fall short of achieving accurate prediction due to their limited ability to handle uncertainty factors, non-linear motion, and non-static characteristics (Liu et al., 2019b). They are also constrained by data quality and physical parameters. In contrast, data-driven methods, particularly machine learning and deep learning techniques, leverage historical data to extract trajectory patterns and features, offering enhanced adaptability to various ship movement patterns and environmental changes (Munim et al., 2020). Among machine learning-based methods (Jordan and Mitchell, 2015), supervised learning relies on labelled data and includes decision trees, Random Forests (RF) (Zhang et al., 2020), and Support Vector Regression (SVR) (Chen et al., 2021b) for effective prediction. Unsupervised learning methods like clustering (Pallotta et al., 2013) and dimensionality reduction (Gao et al., 2023) identify inherent patterns in historical trajectory data. Reinforcement learning (Wang et al., 2024), though limited in STP applications due to data complexity, exists. Deep learning methods can handle non-linear relationships and process large-scale data (Gao et al., 2023b; Liu et al., 2022a; Wang et al., 2019a, 2021), including Recurrent Neural Networks (RNN) (Karatas et al., 2021), Bi-directional Recurrent Neural Networks (BiRNN) (Hochreiter, 1998), Convolutional Neural Networks (CNN) (Kim and Lee, 2018), Attention Mechanisms (AM) (Capobianco et al., 2021), and Graph Neural Networks (GNN) (Zhao et al., 2022b). Hybrid models that combine different deep learning architectures have also been proposed to enhance STP accuracy by leveraging the strengths of each method.

Within this context, this paper proposes a novel STP method called Triple Bidirectional Enhanced Network (TBENet), which combines two bi-directional models. It aims to leverage the strengths of different models to improve the accuracy and stability of STP to a new level at which the current methods fail to arrive. Bi-directional Gated Recurrent Unit (BiGRU) unit enhances short-term information, while Bi-directional Long Short-Term Memory (BiLSTM) unit strengthens long-term information. The proposed method employs a sequence of BiGRU, BiLSTM, and BiGRU, which is applied to short-term prediction tasks. To verify the effectiveness and reliability of the proposed TBENet method, different AIS datasets from three representative water areas are used. Furthermore, six metrics are applied to evaluate the predictive performance of the proposed model. Additionally, the proposed TBENet method is compared with the other twenty predictive models to demonstrate its effectiveness.

More specifically, the remaining sections of this paper are structured as follows: Section 2 introduces a systematic review of STP. Section 3 outlines the mathematical definitions related to trajectory prediction and provides a detailed analysis of the specific tasks involved. Additionally, it includes comparison analyses of classical models. Section 4 presents a detailed description of the overall framework and the theoretical essence of the proposed TBENet method. Section 5 describes the experimental results, offers an in-depth analysis of the findings, and discusses the implications. Finally, Section 6 draws conclusions and discusses research directions for future development.

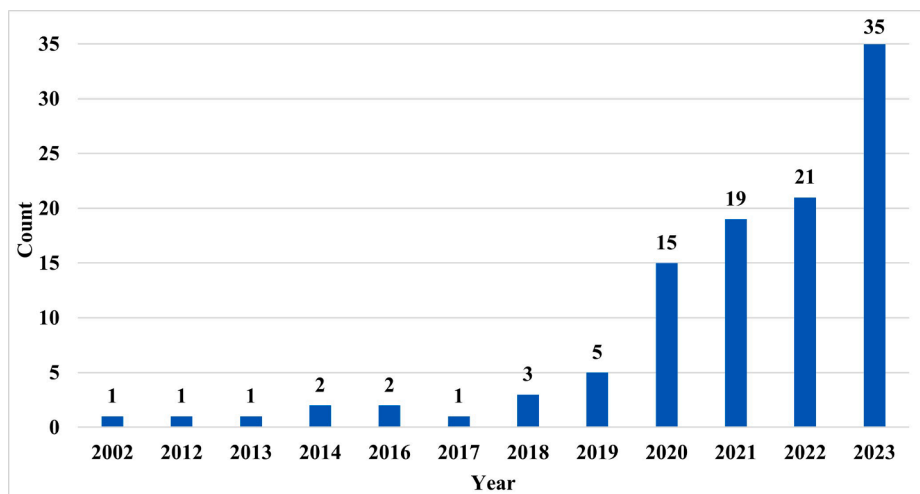


Fig. 1. The number of publications from 2002 to December 2023.

Table 1

Various data characteristics and the corresponding number of citations.

Feature	Latitude	Longitude	Speed-w	SOG	COG	Course-w
Count	101	101	26	35	35	15

2. Literature review

This section investigates an overview of ship trajectory features analysis in the literature. It is followed by an in-depth analysis of STP methods based on traditional methods, machine learning, and deep learning techniques.

To ensure high-quality retrieval and analysis results, the search process from the Web of Science (WoS) Core Collection database only includes the Science Citation Index Expanded (SCI-EXPANDED) and Social Sciences Citation Index (SSCI). An initial collection of 793 journal papers was gathered by using the keywords ‘ship trajectory prediction’ and ‘vessel trajectory prediction’. A thorough review of the relevance of each paper is conducted by assessing their titles, keywords and abstracts. As a result, a final set of 107 journal papers published in the past twenty years (i.e., between 2002 and December 2023) is selected. Fig. 1 illustrates the relationship between the number of published articles and the years, indicating a notable increase in research interest in STP since 2020. The 107 screened papers are then comprehensively analysed from both the input data and methodological perspectives. The methods employed are categorised into three directions: traditional, machine learning-based, and deep learning-based methods.

Among the retrieval results, traditional trajectory prediction methods primarily rely on kinematic or mathematical models. Only a limited number of articles use traditional methods for trajectory prediction (e.g., Ding et al., 2022; Miller and Walczak, 2020; Sutulo et al., 2002). In some studies, traditional models are combined with other approaches for improved prediction (e.g., Chen et al., 2021a; Kanazawa et al., 2021; Last et al., 2019; Luo and Zhang, 2020; Papadimitrakakis et al., 2021; Qiang et al., 2020; Sang et al., 2016; Wang et al., 2022b; Xiao et al., 2020b). Regarding machine learning-based trajectory prediction, this paper specifically focuses on the characteristics and applications of clustering methods in unsupervised learning. For supervised learning methods, the usage characteristics of various methods are discussed based on statistical analysis, with specific examples provided. Deep learning-based trajectory prediction mainly leverages diverse neural network models to learn and simulate ship trajectory behaviour. It is highly generalisable and transferable after training using large-scale data (Li et al., 2023a; Liu et al., 2022a). In recent research methods over the past two years, the predominant emphasis has centred on RNN, Transformers, and GNN. Additionally, AM methods have been widely applied.

2.1. An overview of data features for ship trajectory prediction

The selection of appropriate data features plays a pivotal role in the development of accurate and reliable trajectory prediction models. Each data feature offers unique information. For instance, latitude and longitude provide essential position information, while speed and course depict crucial movement characteristics. Environmental factors affecting the ship are reflected in meteorological conditions. Table 1 illustrates the six most frequently utilised data features in the retained 107 research papers, supporting model development and analysis. The frequency of these features highlights their importance in analysis and modelling. Latitude and longitude serve as the fundamental trajectory data features, forming the basis for analysing historical position information. Speed over water (Speed-w) and Course over water (Course-w) account for the influence of water flow and tidal currents in the prediction. SOG

Table 2

The value of kinematic or mathematical models to aid STP.

References	Advantages
(Kanazawa et al., 2021; Wang et al., 2022b)	Incorporate physical constraints or environmental factors.
(Chen et al., 2021a)	Construct models when faced with data scarcity.
(Last et al., 2019; Papadimitrakakis et al., 2021; Qiang et al., 2020; Sang et al., 2016; Xiao et al., 2020b)	Provide strong interpretability and portability.
(Luo and Zhang, 2020)	Detect and rectify outliers or noise in trajectory data, as well as fill in missing data.

Table 3

The statistical analysis based on clustering methods.

Reference	Method	Specific features
(Pallotta et al., 2013; Suo et al., 2020; Tang et al., 2020)	DBSCAN	Find arbitrarily shaped clusters by density accessibility and allow noise points to be excluded.
(Murray and Perera, 2021)	HDBSCAN	Efficiently and accurately adaptively discover clusters of varying densities and exclude noisy points.
(Murray and Perera, 2022)	GMM	Assume that the data consists of multiple Gaussian distributions and estimate the parameters by maximum likelihood when modelling.
(Ma et al., 2022b)	HierarchicalClustering	Hierarchical clustering is constructing from the bottom-up or top-down through a tree structure, gradually merging similar clusters.
(Park et al., 2021)	SpectralClustering	The data is projected into a low-dimensional space, followed by constructing a similarity matrix based on the data's similarity, which is then eigen-decomposed to facilitate the discovery of non-convex-shaped clusters.
(Last et al., 2019)	EMClustering	Assuming that the data consists of multiple Gaussian distributions, the likelihood function of the data is maximised by iteratively optimising the parameters.
(Xu et al., 2023)	Grid-basedClustering	Grid-based clustering is a method that partitions data space into grid cells and performs clustering on each cell individually.

and COG represent the speed and course over the ground, respectively. Different speed and course parameters can help predict the trajectory during navigation under various environmental conditions.

Moreover, other relevant features used include heading (indicating the direction of a ship's bow), ship type, acceleration, as well as environmental and meteorological factors like wind speed, current direction, and wave height. A method using extreme short-term trajectory prediction under the influence of sea currents is discussed (Zhang et al., 2023a). The incorporation of diverse and detailed data features can enhance the accuracy of STP. However, it also poses challenges in precise data modelling. In practical applications, it is essential to strike a good balance between the quantity and quality of data features, selecting them thoughtfully based on specific methodologies and requirements.

2.2. An overview of trajectory prediction based on traditional methods

Among the 107 journal papers, only three focused on kinematic or mathematical models to simulate the behaviour of ships (i.e., Ding et al., 2022; Miller and Walczak, 2020; Sutulo et al., 2002). However, a common limitation of these two methods is their reliance on overly idealised assumptions, which are not well-suited for complex real-world situations. Consequently, numerous methods combining these models with machine learning or deep learning techniques have been developed to improve prediction accuracy. Table 2 highlights the advantages of incorporating kinematic knowledge or mathematical models, as identified in relevant literature. In summary, the integration of kinematics or mathematical models with other methods addresses issues like idealised assumptions, limited adaptability to complex environments, and inherent model constraints. This combination significantly enhances the accuracy and reliability of STP.

2.3. An overview of trajectory prediction based on machine learning methods

Based on the screened literature, machine learning methods employed in STP can mainly be categorised into unsupervised and supervised learning. Unsupervised learning methods, which do not require labelled training data, focus on discovering inherent structures and patterns through techniques like clustering or dimensionality reduction. These methods can be applied to data analysis and feature extraction.

Clustering methods, a key type of unsupervised learning, are extensively used for data preprocessing, pattern identification, and knowledge discovery. They are vital in detecting and removing invalid or outlier data points. These methods also reveal movement patterns across different segments or time frames, facilitating more effective route planning. By grouping similar trajectories, clustering methods enable the prediction of future paths for each cluster.

Various clustering methods are discussed in the literature for STP. These include K-Means, Density-Based Spatial Clustering of Applications with Noise (DBSCAN), Hierarchical Density-Based Spatial Clustering of Applications with Noise (HDBSCAN), Gaussian

Table 4

The statistical analysis based on supervised learning methods.

References	Methods	Characteristics
(Wang et al., 2022a; Zhang et al., 2020)	RF	Multiple decision trees are trained by randomly selecting features and samples, and their results are combined to efficiently handle high-dimensional data and capture non-linear relationships.
(Maskooki et al., 2021; Zhang et al., 2022b)	KNN	Predictions are made from the position and speed information of the K nearest sample points to the target point. It is suitable for more localised trajectory data, but may not perform well for higher dimensionality and noisier data.
(Liu et al., 2019a)	k-MC	It assumes that the current state is only related to the previous k states. It is suitable for dealing with sequential data with long-term dependencies, but requires the determination of the appropriate order and state transfer probabilities.
(Perera et al., 2012)	EKF	It is effective for predicting trajectories using linear dynamic models and Gaussian noise. However, its performance may be limited when dealing with non-linear models and non-Gaussian noise.
(Chen et al., 2021b; Liu et al., 2020; Liu et al., 2019b)	SVR	It transforms data into a higher-dimensional space using kernel functions and identifies the best hyperplane. It is capable of handling high-dimensional data and non-linear connections, making it suitable for small sample sizes and non-linear regression problems.
(Chen et al., 2020c; Volkova et al., 2021; Zhao et al., 2022a)	Artificial Neural Network (ANN)	It achieves automatic learning of feature representations and processing of non-linear relationships through the computation of multilayer neurons and the action of non-linear activation functions. It is applicable to deal with complex trajectory prediction problems.
(Zhou et al., 2019)	Backpropagation Neural Network (BPNN)	It involves fitting and categorising complex functions by applying non-linear transformations through multiple layers of neurons and error backpropagation. However, it necessitates abundant data and relies on substantial training data and feature engineering support.
(Gao et al., 2023a; Rong et al., 2019, 2022)	Gaussian Process (GP)	The trajectory data is assumed to obey a Gaussian distribution, which is estimated and predicted by means and covariance matrices of the data. It is appropriate for handling data with strong linear relationships and Gaussian noise.
(Tu et al., 2020)	Extreme Learning Machines (ELM)	It is a rapid learning algorithm grounded in a single-layer feed-forward neural network. The output layer weights can be derived in just one training session through the random generation of connection weights and biases from the input layer to the hidden layer.
(Scheepens et al., 2014)	MCM	Information on the distribution of the output results is obtained by random sampling and simulation of the input parameters. It is adapted to deal with complex trajectory prediction problems and uncertainty analysis.
(Alizadeh et al., 2021b, 2021a; Nguyen et al., 2018; Scheepens et al., 2014)	Similarity search method	The most similar trajectory is found as the prediction result by comparing the trajectories to be matched with similar trajectories in the existing trajectory database. It is suited for handling trajectory data with strong local similarity.

Mixture Model (GMM), hierarchical clustering, and Expectation-Maximization (EM). The statistical analysis of these methods is presented in Table 3. A comprehensive description of these seven clustering methods is provided to facilitate their choice in pattern generation for ship prediction.

In addition to the above methods, the Next-Point Connection (NPC) clustering technique is introduced. This density-based approach is suitable for identifying clusters with irregular shapes by linking points through their nearest neighbours (Chen et al., 2020a). The DBSCAN algorithm and its variants are adept at discovering clusters and removing noise points, effectively handling the noise and uncertainty hidden in trajectory data. They offer scalability, efficiency, and data-dependent automatic parameter tuning based on data characteristics. As discussed in Gao et al. (2023), the Laplacian Eigenmaps Self-Organizing Maps (LE-SOM) approach is proficient in feature extraction from high-dimensional, unevenly spaced data by mapping it to a lower-dimensional topological space. These methods train a prediction model using a set of features and a target value, leveraging the relationships among these data points.

Supervised learning methods like RF, k-Nearest Neighbors (KNN), and SVR utilise historical trajectory data and other relevant information to predict future positions and movements. Additionally, knowledge-based methods such as k-order Markov Chain (k-MC), similarity-based methods, Extended Kalman Filter (EKF), and Monte Carlo Method (MCM) are also used in STP, where historical data is employed to train a predictive model. An analysis of these methods is summarised in Table 4.

The most frequently used methods in the above literature are RF, KNN, SVR, ANN, GP, and similarity search methods. RF is applied to time series data using a sliding window approach to update the model incrementally for speed prediction in future time intervals (Wang et al., 2022a). Feature selection using KNN algorithm is employed to identify the most relevant features from historical trajectories for prediction (Tu et al., 2020). The Adaptive Chaos Differential Evolution (ACDE) algorithm is used to optimise the parameters of the SVR model for improving prediction performance (Liu et al., 2019b). Data is processed through trajectory separation, noise removal, and normalisation, followed by trajectory prediction using ANN on a uniformly distributed data sequence (Chen et al., 2020c). The historical ship trajectory data and marine environment data are combined, utilising a GP model for trajectory modelling and prediction while assessing prediction uncertainty through confidence values (Rong et al., 2019). Similarity search methods can be further classified into point-level similarity and trajectory-level similarity. Additionally, the uncertainty and noise issues in AIS data are addressed by introducing decision trees, RF, and Extreme Gradient Boosting (XGBoost) to enhance data processing, prediction accuracy, and robustness (Last et al., 2014).

Table 5

The statistical analysis based on deep learning methods.

Refs.	Methodology	Refs.	Methodology
(Gao et al., 2021)	Multi-step Prediction LSTM(MP-LSTM)	(Zhang et al., 2022a)	KNN-LSTM
(Karatas et al., 2021; Ma et al., 2022b; Tang et al., 2022; Wang et al., 2023b,a; Nguyen et al., 2018)	LSTM	(Chen et al., 2022; Gao et al., 2018; Park et al., 2021)	BiLSTM
(Liu and Ma, 2022)	attention-based LSTM	(Qian et al., 2022)	Genetic Algorithm (GA)-LSTM
(Mehri et al., 2021)	context-aware LSTM	(Zhao et al., 2022b)	k-GCN-LSTM
(Hu et al., 2021)	dual-pass LSTM	(Sorensen et al., 2022)	BiLSTM-Mixture Density Networks (MDN)
(Abebe et al., 2022)	a hybrid Autoregressive Integrated Moving Average (ARIMA) and LSTM	(Chen et al., 2020b)	LSTM-MDN
(Syed and Ahmed, 2023)	CNN and LSTM	(Jia et al., 2023)	attention-based Bi-LSTM
(Wang et al., 2023a)	GAT and LSTM	(Wang et al., 2023c)	MCHN
(Lin et al., 2023)	TTCN-Attention-GRU	(Han et al., 2023; Jia and Ma, 2023)	GAN
(Jiang et al., 2023)	Transformer and LSTM	(Zhang et al., 2023b)	G-STGAN
(Bao et al., 2022)	Multi-head Attention Mechanism (MHA) and BiGRU	(Suo et al., 2020)	GRU
(Xu et al., 2022)	Stacked-BiGRUs	(Zhang et al., 2021)	MSCNN Fusion with GRU-AM and AR
(Xiao et al., 2023b)	BiGRU	(Wei, 2020)	Image Processing
(Wang and He, 2021)	GAN-AI	(Feng et al., 2022)	IS-STGCNN
(Ma et al., 2022b)	RNN	(Liu et al., 2022b)	STMGCN
(You et al., 2020)	GRU encoder-decoder	(Billah et al., 2022; Venskus et al., 2021)	LSTM encoder-decoder
(Murray and Perera, 2020)	dual linear autoencoder	(Kim and Lee, 2018)	CNN and FCNN
(Liu et al., 2021)	CNN and attention-based Bi-LSTM	(Capobianco et al., 2021)	attention-based LSTM encoder-decoder
(Huang et al., 2022)	Transformer with CNN and MHA (TripleConvTransformer)	(Nguyen and Fablet, 2021)	Transformer
(Li et al., 2024)	BiLSTM, BiGRU, and attention mechanism		

In summary, Tables 3 and 4 highlight the unique features and applicability of each method. When selecting an appropriate method, it is essential to take into account the practical application scenario and available conditions. For situations involving complex non-linear relationships and large datasets, machine learning-based methods may have limitations, necessitating the consideration of deep learning methods.

2.4. An in-depth analysis of trajectory prediction based on deep learning methods

Deep learning is an advanced algorithm that utilises deep structures and multiple layers of neural networks to learn and model input data. It enables feature extraction and representation, allowing in-depth analysis (LeCun et al., 2015). In STP, deep learning is beneficial as it can learn from large amounts of multidimensional data, capturing the influences of various factors like position, movement, and environment. It demonstrates proficiency in handling non-linear relationships and exhibits adaptability and generalisation capabilities (Zhang et al., 2022c). Table 5 provides an overview of deep learning methods mentioned in the investigated literature. A total of 67 papers discuss the application of deep learning methods, indicating significant progress in methodology.

Among the deep learning-based methods involved in STP, the most commonly used ones are the Long Short-Term Memory (LSTM) and the Gate Recurrent Unit (GRU), along with their respective variants. These models demonstrate strong performance in modelling time series data based on their effective memory capabilities. BiLSTM and BiGRU are bi-directional network structures that enhance feature extraction in time series by adding a reverse recurrent layer. Many scholars have actively explored the combination of other machine learning or deep learning methods with LSTM, GRU, and their bi-directional network models to improve trajectory prediction. LSTM model was improved by incorporating the attention mechanism, enabling adequate capture of feature information relevant to prediction (Liu and Ma, 2022). A multi-head attention mechanism was introduced to optimise the BiGRU network (Bao et al., 2022). A genetic algorithm was used to optimise the hyperparameters of the LSTM, thus eliminating the uncertainty associated with manual parameter tuning (Qian et al., 2022). Graph Convolutional Network (GCN) was employed to capture the spatial correlation between nodes, while LSTM was used to exploit their spatio-temporal correlations for prediction (Zhao et al., 2022b). A prediction method based on a Multi-Scale Convolutional Neural Network (MSCNN) combining a GRU and Attention Mechanism (GRU-AM) and a fusion with an AutoRegressive (AR) model was proposed (Zhang et al., 2021). MSCNN was applied to extract multi-scale features from high-frequency radar data, followed by feature fusion and prediction using GRU-AM models. Additionally, an AR model was introduced to model the autoregressive relationship of trajectories, enhancing prediction accuracy and robustness. Furthermore, the utilisation of LSTM and GRU networks in an encoder-decoder structure was discussed (Billah et al., 2022; Capobianco et al., 2021; Venskus et al., 2021; Wang and He, 2021; You et al., 2020). This structure provided improved sequence modelling capabilities, reduced overfitting, and increased robustness. An LSTM encoder-decoder structure with interaction and attention mechanisms was

Table 6

The statistical analysis of future improvements based on deep learning methods.

Future Improvements	Count
Improve prediction accuracy.	48
Consider additional factors, such as weather and sea conditions.	23
Enhance real-time processing capabilities.	18
Use more data and improve generalisation.	16
Reduce computational costs and improve predicting efficiency.	15
Improve network structure to predict ship trajectories over more extended periods.	10

incorporated as a subframe within the Generative Adversarial Networks (GAN), resulting in significant improvements compared to Sequence to Sequence (Seq2Seq) and Kalman Filter (KF) models (Wang and He, 2021).

The Convolutional Neural Network (CNN) is mainly used to extract features from ship motion data. A hybrid model based on CNN and the fully connected neural network was developed to predict medium-term and long-term traffic in the investigated area (Kim and Lee, 2018). A CNN-LSTM architecture was developed to capture the spatiotemporal characteristics of the trajectory more effectively (Syed and Ahmed, 2023).

GNNs are specialised neural networks designed to handle graph-structured data. They learn by propagating information through nodes and edges, capturing complex relationships and patterns. For STP, GNNs are suitable due to their ability to effectively handle spatio-temporal connections between ships. They leverage interactions among ships, historical trajectory data, and other pertinent information to develop node feature representations, using these to predict future trajectories. GNNs can adapt to irregular graph structures and update models in real-time to accommodate dynamic trajectory data, thereby enhancing their accuracy in predicting future ship trajectories. The Spatiotemporal Multi-Graph Convolutional Neural network (STMGCN) is a deep learning model based on GCN. It is specifically designed to handle multiple spatio-temporal sequence data and effectively model them in space and time. The prediction accuracy can be improved due to the ability to capture correlations between different spatio-temporal sequences effectively. STMGCN model is reconstructed using three different graphs based on social forces, time to the nearest approach point, and the size of surrounding ships (Liu et al., 2022b). Subsequently, a spatio-temporal multi-graph convolutional layer is utilised to embed these three graphs into the prediction framework jointly. Additionally, a self-attentive temporal convolution layer is introduced to improve prediction performance with fewer parameters. A new method was developed for vessel trajectory prediction based on a sparse multi-graph convolutional hybrid network with spatio-temporal awareness (Wang et al., 2023b).

Transformer is a deep learning model grounded in the attention mechanism, noted for its high processing power, parallelism, and adaptability. Trajectory and meteorological data were combined after feature discretisation to capture the multi-scale features of ocean-going ships effectively (Huang et al., 2022). A generative Transformer model was proposed, leveraging a multi-headed self-attentive mechanism to discern the connections within input data. Additionally, it incorporated a new location embedding approach to enhance the spatial awareness of the model (Nguyen and Fablet, 2021).

Beyond the networks already discussed, AM is widely used in trajectory prediction. These mechanisms enable models to dynamically adjust the significance of different time steps or vessels during prediction, concentrating on the information most relevant to the outcome. This approach helps enhance the model's ability to detect key moments or particular vessel behaviours, resulting in more accurate and reliable prediction outcomes. The incorporation of AM is now a standard practice in network design. In addition, image processing techniques have been applied for trajectory prediction (Wei, 2020). For instance, images taken during ship navigation were analysed using computer vision techniques to determine ship positions and trajectories.

Table 6 provides an overview of the future improvement strategies for deep learning methods, as detailed in the literature presented in Table 5. While deep learning methods are effective, they typically require a significant amount of training data and computational resources, and their models can be intricate, posing implementation challenges. Therefore, it is essential to optimise the network structure, as it can significantly improve prediction accuracy, computational efficiency, and overall predictive capability. Furthermore, Table 6 outlines the ongoing research efforts in the field of STP.

2.5. Research gaps and contributions

The innovative TBENet model integrates short-term and long-term features, drawing inspiration from advancements across various research areas. This innovative fusion in deep learning is exemplified similarly to approaches already demonstrated in other domains.

In computer vision, particularly facial recognition, the fusion of multiple facial features has proven effective in achieving accurate classification and prediction (Qin et al., 2023; Xia et al., 2024; Xiao et al., 2023a; Yan et al., 2023).

In healthcare, multimodal fusion is employed for disease diagnosis, integrating imaging data (such as Magnetic Resonance Imaging (MRI) and Computed Tomography (CT) scans) with genetic information to enhance diagnostic accuracy and prognostics. These models often use deep learning architectures to combine diverse types of medical data, offering a comprehensive view of a patient's health (Muhammad et al., 2021; Qiu et al., 2024; Qu et al., 2023; Shaik et al., 2024; Tan et al., 2020; Wang et al., 2024a).

Autonomous driving systems combine data from LIDAR, radar, Global Positioning System (GPS), and cameras to thoroughly understand the vehicle's environment. This fusion of features with deep learning models aids in accurate navigation, object detection, and decision-making under various conditions (Wang et al., 2020; Wu et al., 2023a; Wu et al., 2023b; Yuan et al., 2022; Zuo et al., 2024).

In financial markets, hybrid models integrate time-series data with sentiment analysis from news articles or social media to predict stock prices or market trends more accurately. These models combine LSTM and BiLSTM (for sequential data) with convolutional layers to process textual data (El Zaar et al., 2024; Tzoumpas et al., 2024; Wang, 2024; Zhang et al., 2024a; Zhang et al., 2024b).

In Natural Language Processing (NLP), innovations like Bidirectional Encoder Representations from Transformers (BERT) leverage bidirectional contexts by fusing textual information from both directions (left-to-right and right-to-left), significantly enhancing language understanding and processing capabilities (Hassan et al., 2024; Kharsa et al., 2024; Makhmudov et al., 2024; Wang et al., 2024b; Zhang et al., 2024c).

The effectiveness of fusion models is verified by relevant methods across various areas. The literature provides a three-layer structure as a baseline model for short-term traffic flow prediction (Ma et al., 2022a). Specifically, a tailored three-layer fusion model is developed for STP tasks. This task requires both short-term and long-term information. Short-term data captures immediate changes in location, speed, and direction, while long-term data helps understand overall trends and routes over a voyage. Therefore, ship trajectory models need to integrate both short-term and long-term features to accurately predict ship paths.

Building on this baseline method and considering the specific characteristics of STP, the best three-layer model is investigated using bidirectional networks to effectively capture both short-term and long-term features.

Given the above review and discussion, it remains a challenging task to realise accurate and reliable STP. Several key issues are wanting new solutions to be explored:

(1) Lack of a systematic research review of the essence of STP.

While previous studies have explored STP, their primary focus has been on comparing and analysing various methods. They have largely overlooked: a) analysis of data features and influential factors, b) description of clustering and dimensionality reduction methods, and c) exploration of the development of the state-of-the-art deep learning models for STP.

This paper conducts a new review analysis of the data features and the influential factors in STP research. It focuses on the application of machine learning techniques in STP and conducts a comprehensive review of trajectory clustering and dimensionality reduction methods, offering valuable insights for researchers in the field. Furthermore, the paper presents a systematic overview of the evolving models used in deep learning approaches for STP, shedding light on the current development trends. Additionally, the paper compares and analyses potential future improvements, focusing specifically on advancements in deep learning models for STP.

(2) Integrated innovation of network structure to improve prediction accuracy.

With the increasing presence of autonomous ships and the complexity they introduce to maritime traffic, there is an urgent need to enhance the accuracy of STP despite the widespread use of deep learning methods in this field. To tackle this challenge, it is essential to invest additional efforts in enhancing prediction accuracy and exploring novel network structures.

The proposed TBENet model is tailored to improve the accuracy of trajectory prediction by leveraging the strengths of two bi-directional models and fusing long-term and short-term features. It is structured with a three-layer cascading bi-directional information network. It is designed specifically to enhance the accuracy of trajectory prediction.

(3) Design comparative experiments by comprehensive evaluation indexes based on three different AIS datasets.

Although AIS datasets have been commonly used for validation in numerous studies, there is a notable lack of thorough testing across a range of evaluation indices and diverse application scenarios representing different levels of traffic complexity.

To address this gap, this paper employs six evaluation indexes to assess the performance of STP across twenty-one models in three distinct application scenarios with different but representative complex traffic flow. It ensures a comprehensive, thorough, and robust analysis.

3. Preliminary

This section sets out to first clarify the definitions of relevant terms and concepts before exploring specific methodology. It will include a mathematical description of the problems tackled in this study. Furthermore, a detailed explanation of the topic's characteristics and challenges will be offered, laying a strong foundation and enhancing the understanding for subsequent research.

3.1. Definitions

A ship's trajectory is its path on the water, recorded as a series of coordinate points representing its position over time. Ship trajectories are important for analysing navigation patterns and predicting future movements. A collection of trajectories, denoted as $T^o = \{T_1, T_2, \dots, T_i, \dots, T_{m-1}, T_m\}$ is gathered within a specific period in a given water area. T^o denotes the set of trajectory sequences in the water area, m represents the total number of trajectories, and T_i indicates i th ($i \in [1, m]$) trajectory.

In particular, a ship's trajectory can be described as a time series of data that captures its movement. It is typically represented by a sequence of consecutive spatio-temporal nodes $T_i = \{N_i^1, N_i^2, \dots, N_i^j, \dots, N_i^{n-1}, N_i^n\}$, where n denotes the total number of nodes captured in the ship trajectory, and N_i^j denotes the j th ($j \in [1, n]$) sampled node. $N_i^j = \{lon_i^j, lat_i^j, t_i^j\}$ means that each node is composed of longitude information (i.e., lon_i^j) and latitude information (i.e., lat_i^j) at the specific sampling time (i.e., t_i^j). In STP tasks, the standard time interval is set at 5 s (Li et al., 2023a, 2024).

Table 7

The comparison of the eight classical neural networks.

Methodology	Refs.	Advantage	Disadvantage
RNN	(Elman, 1990)	It was the first neural network to be proposed capable of processing sequential data.	It suffers from the problem of vanishing or exploding gradients, making it difficult to deal with long-term dependencies in long sequences.
LSTM	(Hochreiter and Schmidhuber, 1997)	It effectively mitigates the problem of vanishing gradients and is good at handling long sequences.	It is computationally time-consuming and can still be difficult to work with long sequences.
GRU	(Chung et al., 2014)	It improves long-term dependency issues through a faster gating mechanism than traditional RNN training.	Although it improves RNNs, it is still difficult to transmit information for excessively long sequences.
BiRNN	(Hochreiter, 1998)	It extends the traditional RNN by processing sequences both forwards and backwards, providing a richer context and improving performance on tasks like speech and text recognition.	Similar to LSTM, it can be computationally intensive and still struggles with the vanishing gradient problem when sequences are very long.
BiLSTM	(Schuster and Paliwal, 1997)	It takes advantage of bi-directionality to better bind the context and improve the robustness of the model.	It is still a challenge to transmit information for very long sequences efficiently.
BiGRU	(Wang et al., 2017)	It combines the advantages of bidirectional and GRU to improve contextual understanding of sequences.	It requires large computing resources and time to train.
Seq2Seq	(Sutskever et al., 2014)	It trains in an end-to-end manner, simplifying the entire training process.	When dealing with complex temporal relationships, the generation effect is uncontrollable.
Transformer	(Vaswani et al., 2023)	It has advantages when dealing with long sequences and large-scale data, as well as strong parallel computing capabilities.	It is data-demanding, requires a large amount of data and computing resources for pre-training and fine-tuning, and is relatively poorly interpretable.

3.2. Problem statement

3.2.1. How to implement ship trajectory prediction?

STP involves the study of movement patterns using various techniques to estimate the future navigation path of a ship based on historical trajectory data. This field has diverse applications, including ship traffic planning, collision avoidance, maritime rescue, and intelligent decision-making.

Given the currently known continuous node information fragments available in the time period (i.e., $\{t_{seg}^p, t_{seg}^{p+1}, \dots, t_{seg}^q\}$) as $T_{seg} = \{N_{seg}^p, N_{seg}^{p+1}, \dots, N_{seg}^q\}$, where p and q denote the serial numbers of the starting and ending nodes in the set, respectively. The location information (i.e., $T_{pre} = \{N_{pre}^{q+1}, N_{pre}^{q+2}, \dots, N_{pre}^{q+l}\}$) corresponding to the time period (i.e., $\{t_{seg}^{q+1}, t_{seg}^{q+2}, \dots, t_{seg}^{q+l}\}$) can be predicted by learning the patterns and rules from a substantial amount of sequential data. Depending on the time span (i.e., l), prediction tasks can be categorised as short-term or long-term predictions.

3.2.2. How to improve the accuracy of ship trajectory prediction?

Trajectory prediction can be conceptualised as a regression problem, where the objective is to find a function (i.e., f) that can generate the predicted points (i.e., $T_{pre} = \{N_{pre}^{q+1}, N_{pre}^{q+2}, \dots, N_{pre}^{q+l}\}$) at future moments, given a trajectory point in T_{seg} , $N_{pre}^k = f_i(T_{seg})$, $k \in [q+1, q+l]$.

Several strategies can be adopted to improve trajectory prediction accuracy, such as selecting appropriate features, combining different models, tuning parameters, enhancing the data, and implementing cross-validation. This paper proposes the TBENet method, which leverages a combination of two models (BiLSTM and BiGRU) to create a cascading network comprising three layers. The technique employs data from three different water areas to enhance its predictive capabilities. It undergoes evaluation using various comparative validation experiments to determine the best prediction results. In particular, the TBENet method utilises the information from four consecutive historical node locations to predict one future location. The formula for the prediction can be represented as follows:

$$(\text{lon}_{pre}^{p+4}, \text{lat}_{pre}^{p+4}) = f_{TBENet}(\{\text{lon}_{seg}^p, \text{lat}_{seg}^p\}, \{\text{lon}_{seg}^{p+1}, \text{lat}_{seg}^{p+1}\}, \{\text{lon}_{seg}^{p+2}, \text{lat}_{seg}^{p+2}\}, \{\text{lon}_{seg}^{p+3}, \text{lat}_{seg}^{p+3}\}) \quad (1)$$

3.2.3. How to evaluate the prediction performance of the proposed TBENet model by various trajectory datasets?

For STP, it is vital to take into account the prediction of movement states across multiple water areas. Therefore, trajectory datasets from various water areas can be selected to ensure comprehensive comparison. These areas should encompass different climates, terrains, vessel types, and other relevant factors. Additionally, suitable data preprocessing techniques are necessary to standardise the original datasets from these varied water areas, ensuring uniform and equitable testing conditions. Typically, the trajectory dataset is split into a training set and a test set using methods like K-Fold cross-validation. This division facilitates multiple iterations of training and testing the model, enabling evaluation of its performance and generalisation capability. Datasets from three distinct water areas, namely Caofeidian water (i.e., a port area), Zhoushan water (i.e., a highly complex water area), and Chengshan Jiao water (i.e., a water area with a ship routing system), are utilized in this paper.

To comprehensively evaluate the performance of trajectory prediction, multiple metrics are selected and employed. In this paper, a combination of six metrics is selected, including Mean Squared Error (MSE), Mean Absolute Error (MAE), Mean Absolute Percentage Error (MAPE), Symmetric Mean Absolute Percentage Error (SMAPE), Fréchet Distance (FD), and Average Euclidean Distance (AED).

The models' performance is ultimately compared using the following equation.

$$\min\{MSE \cap MAE \cap MAPE \cap SMAPE \cap FD \cap AED\} \quad (2)$$

3.3. Comparison among classical models

Table 7 presents a comparison of eight classical neural networks: RNN, LSTM, GRU, BiRNN, BiLSTM, BiGRU, Seq2Seq, and Transformer, highlighting their strengths and weaknesses. RNNs are the first to handle sequential data but struggle with long-term dependencies due to vanishing gradients. LSTMs improve on this by effectively handling longer sequences and mitigating gradient issues, though they are computationally intensive. GRUs further address these long-term dependencies more efficiently with a gating mechanism. BiRNNs improve upon traditional RNNs by processing sequences both forwards and backwards, providing a more complete understanding of the data. This bidirectional processing helps better manage sequence-related information and mitigates some challenges of vanishing gradients, although handling very long sequences may still be problematic without mechanisms like those in LSTMs or GRUs. BiLSTMs and BiGRUs leverage bidirectionality to enhance model robustness and context understanding, respectively, but face challenges in managing very long sequences and require significant computational resources. Seq2Seq models streamline the training process with an end-to-end approach but can produce uncontrollable outputs in complex temporal patterns. Finally, Transformers perform well with extensive data and long sequences due to strong parallel processing capabilities but are data-intensive and have interpretability challenges.

3.4. The bidirectional recurrent network

The BiLSTM and BiGRU models learn bidirectionally from time series data, integrating hidden layer variables at each time step. BiLSTM and BiGRU are two common types of recurrent neural network architectures that differ in their handling of sequential data. The main distinction lies in their internal gating mechanisms. BiLSTM features three gates: the forget gate, input gate, and output gate. These gates control the flow of information through the network, aiding in capturing long-term dependencies. BiGRU is comparatively simpler, comprising only two gates: the update gate and the reset gate. With a more concise structure and fewer parameters, BiGRU is more computationally efficient than BiLSTM. While BiLSTM excels at capturing long-term dependencies, BiGRU may be easier to train in certain scenarios and can be advantageous in resource-constrained environments. The structure of BiLSTM is shown in Fig. 2.

BiGRU is commonly more efficient and easier to handle than BiLSTM due to its simpler structure with fewer parameters and lower memory requirements. Its straightforward design makes implementation and debugging easier, especially for resource-limited scenarios. In BiGRU, whether it is forward or backward learning, each gated recurrent unit consists of the update gate, the reset gate, a new candidate state, and the updated hidden state. The structure of BiGRU is displayed in Fig. 3.

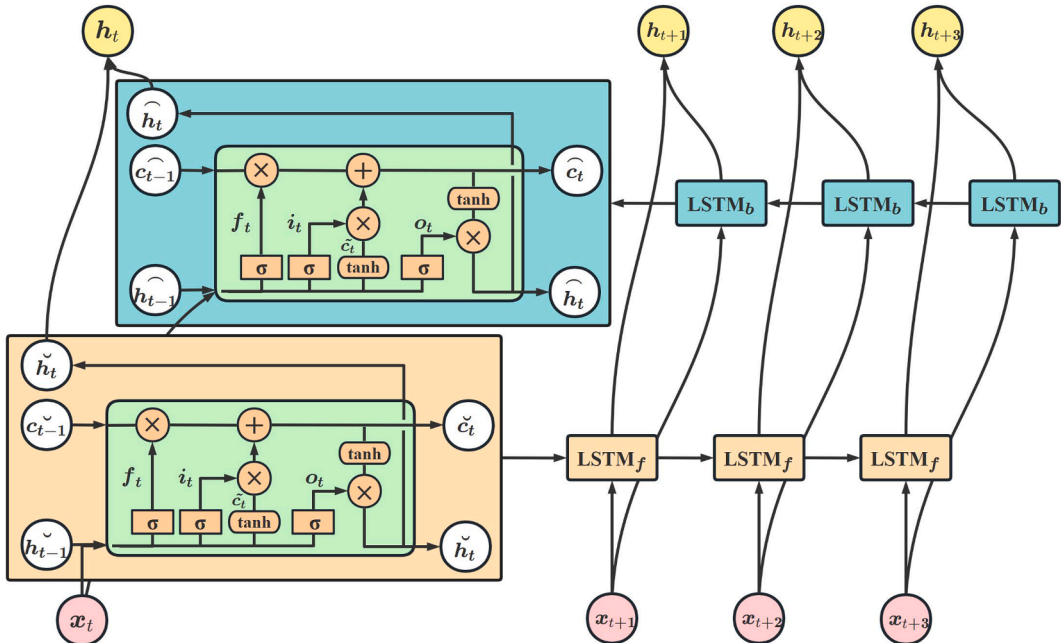


Fig. 2. The framework of the BiLSTM.

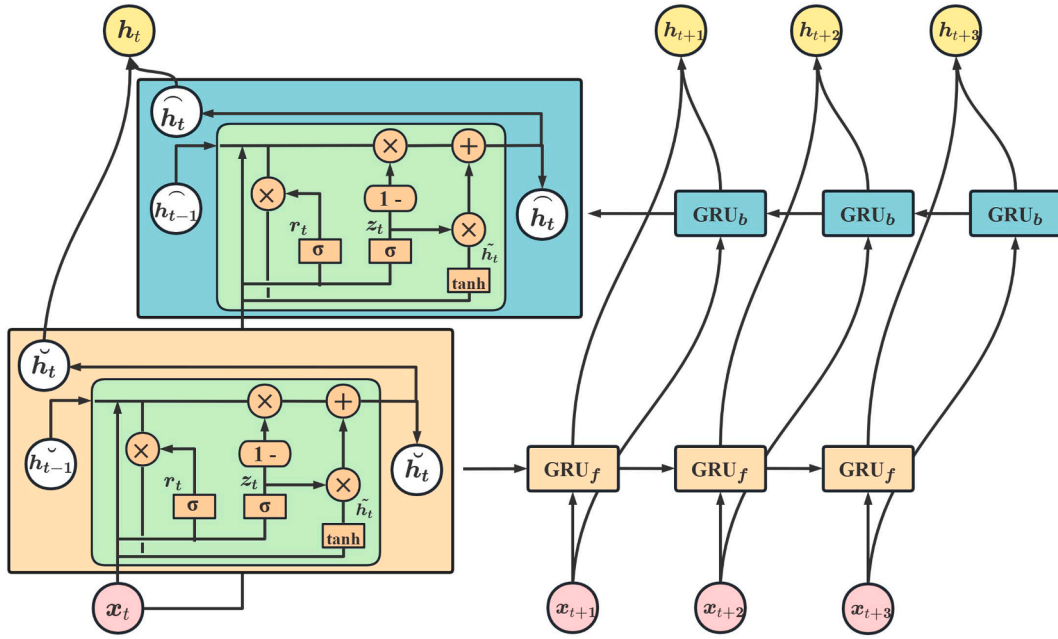


Fig. 3. The framework of the BiGRU.

4. Methodology

4.1. The theoretical essence of the proposed model

The proposed TBNNet model represents a sophisticated approach to predicting ship trajectories, which is crucial for navigation safety and collision avoidance. This model is founded on a robust mathematical and theoretical framework, specifically designed to harness both short-term and long-term information essential for accurate STP.

TBNNet employs a unique three-layer architecture, consisting of BiGRU, BiLSTM, and BiGRU layers, strategically sequenced to maximise each of their strengths. The BiGRU layers are adept at capturing short-term dependencies efficiently, thanks to their gating mechanisms, which swiftly manage recent information. The central BiLSTM layer, positioned between the BiGRU layers, effectively processes long-term dependencies due to its robust memory mechanism. This configuration not only ensures comprehensive handling of data but also maintains the integrity of information over extended periods, which is vital for the complex temporal patterns seen in maritime routes.

This innovative model structure arises from a deep theoretical understanding that different RNN variants are effective at managing varying temporal dependencies. The layering in TBNNet is designed to leverage these insights, ensuring that short-term changes are rapidly processed and long-term trends are thoroughly integrated. This synergy enhances the model's overall predictive performance, as empirically validated through extensive testing against twenty other state-of-the-art models. These included eight single-layer models, four two-layer models (i.e., BiGRU-BiGRU, BiLSTM-BiLSTM, BiGRU-BiLSTM, BiLSTM-BiGRU), eight three-layer models (including BiLSTM-BiLSTM-BiLSTM and BiLSTM-BiGRU-BiLSTM), and one four-layer model (BiGRU-BiLSTM-BiGRU-BiLSTM).

TBNNet integrates cross-disciplinary innovations to enrich its feature fusion capabilities. This approach not only broadens the theoretical underpinnings of the model but also enhances its functionality across diverse applications, demonstrating its versatility and effectiveness in real-world settings.

4.2. The structure of the proposed model

This section provides a comprehensive description of the development of the proposed framework, including the essence and mathematical foundation of the proposed TBNNet model.

BiGRU and BiLSTM are highly capable bi-directional recurrent neural networks known for their proficiency in extracting deep features from time series data (i.e., ship trajectories) by considering both past and future contexts. BiGRU units can be employed to capture dependencies in short sequences while mitigating issues like gradient vanishing or exploding. Moreover, BiLSTM units can be utilised in handling moderate-length sequences and recognising long-term dependencies. BiGRU units enhance short-term information, while BiLSTM units strengthen long-term information. A novel approach is proposed to improve the performance of STP by integrating bi-directional information and leveraging their respective short-term and long-term forecasting capabilities. This approach culminates in the development of a new model named TBNNet, which combines the strengths of BiLSTM and BiGRU to enhance prediction accuracy.

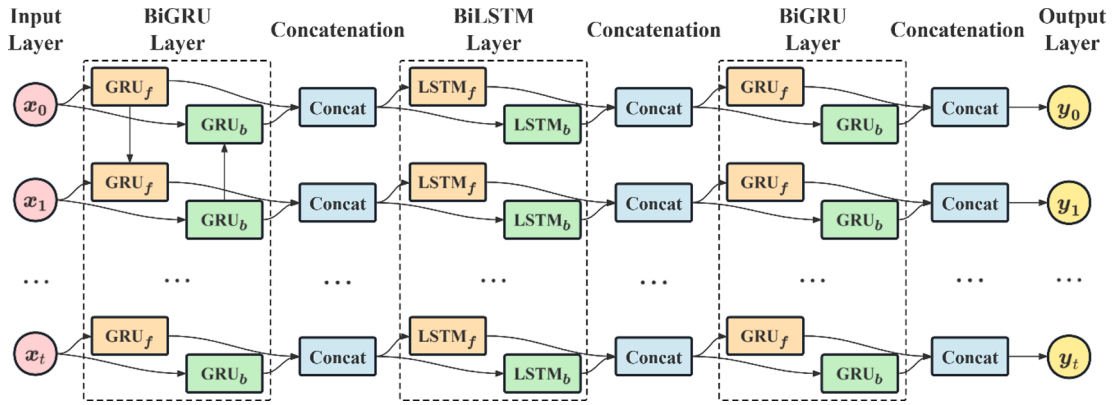


Fig. 4. The structure of the proposed TBENet model.

This new idea draws inspiration from advancements in various research areas, particularly the fusion of multiple features (Ma et al., 2022a). A BiGRU unit is chosen as the first layer model to focus on short-term sequences, and BiLSTM as the second layer model to emphasise long-term patterns. The third layer further enhances prediction accuracy and stability, particularly in short-term trajectory prediction tasks. To combine both short and long-term information effectively, BiGRU is selected as the third layer network unit.

To enhance non-linear processing and adaptability, each network unit is followed by fully connected layers. The structure of the proposed TBENet model is shown in Fig. 4. This fusion three-layer model, sequentially combining BiGRU, BiLSTM, and BiGRU, enables improved accurate and efficient extraction of feature information from short- and long-term perspectives. This method breaks down the overall task into smaller, manageable subtasks, with each subnetwork focusing on a particular aspect. Each component within this network can have unique structures tailored to different functions, including enhancing long-term and short-term features. The output of one subnetwork serves as the input for the next, with its process continuing until the final subnetwork outputs the ultimate result. Consequently, the generalisation ability of the model is enhanced. This structural design enhances data-fitting capabilities and leverages the complementary strengths of these different network units, resulting in an overall performance boost.

The proposed TBENet model, specifically designed for STP, presents an innovative sequence of BiGRU, BiLSTM, and BiGRU. By effectively modelling ship trajectory data and drawing on the advantages of each network unit, TBENet shows superior performance compared to models using a single, two-layer, or four-layer neural network. Its architecture, capable of capturing both short-term dynamics and long-term trends, is instrumental in its success in STP tasks.

4.3. The overall research framework

The comprehensive framework of this paper is illustrated in Fig. 5. To effectively capture spatio-temporal features within ship trajectory sequences, data preprocessing is first conducted to clean and simplify the raw data. These steps include data cleaning, trajectory extraction, data normalisation, and dataset partitioning using sliding windows. Following the data preprocessing stage, comparative experiments are carried out using the proposed methods in the training dataset, with the model parameters saved for each experiment. Subsequently, the results of STP are generated on the test dataset, and a comprehensive evaluation of the results is performed using six evaluation metrics.

5. Experimental results and analysis

This section details the experimental process and provides an in-depth analysis of the results, with the goal of assessing the effectiveness of the TBENet model. To this end, a comparative study of twenty-one different models is conducted, including traditional models and various combined models. The experiments are performed using AIS data collected from three distinct water areas. Six evaluation metrics are used to evaluate the performance of these models. Additionally, the visual representation results are presented to illustrate the model's effectiveness in accurately capturing and predicting ship trajectories. The analysis and discussion drawn from this experimental evaluation are then presented. This analysis provides a clear perspective on the relative strengths and limitations of the various model configurations, highlighting the key factors that influence the TBENet model's overall effectiveness.

5.1. Experimental datasets description and parameter setting

AIS trajectory datasets from three different water regions, namely the Caofeidian water area, Zhoushan water area, and Chengshan Jiao water area, are employed to assess and validate the prediction performance of the proposed TBENet model. Table 8 provides information on three distinct water areas, encompassing descriptions of three datasets and the rationale behind their selection in these particular aquatic regions. A comparative analysis is conducted, comparing the performance of the TBENet model with twenty other models. The trajectory visualisation of the three datasets is shown in Fig. 6. The selection of the three tropical water areas takes into

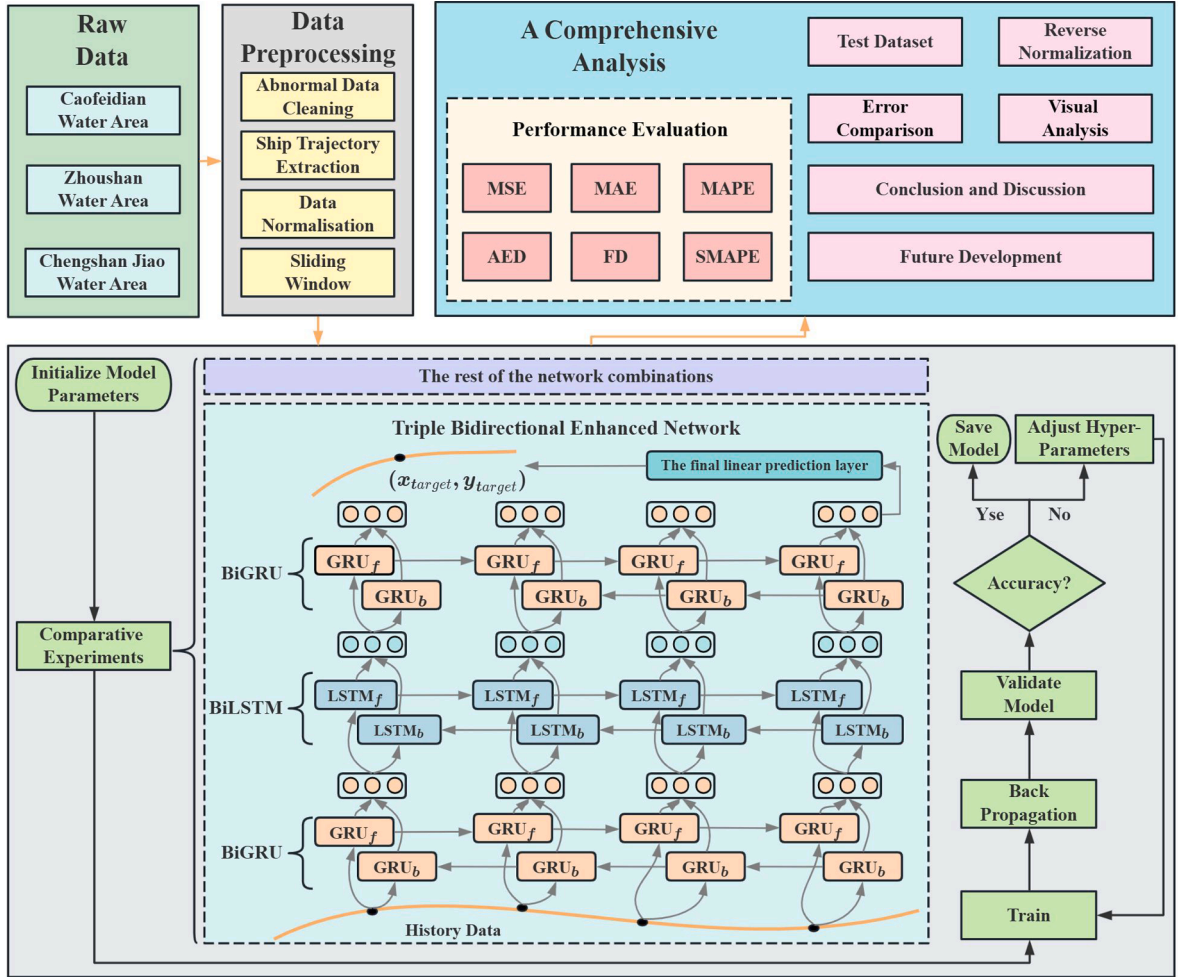
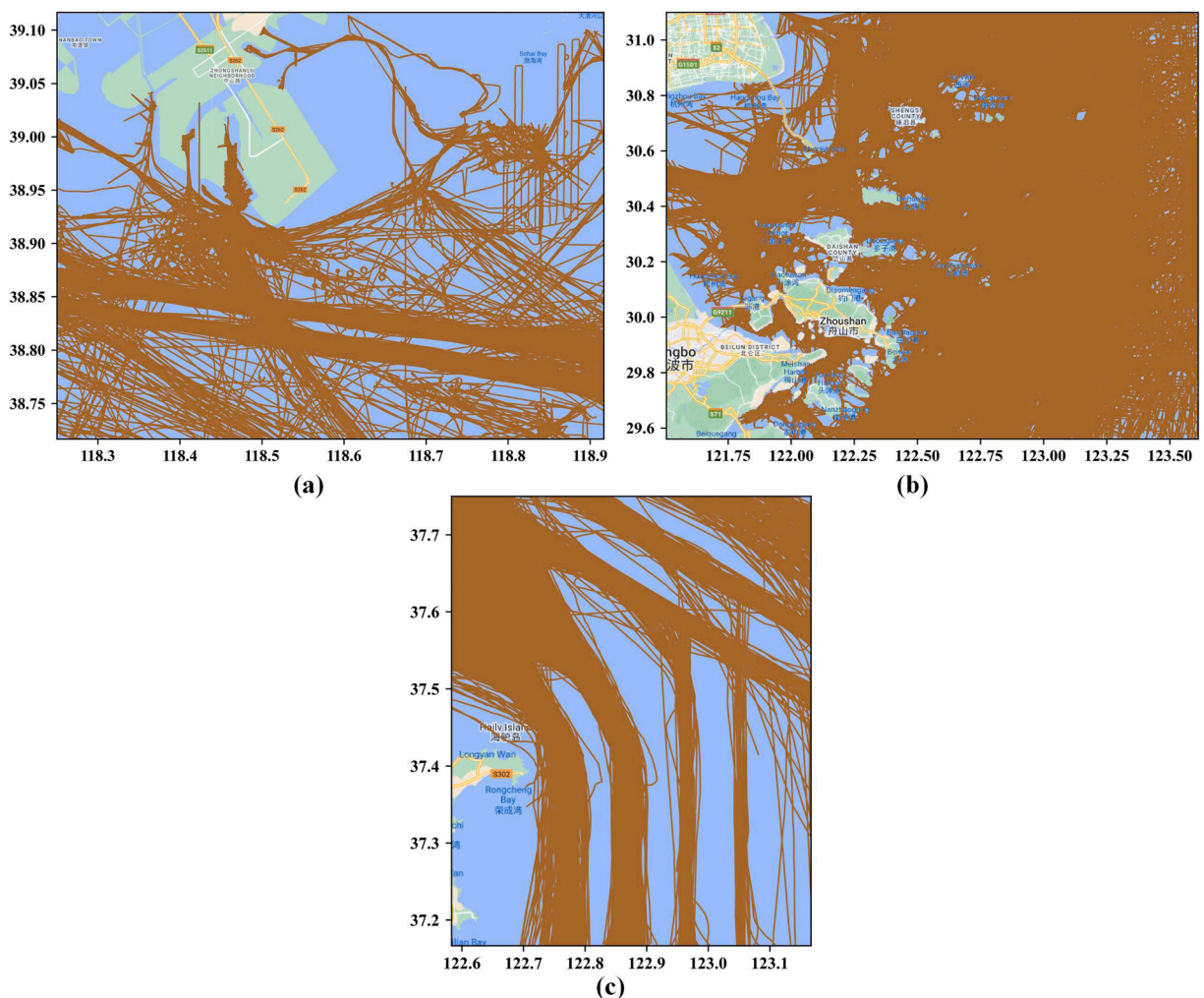


Fig. 5. The overall framework of this paper.

Table 8

The details of three representative water areas.

Water areas	Time	Number of ship trajectories	Number of timestamped points	Range	Representative features
Caofeidian Port water area	Jul. 2017	1284	1,261,875	Longitude from 118°25'E to 118°92'E and latitude from 38°72'N to 39°10'N	1) the largest bay in the western Bohai Sea; 2) large deepwater ports; 3) the highest waterway traffic in the western Bohai Sea.
Zhoushan Archipelago water area	Apr. 2018	9440	8,375,693	Longitude from 121°51'E to 123°61'E and latitude from 29°56' to 31°10'N	1) the most complex traffic area with the highest density in China; 2) mixed traffic of ocean-going and domestic fishing boats; 3) the adverse weather conditions such as typhoons and seasonal storms.
Chengshan Jiao Promontory	Jan. 2018	2000	1,492,889	Longitude from 122°58'E to 123°17'E and latitude from 37°16'N to 37°75'N	1) separate lanes and a traffic separation scheme; 2) a busy maritime route with commercial vessels and fishing boats; 3) unpredictable weather conditions like typhoons and seasonal storms.

**Fig. 6.** Visualisation of the trajectory datasets, (a) visualisation in Caofeidian water area, (b) visualisation in Zhoushan water area, (c) visualisation in Chengshan Jiao water area.

account different perspectives, including the port area (i.e., Fig. 6 (a)), the most complex region (i.e., Fig. 6 (b)), and an area with an existing ship routing system (i.e., Fig. 6 (c)).

The Caofeidian water area, situated in northern China, is the largest bay in the region and plays a vital role in the coastal economic belt and Bohai Sea economic zone. It possesses favourable economic and geographical resources for constructing large deepwater ports, making it the area with the highest waterway traffic in the western Bohai Sea. The AIS dataset for this water area was collected in July 2017. Following data cleaning, the dataset consists of 1,284 trajectories, encompassing a total of 1,261,875 timestamp points. The research area extends from 118°25'E to 118°92'E and 38°72'N to 39°10'N.

Located along the middle section of the Chinese coastline, the Zhoushan water area boasts abundant port resources and serves as a key hub in the East Asian shipping network. With its winding coastline, diverse water depth, and numerous islands and bays, it is widely acknowledged as the most complex traffic area with the highest density in China. The AIS dataset for this water area was collected in April 2018. It comprises 9,440 trajectories with a total of 8,375,693 timestamp points. The trajectory range covers the longitude of 121°51'E to 123°61'E and the latitude of 29°56' to 31°10'N.

The Chengshan Jiao water area serves as a crucial maritime transportation channel, connecting various ports in the Bohai Sea and the northern Yellow Sea in China. It is also renowned as a prominent fishing ground with a substantial number of fishing vessels. Given its unique geographical location, this water area is often affected by weather and sea conditions. Additionally, the high density of ship traffic and complex traffic environment pose risks of collisions and grounding accidents. Therefore, a ship routing system is established to mitigate these risks. The AIS dataset for this water area was collected in January 2018. The research area spans from longitude 122°58'E to 123°17'E and latitude 37°16'N to 37°75'N. After data cleaning, the dataset consists of 2,000 trajectories with 1,492,889 timestamp points.

In this paper, the goal is to predict future location based on four consecutive timestamps of position. Each trajectory undergoes a normalisation process to facilitate the prediction process, resulting in the creation of corresponding input and label data. Normalisation is crucial for unifying data with varying scales and magnitudes into a consistent and relative range. This, in turn, enables the neural network to learn the inherent relationships and patterns within the data effectively. Larger values may disproportionately influence the training process without normalisation, potentially causing convergence issues or reduced prediction accuracy. To tackle this issue, the min-max normalisation method is employed to normalise the latitude and longitude data of each trajectory, scaling them to a range between 0 and 1, as illustrated in Eqs (3)–(4).

$$lon_{std} = \frac{lon_{raw} - lon_{min}}{lon_{max} - lon_{min}} \quad (3)$$

$$lat_{std} = \frac{lat_{raw} - lat_{min}}{lat_{max} - lat_{min}} \quad (4)$$

where lon and lat indicate the latitude and longitude information of the trajectory, respectively. raw represents the original position data of the node. min and max express the minimum and maximum values of the trajectory data, respectively. std denotes the normalised standard value.

After the above normalisation process, the original i th trajectory data $T_i^o = \{N_i^1, N_i^2, \dots, N_i^j, \dots, N_i^{n-1}, N_i^n\}$ can be converted into $T_{std-i}^o = \{N_{std-i}^1, N_{std-i}^2, \dots, N_{std-i}^j, \dots, N_{std-i}^{n-1}, N_{std-i}^n\}$ with $N_{std-i}^j = \{lon_{std-i}^j, lat_{std-i}^j\}$. Subsequently, the data is segmented and organised into the appropriate training set, following the prediction task, utilising a sliding window approach. For each trajectory, the position information of the four consecutive nodes is considered as the input data, while the position information of the subsequent node is set as the corresponding label data. This process is visually depicted in Fig. 7.

The sliding window technique enables efficient and real-time processing of large volumes of data in sequential order. In this study, each dataset is processed using this technique. The processed dataset is then divided, with 80 % allocated for the training and validation sets and the remaining 20 % used as the test set. For this, nine representative trajectories are selected to display results and perform visualisation analyses in three water areas. These trajectories are specifically chosen to reflect a range of navigational features, movement patterns, and channel characteristics.

The experiments are conducted on a 64-bit Windows 10 system with a 3.10 GHz Intel Core i5-11300H CPU, GPU, and 16 GB of memory. The experiment programming is implemented using the PyTorch framework and developed in Python. It is crucial to control the hyperparameters of all the models. The optimal parameter setting is determined through experimental comparisons and listed in Table 9.

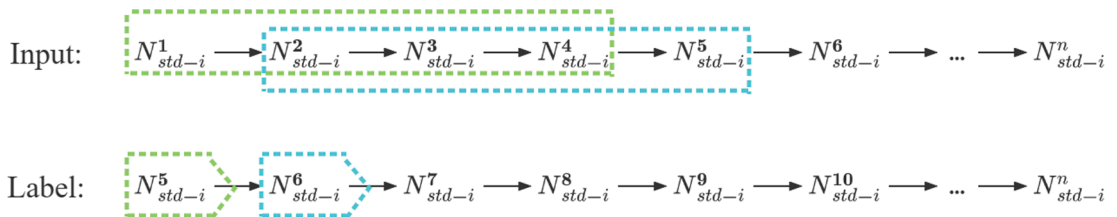


Fig. 7. The process of the assembled dataset.

Table 9

The optimal parameter setting.

Batch size	Input dimension	Hidden layers	Output dimension	Network layers
64	2	128	2	4

To ensure fast and stable convergence during training, the initial learning rate is set to 0.0001. As the number of iterations increases, the learning rate is adjusted to decrease gradually. This approach helps the model avoid oscillations when approaching the optimal solution and allows for more refined updates. Additionally, a validation-based stopping criterion is employed in the experiment. After each iteration, the model's performance is evaluated using the validation set. Training is stopped when the performance on the validation set starts to decline. This strategy helps prevent overfitting and enhances the efficiency of the multiple comparative experiments.

5.2. Comparative experiment

A total of twenty-one comparative experiments are designed to evaluate the effectiveness of the proposed TBENet model and explore how different combinations of STP models perform. Firstly, the baseline comparative experiments by listing the eight most commonly used individual networks in Table 10, which include RNN, LSTM, GRU, Seq2Seq, BiRNN, BiLSTM, BiGRU, and Transformer. Furthermore, different combinations of two bidirectional networks are displayed in Table 11, facilitating in-depth analysis of results and conducting ablation experiments. For clarity, 'A' indicates BiGRU, while 'B' represents BiLSTM. These comparative experiments encompass both single-network models and multiple fusion networks. The investigated model in this study, the proposed TBENet model (i.e., ABA), is compared against twenty other models in Tables 10 and 11.

To maintain consistency and control variables, the parameter configurations for both network units, BiGRU and BiLSTM, adhere to the parameter combinations outlined in Section 5.1. Additionally, following each network unit, a fully connected layer with 256 input features and 2 output features is incorporated to introduce additional parameters and enhance non-linear transformations. To facilitate

Table 10

The description of eight individual networks.

Abbreviations	Models	Abbreviations	Models
RNN	RNN	GRU	GRU
LSTM	LSTM	BiGRU	BiGRU (A)
BiLSTM	BiLSTM (B)	Transformer	Transformer
Seq2Seq	Seq2Seq	BiRNN	BiRNN

Table 11

The description of twelve different combinations of two bidirectional units.

Abbreviations	Specific combinations	Abbreviations	Specific combinations
AB	BiGRU-BiLSTM	AAB	BiGRU-BiGRU-BiLSTM
BA	BiLSTM-BiGRU	BBA	BiLSTM-BiLSTM-BiGRU
AA	BiGRU-BiGRU	BAB	BiLSTM-BiGRU-BiLSTM
BB	BiLSTM-BiLSTM	ABB	BiGRU-BiLSTM-BiLSTM
AAA	BiGRU-BiGRU-BiGRU	BAA	BiLSTM-BiGRU-BiGRU
BBB	BiLSTM-BiLSTM-BiLSTM	ABAB	BiGRU-BiLSTM-BiGRU-BiLSTM

Table 12

A detailed description of the six indexes.

Indexes	Features	Equations	Descriptions
MSE	Overall error	$MSE = \frac{1}{n} \sum_{i=1}^n (\hat{y}_i - y_i)^2$	MSE gives higher weight to larger prediction deviations.
MAE	Overall error	$MAE = \frac{1}{n} \sum_{i=1}^n \hat{y}_i - y_i $	MAE is not sensitive to abnormal values in the data.
MAPE	Overall error	$MAPE = \frac{1}{n} \sum_{i=1}^n \left \frac{\hat{y}_i - y_i}{y_i} \right \times 100\%$	MAPE can take into account the effect of relative errors.
SMAPE	Overall error	$SMAPE = \frac{1}{n} \sum_{i=1}^n \frac{ \hat{y}_i - y_i }{(\hat{y}_i + y_i)/2} \times 100\%$	SMAPE ensures that over- or under-prediction has an equal impact on the error.
FD	Similarity	$FD = \max(\sqrt{\sum_{i=1}^n (\hat{y}_i - y_i)^2})$	FD represents the degree of difference between the actual probability distribution and the predicted probability distribution. It is often used to describe path similarity.
AED	Similarity	$AED = \frac{1}{n} \sqrt{\sum_{i=1}^n (\hat{y}_i - y_i)^2}$	AED is usually used to measure the distance between two points in space.

Table 13

The results of six indexes for nine selected trajectories across eight single-layer models in the Caofeidian water area.

	Criteria	RNN	GRU	LSTM	Transformer	Seq2Seq	BiRNN	BiGRU	BiLSTM
1	MSE	2.1E-04	7.4E-05	5.7E-07	1.7E-06	6.3E-04	2.8E-06	1.0E-07	3.8E-07
	MAE	8.9E-03	6.5E-03	4.5E-04	9.5E-04	1.1E-02	1.2E-03	1.7E-04	4.6E-04
	MAPE	9.6E-03	9.5E-03	4.0E-04	1.0E-03	1.2E-02	1.6E-03	2.8E-04	9.7E-04
	SMAPE	9.6E-03	9.5E-03	4.0E-04	1.0E-03	1.2E-02	1.6E-03	2.8E-04	9.7E-04
	FD	5.1E-02	5.0E-02	6.5E-03	5.4E-03	1.1E-01	9.5E-03	5.3E-03	6.1E-03
	AED	1.6E-02	1.0E-02	8.7E-04	1.7E-03	2.0E-02	2.1E-03	2.7E-04	7.4E-04
2	MSE	2.0E-04	4.8E-05	3.5E-06	9.6E-06	2.2E-04	9.9E-06	1.5E-07	2.1E-07
	MAE	9.4E-03	3.7E-03	1.3E-03	2.2E-03	6.0E-03	2.6E-03	3.2E-04	3.6E-04
	MAPE	9.4E-03	5.2E-03	1.3E-03	2.2E-03	6.5E-03	4.9E-03	4.5E-04	6.3E-04
	SMAPE	9.4E-03	5.2E-03	1.3E-03	2.2E-03	6.5E-03	4.9E-03	4.5E-04	6.3E-04
	FD	5.1E-02	4.5E-02	8.9E-03	1.3E-02	1.0E-01	1.1E-02	2.2E-03	2.5E-03
	AED	1.7E-02	5.9E-03	2.4E-03	3.9E-03	1.0E-02	4.1E-03	5.1E-04	5.5E-04
3	MSE	6.1E-05	3.2E-05	7.4E-07	8.5E-06	8.4E-05	2.8E-06	1.3E-07	7.6E-07
	MAE	5.9E-03	3.8E-03	5.4E-04	2.4E-03	4.8E-03	1.4E-03	2.7E-04	6.6E-04
	MAPE	7.5E-03	6.8E-03	7.4E-04	3.1E-03	6.5E-03	2.0E-03	3.4E-04	8.6E-04
	SMAPE	7.5E-03	6.8E-03	7.4E-04	3.1E-03	6.5E-03	2.0E-03	3.4E-04	8.6E-04
	FD	2.7E-02	2.7E-02	4.8E-03	9.3E-03	5.7E-02	5.3E-03	2.3E-03	3.1E-03
	AED	9.4E-03	6.1E-03	8.5E-04	3.7E-03	7.4E-03	2.1E-03	4.5E-04	1.1E-03
4	MSE	5.5E-07	5.7E-07	3.6E-07	1.4E-06	4.0E-06	8.4E-06	1.3E-07	1.2E-06
	MAE	2.8E-04	4.4E-04	2.3E-04	2.2E-04	1.3E-03	2.6E-03	2.3E-04	7.7E-04
	MAPE	4.0E-04	7.2E-04	2.5E-04	3.9E-04	1.3E-03	4.1E-03	2.1E-04	7.0E-04
	SMAPE	4.0E-04	7.2E-04	2.5E-04	3.9E-04	1.3E-03	4.1E-03	2.1E-04	7.0E-04
	FD	1.6E-02	1.8E-02	1.9E-02	3.0E-02	2.3E-02	1.1E-02	1.6E-03	3.2E-03
	AED	4.3E-04	6.3E-04	4.2E-04	3.6E-04	2.6E-03	3.7E-03	4.4E-04	1.5E-03
5	MSE	4.1E-05	3.6E-05	3.4E-07	1.2E-06	1.6E-05	3.4E-06	1.5E-07	8.6E-07
	MAE	5.7E-03	4.7E-03	3.2E-04	5.9E-04	3.4E-03	1.6E-03	2.9E-04	7.1E-04
	MAPE	7.9E-03	7.1E-03	4.4E-04	8.4E-04	4.5E-03	2.4E-03	3.8E-04	8.6E-04
	SMAPE	7.9E-03	7.1E-03	4.4E-04	8.4E-04	4.5E-03	2.4E-03	3.8E-04	8.6E-04
	FD	1.1E-02	2.2E-02	6.0E-03	7.5E-03	1.8E-02	5.4E-03	2.3E-03	3.1E-03
	AED	8.7E-03	7.6E-03	5.1E-04	9.8E-04	5.4E-03	2.4E-03	4.8E-04	1.2E-03
6	MSE	3.0E-05	2.7E-05	1.4E-05	1.0E-04	4.8E-05	1.4E-06	2.0E-07	1.2E-06
	MAE	4.2E-03	3.8E-03	1.8E-03	5.2E-03	4.3E-03	1.0E-03	2.1E-04	7.6E-04
	MAPE	5.6E-03	5.1E-03	2.3E-03	6.6E-03	5.6E-03	1.4E-03	2.1E-04	7.0E-04
	SMAPE	5.6E-03	5.1E-03	2.3E-03	6.6E-03	5.6E-03	1.4E-03	2.1E-04	7.0E-04
	FD	2.2E-02	2.3E-02	2.2E-02	5.6E-02	3.0E-02	3.1E-03	1.3E-02	1.4E-02
	AED	6.7E-03	5.9E-03	2.9E-03	8.7E-03	7.2E-03	1.6E-03	3.9E-04	1.5E-03
7	MSE	9.5E-05	2.4E-05	1.6E-06	6.1E-06	3.4E-04	1.9E-06	3.2E-07	1.7E-06
	MAE	6.6E-03	3.7E-03	9.0E-04	1.8E-03	1.1E-02	1.0E-03	3.3E-04	9.7E-04
	MAPE	7.4E-03	6.2E-03	9.2E-04	1.9E-03	1.3E-02	2.1E-03	3.7E-04	1.0E-03
	SMAPE	7.4E-03	6.2E-03	9.2E-04	1.9E-03	1.3E-02	2.1E-03	3.7E-04	1.0E-03
	FD	2.4E-02	1.4E-02	7.0E-02	5.1E-02	5.0E-02	7.2E-03	1.5E-02	1.6E-02
	AED	1.1E-02	5.3E-03	1.6E-03	3.1E-03	1.9E-02	1.8E-03	5.8E-04	1.7E-03
8	MSE	1.8E-05	1.8E-05	2.3E-07	1.3E-06	3.8E-06	5.7E-06	1.4E-07	9.0E-08
	MAE	3.6E-03	3.5E-03	3.3E-04	6.6E-04	1.7E-03	1.7E-03	2.7E-04	2.6E-04
	MAPE	4.8E-03	5.1E-03	3.9E-04	8.5E-04	2.8E-03	3.8E-03	3.0E-04	4.2E-04
	SMAPE	4.8E-03	5.1E-03	3.9E-04	8.5E-04	2.8E-03	3.8E-03	3.0E-04	4.2E-04
	FD	8.5E-03	8.1E-03	3.9E-03	7.4E-03	7.1E-03	1.2E-02	1.6E-03	1.9E-03
	AED	5.6E-03	5.2E-03	5.5E-04	1.1E-03	2.7E-03	2.8E-03	4.8E-04	3.9E-04
9	MSE	4.5E-02	4.3E-02	4.5E-02	4.5E-02	4.1E-02	2.3E-06	1.0E-07	3.8E-07
	MAE	1.3E-01	1.3E-01	1.3E-01	1.4E-01	1.3E-01	1.3E-03	1.7E-04	4.6E-04
	MAPE	1.3E-01	1.3E-01	1.3E-01	1.3E-01	1.2E-01	2.4E-03	2.8E-04	9.7E-04
	SMAPE	1.3E-01	1.3E-01	1.3E-01	1.3E-01	1.2E-01	2.4E-03	2.8E-04	9.7E-04
	FD	4.9E-01	4.9E-01	4.9E-01	4.9E-01	4.8E-01	7.3E-03	5.3E-03	6.1E-03
	AED	2.5E-01	2.5E-01	2.5E-01	2.5E-01	2.4E-01	1.9E-03	2.7E-04	7.4E-04

effective comparative analysis, the parameters of the two bidirectional units remain consistent throughout the experiment. This uniformity is maintained across all experimental combinations and contributes significantly to the overall performance of the trajectory prediction models.

Subsequent experiments involved testing both two-layer and three-layer fusion models incorporating BiGRU, BiLSTM, and BiRNN. Despite various configurations, all models consistently encountered Not a Number (NaN) issues during training, primarily attributed to gradient explosion or vanishing. The experimental results further validate the effectiveness of selectively fusing specific bi-directional networks.

Table 14

The results of six indexes for nine selected trajectories across 13 multilayer models in the Caofeidian water area (A denotes BiGRU, and B indicates BiLSTM).

	Criteria	AB	BA	AA	BB	AAA	BBB	AAB	BBA	TBNet	BAB	ABB	BAA	ABAB
1	MSE	6.0E-08	9.2E-08	7.3E-08	1.5E-07	8.3E-08	7.9E-08	9.5E-08	1.1E-07	5.7E-08	6.8E-08	8.2E-08	8.0E-08	1.1E-07
	MAE	1.5E-04	1.9E-04	1.32E-04	2.3E-04	1.6E-04	1.5E-04	1.9E-04	2.3E-04	1.28E-04	1.31E-04	1.5E-04	1.4E-04	2.4E-04
	MAPE	2.8E-04	3.7E-04	2.2E-04	4.5E-04	2.153E-04	3.0E-04	4.0E-04	4.6E-04	2.151E-04	2.4E-04	2.3E-04	2.5E-04	5.0E-04
	SMAPE	2.8E-04	3.7E-04	2.2E-04	4.5E-04	2.153E-04	3.0E-04	4.0E-04	4.6E-04	2.151E-04	2.4E-04	2.3E-04	2.5E-04	5.0E-04
	FD	5.0E-03	5.3E-03	5.2E-03	5.2E-03	5.3E-03	5.3E-03	5.1E-03	5.2E-03	4.5E-03	5.0E-03	5.0E-03	5.4E-03	5.0E-03
	AED	1.9E-04	2.9E-04	2.0E-04	3.6E-04	1.9E-04	2.4E-04	3.1E-04	3.6E-04	1.8E-04	2.0E-04	2.6E-04	2.1E-04	3.8E-04
2	MSE	9.3E-08	7.2E-08	6.9E-08	2.1E-07	7.3E-08	6.7E-08	1.6E-07	6.9E-08	5.4E-08	7.2E-08	2.1E-07	6.2E-07	1.2E-07
	MAE	2.2E-04	2.2E-04	2.1E-04	3.7E-04	2.1E-04	2.0E-04	3.3E-04	2.1E-04	1.8E-04	1.9E-04	3.2E-04	1.9E-04	2.4E-04
	MAPE	2.9E-04	3.8E-04	3.3E-04	5.6E-04	3.7E-04	3.2E-04	4.5E-04	3.2E-04	2.4E-04	2.9E-04	3.9E-04	3.1E-04	3.6E-04
	SMAPE	2.9E-04	3.8E-04	3.3E-04	5.6E-04	3.7E-04	3.2E-04	4.5E-04	3.2E-04	2.4E-04	2.9E-04	3.9E-04	3.1E-04	3.6E-04
	FD	2.3E-03	2.1E-03	2.1E-03	2.4E-03	2.0E-03	1.7E-03	2.1E-03	1.8E-03	1.6E-03	2.2E-03	2.6E-03	1.8E-03	2.2E-03
	AED	3.7E-04	3.2E-04	3.3E-04	5.9E-04	3.3E-04	3.1E-04	5.2E-04	3.2E-04	2.2E-04	3.1E-04	5.6E-04	3.1E-04	3.9E-04
3	MSE	5.4E-08	1.1E-07	1.3E-07	1.3E-07	1.2E-07	1.5E-07	3.5E-07	1.8E-07	4.0E-08	5.6E-08	8.6E-08	1.6E-07	6.6E-08
	MAE	1.7E-04	2.8E-04	2.7E-04	2.6E-04	2.6E-04	2.9E-04	4.2E-04	3.4E-04	1.4E-04	1.6E-04	2.2E-04	2.8E-04	2.0E-04
	MAPE	2.7E-04	4.7E-04	3.8E-04	3.9E-04	3.4E-04	4.4E-04	4.6E-04	4.6E-04	1.6E-04	1.9E-04	3.0E-04	4.0E-04	2.9E-04
	SMAPE	2.7E-04	4.7E-04	3.8E-04	3.9E-04	3.4E-04	4.4E-04	4.6E-04	4.6E-04	1.6E-04	1.9E-04	3.0E-04	4.0E-04	2.9E-04
	FD	1.8E-03	2.1E-03	2.2E-03	2.3E-03	2.0E-03	2.1E-03	3.0E-03	2.1E-03	1.3E-03	2.2E-03	1.6E-03	2.3E-03	2.0E-03
	AED	3.0E-04	4.2E-04	4.2E-04	4.1E-04	4.2E-04	4.8E-04	7.4E-04	5.5E-04	2.4E-04	2.6E-04	3.5E-04	4.6E-04	3.2E-04
4	MSE	8.6E-08	1.1E-07	7.5E-08	6.7E-08	2.9E-07	1.8E-07	2.1E-07	3.6E-07	6.5E-08	6.6E-08	1.9E-07	7.2E-07	2.0E-07
	MAE	1.9E-04	2.2E-04	1.3E-04	1.5E-04	3.4E-04	2.9E-04	2.8E-04	4.1E-04	1.0E-04	1.6E-04	2.7E-04	1.2E-04	3.0E-04
	MAPE	1.8E-04	2.2E-04	1.3E-04	1.7E-04	3.1E-04	2.8E-04	2.6E-04	3.7E-04	1.0E-04	1.5E-04	2.5E-04	1.2E-04	2.8E-04
	SMAPE	1.8E-04	2.2E-04	1.3E-04	1.7E-04	3.1E-04	2.8E-04	2.6E-04	3.7E-04	1.0E-04	1.5E-04	2.5E-04	1.2E-04	2.8E-04
	FD	1.7E-03	1.8E-03	1.6E-03	2.2E-03	2.4E-03	1.9E-03	2.1E-03	2.4E-03	1.0E-03	1.6E-03	2.5E-03	1.7E-03	2.1E-03
	AED	3.6E-04	4.1E-04	2.3E-04	2.5E-04	6.6E-04	5.3E-04	5.3E-04	7.8E-04	1.9E-04	2.9E-04	5.0E-04	2.2E-04	5.6E-04
5	MSE	7.6E-08	1.3E-07	1.5E-07	1.3E-07	1.6E-07	1.5E-07	3.9E-07	2.3E-07	7.4E-08	7.6E-08	9.4E-08	1.2E-07	9.6E-08
	MAE	1.7E-04	2.9E-04	2.8E-04	2.6E-04	3.0E-04	2.9E-04	4.7E-04	3.9E-04	1.6E-04	1.9E-04	2.2E-04	2.5E-04	2.4E-04
	MAPE	2.7E-04	4.6E-04	4.0E-04	3.9E-04	4.1E-04	4.3E-04	5.3E-04	5.1E-04	2.4E-04	2.7E-04	3.1E-04	3.8E-04	3.5E-04
	SMAPE	2.7E-04	4.6E-04	4.0E-04	3.9E-04	4.1E-04	4.3E-04	5.3E-04	5.1E-04	2.4E-04	2.7E-04	3.1E-04	3.8E-04	3.5E-04
	FD	1.9E-03	1.7E-03	1.9E-03	2.0E-03	2.0E-03	1.8E-03	2.4E-03	2.5E-03	1.6E-03	1.8E-03	2.0E-03	1.8E-03	1.8E-03
	AED	3.9E-04	4.5E-04	4.4E-04	4.0E-04	4.8E-04	4.7E-04	8.2E-04	6.4E-04	3.0E-04	3.1E-04	3.6E-04	4.0E-04	3.8E-04
6	MSE	1.2E-07	1.7E-07	1.2E-07	1.3E-07	2.9E-07	2.3E-07	3.6E-07	3.3E-07	1.0E-07	1.3E-07	2.6E-07	1.2E-07	1.4E-07
	MAE	1.2E-04	2.1E-04	1.3E-04	1.5E-04	3.0E-04	2.8E-04	3.7E-04	3.4E-04	1.0E-04	1.4E-04	2.5E-04	1.1E-04	1.7E-04
	MAPE	2.3E-04	2.5E-04	1.9E-04	1.8E-04	2.9E-04	3.1E-04	3.5E-04	3.4E-04	1.7E-04	1.8E-04	2.4E-04	2.4E-04	1.9E-04

(continued on next page)

Table 14 (continued)

	Criteria	AB	BA	AA	BB	AAA	BBB	AAB	BBA	TBENet	BAB	ABB	BAA	ABAB
7	SMAPE	2.3E-04	2.5E-04	1.9E-04	1.8E-04	2.9E-04	3.1E-04	3.5E-04	3.4E-04	1.7E-04	1.8E-04	2.4E-04	2.4E-04	1.9E-04
	FD	1.3E-02	1.3E-02	1.3E-02	1.2E-02	1.3E-02	1.3E-02	1.3E-02	1.3E-02	1.0E-02	1.3E-02	1.3E-02	1.3E-02	1.3E-02
	AED	2.2E-04	3.7E-04	2.2E-04	2.6E-04	5.6E-04	4.9E-04	7.0E-04	6.2E-04	2.1E-04	2.5E-04	4.7E-04	2.8E-04	2.9E-04
	MSE	2.9E-07	2.8E-07	3.1E-07	2.8E-07	8.5E-07	3.0E-07	4.8E-07	3.8E-07	2.6E-07	2.9E-07	3.7E-07	3.1E-07	3.1E-07
	MAE	2.4E-04	2.6E-04	3.3E-04	2.6E-04	4.5E-04	3.1E-04	4.3E-04	3.6E-04	2.3E-04	2.5E-04	3.2E-04	3.1E-04	2.6E-04
	MAPE	3.1E-04	3.4E-04	4.0E-04	2.9E-04	4.9E-04	3.8E-04	4.4E-04	4.3E-04	2.5E-04	2.7E-04	3.5E-04	3.7E-04	3.0E-04
	SMAPE	3.1E-04	3.4E-04	4.0E-04	2.9E-04	4.9E-04	3.8E-04	4.4E-04	4.3E-04	2.5E-04	2.7E-04	3.5E-04	3.7E-04	3.0E-04
8	FD	1.5E-02	1.5E-02	1.42E-02	1.5E-02	1.5E-02	1.5E-02	1.5E-02	1.5E-02	1.39E-02	1.5E-02	1.5E-02	1.5E-02	1.5E-02
	AED	4.1E-04	4.0E-04	5.6E-04	4.5E-04	7.9E-04	5.3E-04	7.7E-04	6.2E-04	3.6E-04	3.9E-04	5.6E-04	5.3E-04	4.5E-04
	MSE	1.5E-07	2.1E-07	2.4E-07	3.3E-07	1.0E-07	1.2E-07	1.7E-07	8.3E-08	5.3E-08	1.7E-07	3.0E-07	3.1E-07	1.6E-07
	MAE	2.9E-04	3.3E-04	3.4E-04	3.7E-04	2.3E-04	2.4E-04	2.7E-04	2.1E-04	1.5E-04	2.8E-04	3.5E-04	4.1E-04	2.7E-04
	MAPE	3.1E-04	3.6E-04	3.6E-04	3.6E-04	2.6E-04	2.7E-04	2.9E-04	2.7E-04	1.7E-04	2.9E-04	3.6E-04	4.2E-04	3.1E-04
	SMAPE	3.1E-04	3.6E-04	3.6E-04	3.6E-04	2.6E-04	2.7E-04	2.9E-04	2.7E-04	1.7E-04	2.9E-04	3.6E-04	4.2E-04	3.1E-04
	FD	1.9E-03	2.1E-03	2.3E-03	2.4E-03	1.8E-03	1.7E-03	1.9E-03	1.5E-03	1.4E-03	1.8E-03	2.3E-03	2.0E-03	1.8E-03
9	AED	5.0E-04	5.8E-04	6.1E-04	7.0E-04	3.8E-04	4.2E-04	4.8E-04	3.5E-04	2.8E-04	5.1E-04	6.4E-04	7.3E-04	4.7E-04
	MSE	6.0E-08	9.2E-08	7.3E-08	1.5E-07	8.3E-08	7.9E-08	9.5E-08	1.1E-07	5.7E-08	6.8E-08	8.2E-08	8.0E-08	1.1E-07
	MAE	1.8E-04	1.9E-04	1.4E-04	2.3E-04	1.4E-04	1.5E-04	1.9E-04	2.3E-04	1.28E-04	1.32E-04	1.5E-04	1.4E-04	2.4E-04
	MAPE	2.8E-04	3.7E-04	2.3E-04	4.5E-04	2.22E-04	3.0E-04	4.0E-04	4.6E-04	2.21E-04	2.4E-04	2.3E-04	2.5E-04	5.0E-04
	SMAPE	2.8E-04	3.7E-04	2.3E-04	4.5E-04	2.22E-04	3.0E-04	4.0E-04	4.6E-04	2.21E-04	2.4E-04	2.3E-04	2.5E-04	5.0E-04
	FD	5.0E-03	5.3E-03	5.2E-03	5.2E-03	5.3E-03	5.3E-03	5.1E-03	5.2E-03	4.5E-03	5.0E-03	5.0E-03	5.4E-03	5.0E-03
	AED	2.0E-04	2.9E-04	2.0E-04	3.6E-04	1.92E-04	2.4E-04	3.1E-04	3.6E-04	1.90E-04	2.0E-04	2.6E-04	2.1E-04	3.8E-04

5.3. Evaluation indexes

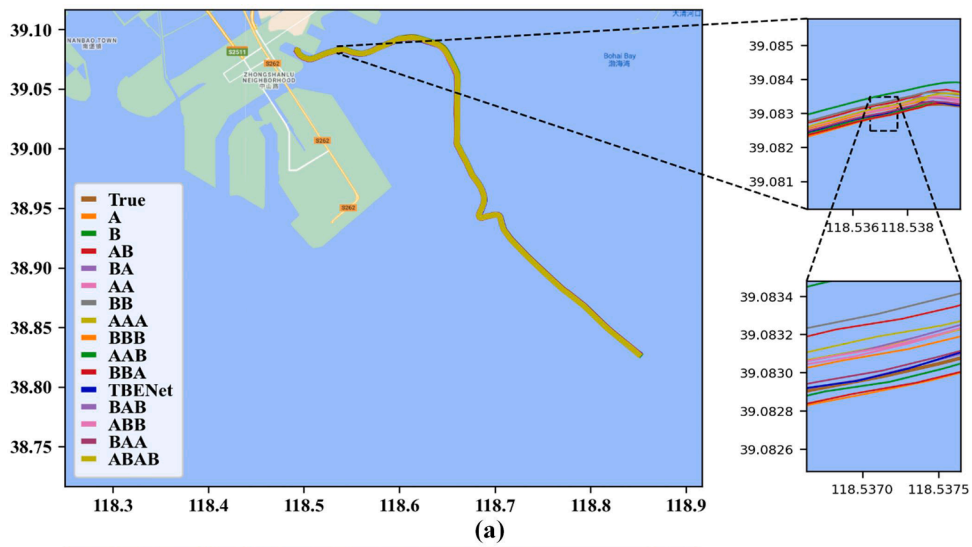
This paper employs six metrics, namely MSE, MAE, MAPE, SMAPE, FD, and AED, to measure the deviation between the predicted values and the ground truth. These metrics collectively assess the performance of twenty-one prediction models, as summarised in Table 12.

5.4. Visualisation analysis of experimental results in three cases

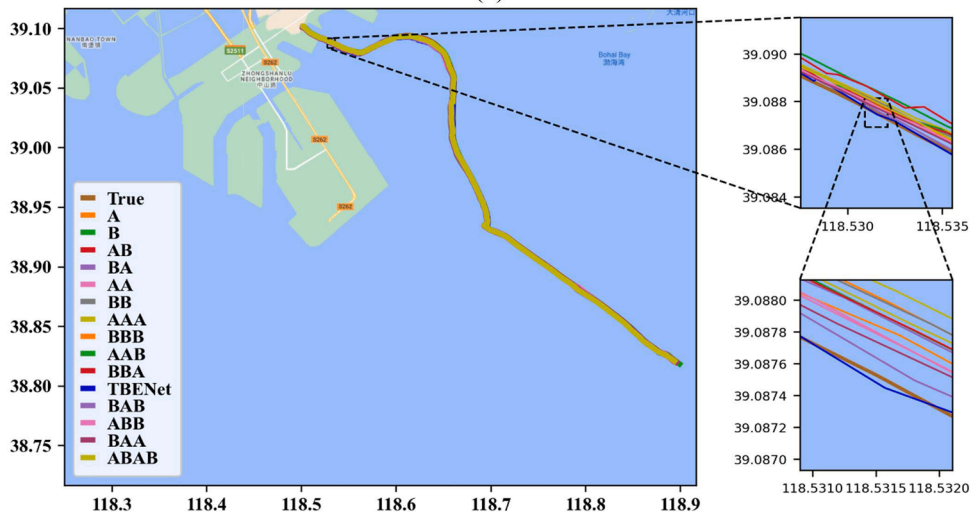
5.4.1. Visualisation analysis in the Caofeidian water area

To conduct the effective analysis, nine trajectories associated with selected Maritime Mobile Service Identity (MMSI) numbers in the Caofeidian water area are numbered 1–9: 209047000, 259739000, 355356000, 373498000, 518100230, 538006066, 566410000, 636091132, 636092704, respectively. Tables 13 and 14 provide a detailed comparison of prediction performance across twenty-one methods applied to nine test trajectories in the Caofeidian water area. Eight single-layer models in Table 13 show better prediction performance with smaller values highlighted in bold, demonstrating BiGRU as the best-performing method, followed by BiLSTM. In Table 14, the TBENet method stands out with bolded minimum values, indicating its superior predictive effectiveness among the thirteen multi-layer models. Moreover, its performance surpasses even the best-performing single-layer method, BiGRU. Tables 13 and 14 quantitatively illustrate the comparative advantage of one method over another for specific evaluation indexes, showcasing the unique strengths of each method in predicting ship trajectories. This consistent superiority of TBENet across all evaluation indices suggests its suitability for future STP tasks. Based on these findings, the proposed TBENet model with the best performance measurements is highly recommended for future STP tasks.

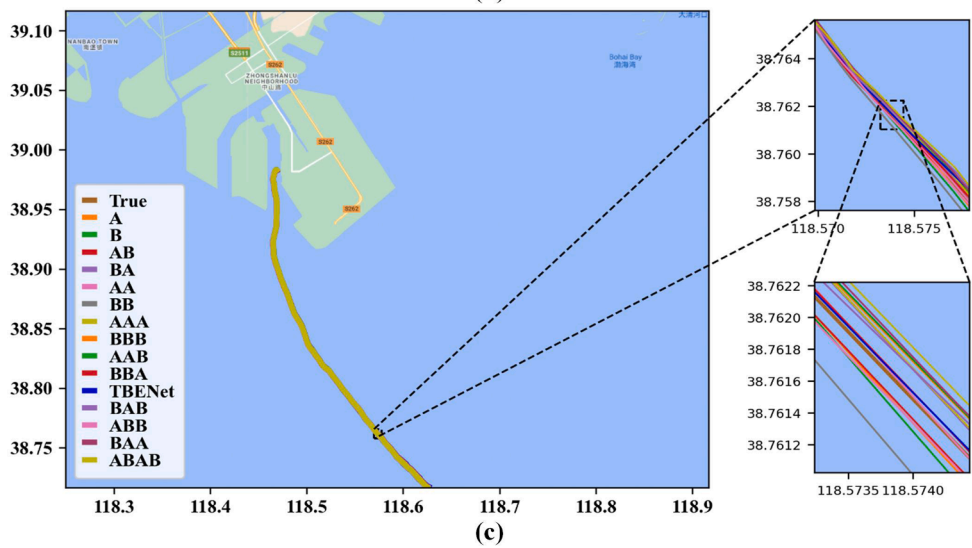
Since the performance of RNN, GRU, LSTM, Seq2seq, and Transformer is significantly worse compared to the other 15 methods, for a clearer visual analysis of the experimental results, the visualisation of the representative trajectories based on the results of these 15



(a)



(b)



(c)

(caption on next page)

Fig. 8. The comparison of predicted and actual trajectories with 15 prediction methods in the Caofeidian water area, (a) the results for MMSI 355356000, (b) the results for MMSI 518100230, (c) the results for MMSI 636092704.

prediction methods is presented in Figs. 8–10. For the test set in the Caofeidian water area, three representative trajectories are further selected for prediction using 15 prediction models. In Fig. 8, the actual trajectories are distinctly marked in bold brown, whereas the prediction results from the other 15 models are shown in various colours. The trajectory predicted by the TBENet method is presented in dark blue for clear comparison. A three-stage zoom-in technique is used to highlight the differences more effectively. Upon examining the visualisation, it is clear that the trajectory curve predicted by the TBENet method closely matches the ground truth, demonstrating superior prediction accuracy over all the other evaluated models.

5.4.2. Visualisation analysis in the Zhoushan water area

Similar to the comparison in Sec. 5.4.1, Tables 15 and 16 present a comprehensive evaluation of the prediction performance of twenty-one methods across nine test trajectories in the Zhoushan water area. The given MMSI numbers are assigned as track numbers 1–9: 249515000, 354336000, 412764670, 412366430, 413438520, 477439900, 538005313, 538007727, 636091992. By examining the results in Tables 15 and 16, it is apparent that TBENet achieves the most favourable prediction results among the tested models.

Tables 15 and 16 present the results of six indexes, with lower error values signifying better prediction performance. The most effective results for all methods are highlighted in bold. An in-depth analysis of the results in Tables 15 and 16 reveals that the proposed TBENet method surpasses the other twenty methods in all six evaluation indexes, as shown by the bolded minimum values. Furthermore, Tables 15 and 16 provide a quantitative overview of how different methods measure up against specific evaluation indices, shedding light on the distinct predictive capabilities of each method. Given these results, the TBENet model, with its superior performance metrics, is strongly recommended for future STP in both manned and unmanned vessels.

For the test data in the Zhoushan water area, three characteristic trajectories are chosen to be predicted using 15 experimental approaches. Fig. 9 illustrates the differences in these trajectories, utilising a three-tier zoom-in method for clarity. The results show that the trajectory predicted by the TBENet model closely matches the actual trajectory, demonstrating its enhanced predictive accuracy over the other fifteen methods evaluated.

5.4.3. Visualisation analysis in the Chengshan Jiao water area

Similar to the comparison in Secs. 5.4.1 and 5.4.2, the prediction errors of twenty-one different methods are listed in Tables 17 and 18 across nine test trajectories in the Chengshan Jiao water area. The nine selected trajectories numbered 1–9 are associated with the following MMSI numbers: 241407000, 241408000, 249020000, 353816000, 412362000, 412536000, 412550870, 412551020, and 413115000. The bolded minimum values signify the best predictive performance among the twenty-one methods in Tables 17 and 18. Through a comprehensive analysis of the results presented in Tables 17 and 18, it is clear that the TBENet method surpasses the other twenty methods in terms of prediction performance across all six evaluation indexes, as denoted by the bolded minimum values. Furthermore, the comparison results provide valuable quantitative insights into the relative advantages of different methods concerning specific evaluation indexes, thereby showcasing the distinct strengths of each method in predicting ship trajectories. Considering these results, the TBENet model demonstrates superior performance and is strongly recommended for future STP tasks, applicable to both manned and unmanned ship scenarios.

Three representative trajectories with different patterns in the Chengshan Jiao water are selected to be predicted by 15 experimental methods. The differences in the prediction performance of different models are shown in Fig. 10 (a)–(c). The variations between the predicted trajectories obtained from other methods are highlighted by visually analysing the enlarged views of the three trajectories. Notably, the brown trajectory predicted by the proposed TBENet model exhibits the best performance (i.e., the smallest error) among the predicted trajectories.

5.5. Prediction performance analysis and ablation experimental analysis

The TBENet's performance is primarily assessed through the downward trends of the loss function curves in three distinct water areas, as depicted in Fig. 11, along with ablation experiment analyses. These curves consistently show a decreasing pattern. Leveraging the advantages of the Pytorch framework, the model exhibits rapid learning in the initial training stages. Following this, the loss values for both training and validation sets continue declining, highlighting the model's proficiency in capturing complex data patterns. Eventually, the gap between the training and validation set losses narrows, indicating the model has the strongest ability to fit unknown data.

The impact of different combinations of two bidirectional network units is fully taken into account to conduct the ablation experiments. Furthermore, since the TBENet method (i.e., ABA) integrates two bidirectional networks, the various other network combinations serve as the foundation for a comprehensive ablation experiment. The error metrics for these combinations (i.e., AAA, ABB, BBA, BAA, BBB, and ABAB) in the ablation experiment are detailed in Tables 14, 16, and 18. However, their predictive outcomes still fall short of the TBENet model's performance. Therefore, the prediction results fully demonstrate the effectiveness of the proposed TBENet model. In addition, the loss decrease curves indicate no substantial overfitting issues. The extensive ablation experiments further confirm the efficacy of the proposed TBENet model.



23

Fig. 9. The comparison of predicted and actual trajectories with 15 prediction methods in the Zhoushan water area, (a) the results for MMSI 412764670, (b) the results for MMSI 413438520, (c) the results for MMSI 538007727.

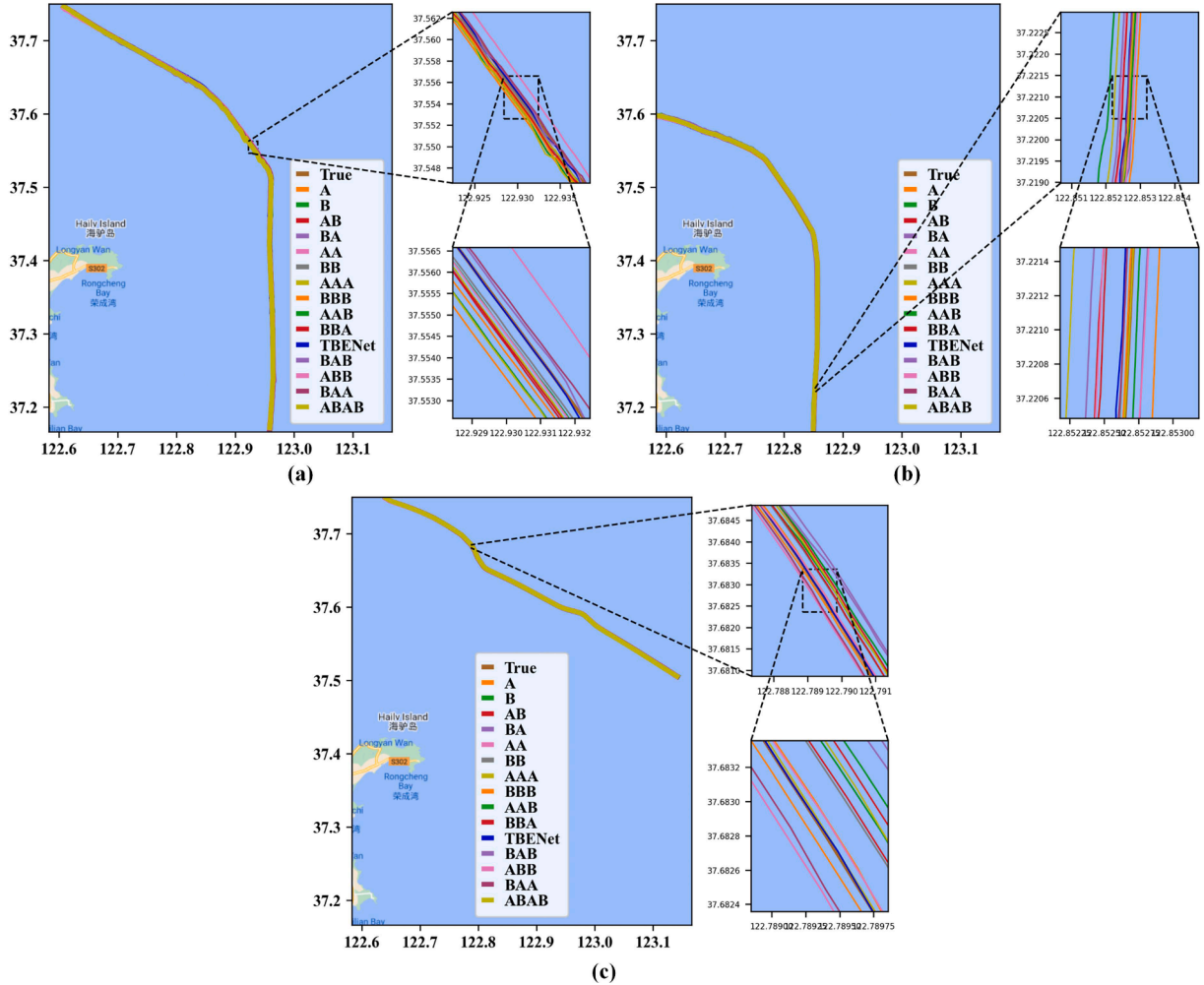


Fig. 10. The comparison of predicted and actual trajectories with 15 prediction methods in the Chengshan Jiao water area, (a) the results for MMSI 412362000, (b) the results for MMSI 412550870, (c) the results for MMSI 413115000.

5.6. Quantitative evaluation

The improved prediction accuracy results of twenty-one models in three water areas are presented in Fig. 12 and Fig. 13. 'A' and 'B' represent the baseline models BiGRU and BiLSTM, respectively. Fig. 12 compares the performance of eight single models. Given the significant differences in performance between single networks and those of BiLSTM and BiGRU, the results in Fig. 12 are shown as multiples indicating either an increase or a decrease. Meanwhile, in Fig. 13, the performance of multi-layer networks is compared to that of BiLSTM and BiGRU and is expressed in terms of percentage improvements. Although different expressions of multiples and percentages are used, they are essentially an overall comparison of the accuracy of the nine trajectories under multiple indicators. The trajectory data from the Zhoushan water area, being simpler and smaller, results in minor differences among the single models, as seen in Fig. 12 (b). Among the single-model comparisons, RNN shows the weakest performance, while GRU stands out as the most effective overall.

In Fig. 13, the TBENet model exhibits significant improvements in prediction accuracy on test trajectories, with average percentage enhancements ranging between 22.97 % and 64.11 % across the three water areas. Notably, the results in the Caofeidian water area demonstrate the most consistent improvements, likely due to the quality and complexity of the original port area trajectories. Moreover, the combined model results from AAB (BiGRU-BiGRU-BiLSTM) and ABAB (BiGRU-BiLSTM-BiGRU-BiLSTM) combinations

show moderate performance in all three water areas. This outcome may relate to the depth of the network structure and the specific sequence of model combinations.

Based on the comprehensive analysis of results across the three water areas, the effectiveness of a three-layer model utilising the BiGRU network as the first layer surpasses that of two-layer and multi-layer models. This is primarily attributed to the BiGRU network's efficacy in capturing short-term features. Furthermore, the proposed TBENet model exhibits approximately a 30 % increase in prediction accuracy compared to the two-layer model, which is solely considering BiGRU and BiLSTM. This further underscores the importance of integrating short-term and long-term information. The results in the [Figs. 12-13](#) provide robust evidence of the efficacy of the proposed TBENet model in this paper.

It's essential to take into account that the quality of AIS trajectory data, along with the patterns and complexity of the trajectories, varies among water areas. The TBENet model's validation across these diverse areas demonstrates its robustness and consistency. In

Table 15

The results of six indexes of nine selected trajectories across eight single-layer models in the Zhoushan water area.

	Criteria	RNN	GRU	LSTM	Transformer	Seq2Seq	BiRNN	BiGRU	BiLSTM
1	MSE	2.3E-06	8.8E-07	7.1E-07	8.0E-07	8.7E-07	2.8E-06	5.8E-07	7.1E-07
	MAE	1.2E-03	5.7E-04	5.2E-04	5.4E-04	5.8E-04	1.2E-03	3.9E-04	4.8E-04
	MAPE	2.5E-03	1.2E-03	1.1E-03	1.5E-03	1.3E-03	1.5E-03	8.0E-04	1.0E-03
	SMAPE	2.5E-03	1.2E-03	1.1E-03	1.5E-03	1.3E-03	1.5E-03	8.0E-04	1.0E-03
	FD	4.2E-02	4.2E-02	4.2E-02	4.3E-02	4.2E-02	9.0E-03	4.2E-02	4.2E-02
	AED	1.9E-03	9.0E-04	7.9E-04	9.0E-04	9.1E-04	2.0E-03	6.0E-04	7.4E-04
2	MSE	1.3E-05	2.4E-05	4.2E-06	2.1E-06	6.5E-06	1.3E-05	1.6E-06	1.9E-06
	MAE	2.3E-03	2.5E-03	1.3E-03	9.2E-04	1.5E-03	3.1E-03	5.3E-04	7.5E-04
	MAPE	3.6E-03	3.7E-03	1.6E-03	1.7E-03	1.8E-03	5.8E-03	7.5E-04	1.1E-03
	SMAPE	3.6E-03	3.7E-03	1.6E-03	1.7E-03	1.8E-03	5.8E-03	7.5E-04	1.1E-03
	FD	9.5E-02	9.4E-02	6.9E-02	5.5E-02	7.3E-02	1.1E-02	5.7E-02	5.5E-02
	AED	3.7E-03	3.9E-03	2.1E-03	1.4E-03	2.7E-03	4.8E-03	8.9E-04	1.2E-03
3	MSE	9.0E-06	3.4E-06	6.2E-07	2.8E-06	1.5E-06	3.1E-06	6.1E-07	1.6E-06
	MAE	2.4E-03	1.2E-03	5.6E-04	1.4E-03	9.5E-04	1.4E-03	6.0E-04	1.1E-03
	MAPE	4.1E-03	2.6E-03	1.2E-03	3.8E-03	2.5E-03	2.0E-03	1.4E-03	2.5E-03
	SMAPE	4.1E-03	2.6E-03	1.2E-03	3.8E-03	2.5E-03	2.0E-03	1.4E-03	2.5E-03
	FD	2.3E-02	2.2E-02	2.1E-02	2.2E-02	2.3E-02	5.8E-03	2.0E-02	2.4E-02
	AED	3.6E-03	1.8E-03	9.2E-04	2.3E-03	1.6E-03	2.2E-03	9.3E-04	1.7E-03
4	MSE	9.0E-06	2.4E-06	1.1E-06	1.9E-06	1.9E-06	8.5E-06	6.9E-07	1.2E-06
	MAE	2.6E-03	9.3E-04	7.9E-04	1.2E-03	1.1E-03	2.6E-03	6.0E-04	8.9E-04
	MAPE	5.2E-03	2.1E-03	1.8E-03	2.7E-03	1.9E-03	4.1E-03	1.3E-03	1.9E-03
	SMAPE	5.2E-03	2.1E-03	1.8E-03	2.7E-03	1.9E-03	4.1E-03	1.3E-03	1.8E-03
	FD	1.7E-02	2.0E-02	1.3E-02	1.1E-02	1.6E-02	1.0E-02	1.2E-02	1.2E-02
	AED	3.7E-03	1.5E-03	1.2E-03	1.8E-03	1.7E-03	3.8E-03	9.2E-04	1.4E-03
5	MSE	8.7E-06	1.6E-06	9.3E-07	1.6E-06	1.6E-06	3.9E-06	7.2E-07	1.1E-06
	MAE	2.2E-03	9.1E-04	6.2E-04	1.0E-03	9.3E-04	1.6E-03	5.4E-04	7.8E-04
	MAPE	3.6E-03	1.8E-03	1.1E-03	2.5E-03	2.2E-03	2.4E-03	1.2E-03	1.5E-03
	SMAPE	3.6E-03	1.8E-03	1.1E-03	2.5E-03	2.2E-03	2.4E-03	1.2E-03	1.5E-03
	FD	3.3E-02	3.2E-02	3.3E-02	3.2E-02	3.1E-02	6.0E-03	3.2E-02	3.2E-02
	AED	3.4E-03	1.4E-03	1.0E-03	1.5E-03	1.4E-03	2.5E-03	8.5E-04	1.2E-03
6	MSE	6.6E-06	2.0E-06	5.2E-07	1.6E-06	1.3E-06	1.3E-06	3.9E-07	1.2E-06
	MAE	1.9E-03	6.9E-04	4.0E-04	8.7E-04	7.2E-04	9.9E-04	3.9E-04	6.3E-04
	MAPE	5.8E-03	2.1E-03	1.2E-03	2.8E-03	2.2E-03	1.4E-03	1.2E-03	1.9E-03
	SMAPE	5.8E-03	2.1E-03	1.2E-03	2.8E-03	2.2E-03	1.4E-03	1.2E-03	1.9E-03
	FD	1.1E-02	1.7E-02	8.9E-03	8.4E-03	8.2E-03	3.1E-03	7.9E-03	9.2E-03
	AED	3.5E-03	1.3E-03	7.1E-04	1.7E-03	1.3E-03	1.5E-03	6.9E-04	1.1E-03
7	MSE	1.2E-06	2.6E-07	6.9E-08	4.8E-07	3.6E-07	1.2E-06	7.5E-08	2.2E-07
	MAE	9.4E-04	3.6E-04	2.3E-04	5.8E-04	4.7E-04	8.2E-04	1.8E-04	3.7E-04
	MAPE	1.7E-03	8.0E-04	3.3E-04	1.5E-03	1.2E-03	1.5E-03	4.2E-04	6.3E-04
	SMAPE	1.7E-03	8.0E-04	3.3E-04	1.5E-03	1.2E-03	1.5E-03	4.2E-04	6.3E-04
	FD	6.3E-03	7.5E-03	6.9E-03	7.2E-03	7.3E-03	6.7E-03	6.9E-03	7.3E-03
	AED	2.6E-03	5.6E-04	2.7E-04	9.0E-04	7.4E-04	1.3E-03	2.8E-04	5.8E-04
8	MSE	8.7E-06	1.6E-06	9.3E-07	1.14E-06	1.6E-06	6.8E-06	1.3E-06	1.9E-06
	MAE	2.2E-03	9.1E-04	6.2E-04	1.0E-03	9.3E-04	2.0E-03	6.5E-04	8.3E-04
	MAPE	3.6E-03	1.8E-03	1.1E-03	2.5E-03	2.2E-03	4.4E-03	1.1E-03	1.3E-03
	SMAPE	3.6E-03	1.8E-03	1.1E-03	2.5E-03	2.2E-03	4.4E-03	1.1E-03	1.3E-03
	FD	3.3E-02	3.2E-02	3.3E-02	3.2E-02	3.1E-02	1.2E-02	3.1E-02	3.6E-02
	AED	3.4E-03	1.4E-03	1.0E-03	1.5E-03	1.4E-03	3.3E-03	1.1E-03	1.3E-03
9	MSE	1.0E-05	3.5E-06	1.7E-06	2.8E-06	2.9E-06	1.6E-06	1.3E-06	1.8E-06
	MAE	2.7E-03	1.0E-03	8.2E-04	1.2E-03	1.0E-03	1.1E-03	6.0E-04	9.1E-04
	MAPE	6.1E-03	2.5E-03	2.0E-03	3.1E-03	2.2E-03	1.8E-03	1.4E-03	2.0E-03
	SMAPE	6.1E-03	2.5E-03	2.0E-03	3.1E-03	2.2E-03	1.8E-03	1.4E-03	2.0E-03
	FD	5.7E-02	5.6E-02	5.6E-02	5.6E-02	5.8E-02	6.5E-03	5.5E-02	5.6E-02
	AED	3.9E-03	1.7E-03	1.3E-03	1.9E-03	1.6E-03	1.6E-03	9.4E-04	1.4E-03

Table 16

The results of six indexes of nine selected trajectories across 13 multilayer models in the Zhoushan water area (A denotes BiGRU, and B indicates BiLSTM).

	Criteria	AB	BA	AA	BB	AAA	BBB	AAB	BBA	TBNet	BAB	ABB	BAA	ABAB
1	MSE	6.3E-07	6.3E-07	6.1E-07	6.3E-07	5.3E-07	1.1E-06	1.6E-06	5.7E-07	4.8E-07	4.9E-07	8.1E-07	5.8E-07	2.5E-06
	MAE	4.2E-04	4.4E-04	4.2E-04	4.5E-04	3.5E-04	7.6E-04	8.5E-04	3.7E-04	2.7E-04	2.9E-04	5.7E-04	3.8E-04	1.1E-03
	MAPE	1.1E-03	9.5E-04	7.7E-04	1.1E-03	8.1E-04	1.6E-03	2.1E-03	8.9E-04	5.6E-04	6.3E-04	1.5E-03	8.3E-04	2.6E-03
	SMAPE	1.1E-03	9.5E-04	7.7E-04	1.1E-03	8.1E-04	1.6E-03	2.1E-03	8.9E-04	5.6E-04	6.3E-04	1.5E-03	8.3E-04	2.6E-03
	FD	4.2E-02	4.3E-02	4.2E-02	4.2E-02	4.2E-02	4.7E-02	4.2E-02	4.9E-02	4.1E-02	4.2E-02	4.2E-02	4.3E-02	4.8E-02
	AED	6.7E-04	6.6E-04	6.5E-04	7.2E-04	5.5E-04	1.2E-03	1.3E-03	5.8E-04	4.2E-04	4.5E-04	9.3E-04	5.9E-04	1.8E-03
2	MSE	1.5E-06	1.5E-06	1.9E-06	2.0E-06	2.0E-06	3.7E-06	2.7E-06	2.0E-06	1.4E-06	1.5E-06	2.1E-06	1.5E-06	1.1E-05
	MAE	4.4E-04	5.5E-04	7.5E-04	7.8E-04	7.1E-04	1.3E-03	9.0E-04	7.5E-04	4.3E-04	4.5E-04	9.5E-04	4.9E-04	2.1E-03
	MAPE	9.1E-04	9.4E-04	1.1E-03	1.3E-03	1.2E-03	2.0E-03	1.4E-03	1.4E-03	6.2E-04	8.0E-04	1.8E-03	7.1E-04	2.8E-03
	SMAPE	9.1E-04	9.4E-04	1.1E-03	1.3E-03	1.2E-03	2.0E-03	1.4E-03	1.4E-03	6.2E-04	8.0E-04	1.8E-03	7.1E-04	2.8E-03
	FD	5.8E-02	5.6E-02	5.8E-02	5.7E-02	5.7E-02	6.1E-02	6.0E-02	5.7E-02	5.4E-02	5.7E-02	5.6E-02	5.7E-02	7.2E-02
	AED	7.9E-04	8.6E-04	1.3E-03	1.3E-03	1.1E-03	2.1E-03	1.5E-03	1.1E-03	7.1E-04	7.0E-04	1.4E-03	8.1E-04	3.5E-03
3	MSE	1.2E-06	7.5E-07	1.2E-06	4.0E-07	3.8E-07	1.3E-06	2.3E-06	1.2E-06	3.3E-07	7.8E-07	1.1E-06	4.6E-07	3.6E-06
	MAE	8.4E-04	6.8E-04	9.1E-04	4.3E-04	4.3E-04	9.0E-04	1.2E-03	8.0E-04	4.1E-04	6.9E-04	8.0E-04	5.3E-04	1.4E-03
	MAPE	2.3E-03	1.6E-03	2.2E-03	9.6E-04	9.4E-04	1.6E-03	2.9E-03	2.2E-03	8.3E-04	1.7E-03	2.0E-03	1.1E-03	3.6E-03
	SMAPE	2.3E-03	1.6E-03	2.2E-03	9.6E-04	9.4E-04	1.6E-03	2.9E-03	2.2E-03	8.3E-04	1.7E-03	2.0E-03	1.1E-03	3.6E-03
	FD	2.1E-02	2.2E-02	2.1E-02	2.1E-02	2.1E-02	2.1E-02	2.3E-02	2.2E-02	2.1E-02	2.1E-02	2.9E-02	2.1E-02	2.6E-02
	AED	1.4E-03	1.1E-03	1.5E-03	6.9E-04	6.8E-04	1.4E-03	1.9E-03	1.3E-03	6.3E-04	1.1E-03	1.3E-03	8.1E-04	2.2E-03
4	MSE	8.6E-07	7.1E-07	1.2E-06	5.4E-07	5.3E-07	1.2E-06	2.1E-06	9.2E-07	5.0E-07	6.2E-07	1.1E-06	5.9E-07	3.7E-06
	MAE	6.7E-04	6.0E-04	8.5E-04	4.6E-04	4.6E-04	8.5E-04	1.1E-03	6.9E-04	4.4E-04	5.3E-04	7.9E-04	5.0E-04	1.5E-03
	MAPE	1.7E-03	1.3E-03	1.7E-03	8.8E-04	9.3E-04	1.6E-03	2.5E-03	1.6E-03	8.7E-04	1.2E-03	1.8E-03	1.0E-03	3.5E-03
	SMAPE	1.7E-03	1.3E-03	1.7E-03	8.8E-04	9.3E-04	1.6E-03	2.5E-03	1.6E-03	8.7E-04	1.2E-03	1.8E-03	1.0E-03	3.5E-03
	FD	1.2E-02	1.1E-02	1.1E-02	1.1E-02	1.1E-02	1.1E-02	1.1E-02	1.2E-02	1.0E-02	1.1E-02	1.2E-02	1.1E-02	1.7E-02
	AED	1.1E-03	9.4E-04	1.3E-03	6.9E-04	7.2E-04	1.3E-03	1.7E-03	1.1E-03	6.6E-04	8.3E-04	1.3E-03	8.0E-04	2.4E-03
5	MSE	7.9E-07	6.6E-07	1.0E-06	5.8E-07	5.5E-07	1.4E-06	2.4E-06	6.7E-07	5.1E-07	6.3E-07	8.0E-07	6.1E-07	2.3E-06
	MAE	5.6E-04	4.8E-04	7.1E-04	4.1E-04	3.6E-04	8.6E-04	1.1E-03	4.8E-04	3.1E-04	4.7E-04	5.4E-04	4.4E-04	1.1E-03
	MAPE	1.3E-03	9.5E-04	1.3E-03	7.7E-04	6.2E-04	1.3E-03	2.3E-03	1.1E-03	5.8E-04	1.0E-03	1.1E-03	9.0E-04	2.8E-03
	SMAPE	1.3E-03	9.5E-04	1.3E-03	7.7E-04	6.2E-04	1.3E-03	2.3E-03	1.1E-03	5.8E-04	1.0E-03	1.1E-03	9.0E-04	2.8E-03
	FD	3.2E-02	3.2E-02	3.3E-02	3.2E-02	3.2E-02	3.4E-02	3.4E-02	3.2E-02	3.1E-02	3.2E-02	3.2E-02	3.2E-02	3.3E-02
	AED	8.8E-04	7.7E-04	1.1E-03	6.4E-04	5.6E-04	1.4E-03	1.7E-03	7.5E-04	5.0E-04	7.2E-04	8.6E-04	6.9E-04	1.8E-03
6	MSE	8.9E-07	4.3E-07	5.5E-07	4.0E-07	3.6E-07	1.3E-06	4.1E-06	9.2E-07	2.6E-07	4.6E-07	9.3E-07	5.9E-07	3.2E-06
	MAE	6.3E-04	4.1E-04	4.6E-04	3.5E-04	3.2E-04	7.7E-04	1.2E-03	5.1E-04	2.7E-04	4.0E-04	5.5E-04	4.8E-04	1.1E-03
	MAPE	2.0E-03	1.2E-03	1.4E-03	1.1E-03	9.6E-04	2.4E-03	3.7E-03	1.6E-03	7.9E-04	1.2E-03	1.7E-03	1.5E-03	3.4E-03

(continued on next page)

Table 16 (continued)

	Criteria	AB	BA	AA	BB	AAA	BBB	AAB	BBA	TBENet	BAB	ABB	BAA	ABAB
7	SMAPE	2.0E-03	1.2E-03	1.4E-03	1.1E-03	9.6E-04	2.4E-03	3.7E-03	1.6E-03	7.9E-04	1.2E-03	1.7E-03	1.5E-03	3.4E-03
	FD	7.8E-03	7.5E-03	7.3E-03	7.9E-03	7.4E-03	8.8E-03	7.7E-03	9.4E-03	7.3E-03	7.3E-03	8.8E-03	7.3E-03	7.5E-03
	AED	1.2E-03	7.1E-04	8.3E-04	6.5E-04	5.8E-04	1.4E-03	2.2E-03	9.6E-04	4.8E-04	7.2E-04	1.0E-03	8.9E-04	2.1E-03
	MSE	1.7E-07	7.1E-08	1.7E-07	8.5E-08	7.9E-08	2.0E-07	1.8E-07	1.0E-07	6.8E-08	1.2E-07	2.3E-07	7.2E-08	6.9E-07
	MAE	3.0E-04	1.61E-04	3.0E-04	2.0E-04	1.8E-04	3.6E-04	3.1E-04	1.8E-04	1.59E-04	2.2E-04	3.8E-04	1.7E-04	6.1E-04
	MAPE	8.4E-04	3.5E-04	8.0E-04	4.6E-04	4.0E-04	6.7E-04	7.3E-04	4.2E-04	3.2E-04	5.9E-04	8.5E-04	3.5E-04	1.6E-03
	SMAPE	8.4E-04	3.5E-04	8.0E-04	4.6E-04	4.0E-04	6.7E-04	7.3E-04	4.2E-04	3.2E-04	5.9E-04	8.5E-04	3.5E-04	1.6E-03
	FD	7.0E-03	7.1E-03	7.1E-03	6.7E-03	7.0E-03	7.1E-03	6.9E-03	7.1E-03	5.9E-03	6.9E-03	6.5E-03	7.1E-03	7.5E-03
	AED	5.0E-04	2.5E-04	5.2E-04	3.1E-04	2.9E-04	5.6E-04	4.9E-04	2.9E-04	2.4E-04	3.7E-04	6.1E-04	2.7E-04	9.8E-04
	MSE	8.8E-07	1.8E-06	1.8E-06	9.2E-07	1.6E-06	2.6E-06	4.4E-06	1.8E-06	1.13E-07	8.6E-07	1.2E-06	1.0E-06	9.3E-06
	MAE	4.9E-04	8.4E-04	8.9E-04	5.4E-04	7.3E-04	1.0E-03	1.7E-03	8.6E-04	4.1E-04	4.6E-04	6.7E-04	6.2E-04	2.1E-03
	MAPE	8.1E-04	1.2E-03	1.2E-03	1.0E-03	9.3E-04	1.3E-03	2.7E-03	1.5E-03	8.0E-04	8.5E-04	1.0E-03	1.0E-03	2.8E-03
	SMAPE	8.1E-04	1.2E-03	1.2E-03	1.0E-03	9.3E-04	1.3E-03	2.7E-03	1.5E-03	8.0E-04	8.5E-04	1.0E-03	1.0E-03	2.8E-03
8	FD	3.2E-02	3.3E-02	3.1E-02	3.3E-02	3.1E-02	3.2E-02	3.3E-02	3.8E-02	3.0E-02	3.1E-02	3.6E-02	3.1E-02	5.5E-02
	AED	7.9E-03	1.4E-03	1.5E-03	1.6E-03	1.3E-03	1.8E-03	2.7E-03	1.4E-03	1.01E-03	1.6E-04	1.1E-03	1.03E-03	3.5E-03
	MSE	1.6E-06	1.3E-06	1.6E-06	1.1E-06	1.0E-06	1.5E-06	2.3E-06	1.6E-06	9.2E-07	1.2E-06	1.7E-06	1.2E-06	5.5E-06
	MAE	7.5E-04	6.0E-04	8.1E-04	4.6E-04	4.8E-04	7.9E-04	9.6E-04	7.3E-04	4.4E-04	5.6E-04	7.8E-04	5.1E-04	1.6E-03
	MAPE	2.0E-03	1.4E-03	1.9E-03	1.1E-03	1.0E-03	1.7E-03	2.4E-03	1.9E-03	9.6E-04	1.4E-03	2.0E-03	1.1E-03	4.2E-03
	SMAPE	2.0E-03	1.4E-03	1.9E-03	1.1E-03	1.0E-03	1.7E-03	2.4E-03	1.9E-03	9.6E-04	1.4E-03	2.0E-03	1.1E-03	4.2E-03
	FD	5.5E-02	5.6E-02	5.4E-02	5.6E-02	5.5E-02	5.5E-02	5.4E-02	5.6E-02	5.1E-02	5.6E-02	5.5E-02	5.5E-02	5.7E-02
	AED	1.3E-03	9.7E-04	1.3E-03	7.3E-04	7.4E-04	1.2E-03	1.5E-03	1.2E-03	6.7E-04	9.2E-04	1.3E-03	8.3E-04	2.7E-03

terms of both accuracy and stability, the prediction performance of the proposed TBENet model surpasses those of other models, as evidenced by the aggregated lift-average statistics from different test sets across the three water areas.

5.7. Discussion and implications

STP task addressed in this paper involves the prediction of ship movement latitude and longitude data for the next time node in the future based on the combination of four consecutive time nodes' latitude and longitude data from the past. The proposed TBENet model effectively utilises the strengths of both BiGRU and BiLSTM to enhance short-term prediction results. Through comparative experiments conducted in three distinct water regions, the TBENet model achieved the best prediction performance.

Compared to using only BiLSTM or BiGRU, the proposed TBENet structure demonstrates improved prediction performance by effectively capturing long-term dependencies and short-term changes in the time series data. On the other hand, the combination of two BiGRU or BiLSTM networks, although increasing network depth, may lead to gradient vanishing or exploding issues, resulting in inferior prediction results. In contrast, the TBENet's configuration, with a combination of BiGRU and BiLSTM followed by another BiGRU unit, leverages cross-layer connections to pass down information learned from the previous two network layers, further enhancing prediction accuracy. This design is particularly suitable for short-term prediction tasks. It is important to note that the superiority of different combinatorial models may vary depending on specific application scenarios. Decisions regarding model complexity, specific trajectory prediction tasks, and the allocation of computational resources and time should be made based on the particular requirements and constraints of the application at hand.

Meantime, the findings of this new TBENet model for STP provide valuable guidance for different stakeholders involved in maritime traffic management, emergency response, and the development of autonomous navigation technology.

(1) The TBENet model exhibits higher accuracy and precision, enabling more accurate prediction of ship trajectories. This is an important finding for various stakeholders, such as maritime traffic management organisations, port operators, and shipping

Table 17

The results of six indexes of nine selected trajectories across eight single-layer models in the Chengshan Jiao water area.

	Criteria	RNN	GRU	LSTM	Transformer	Seq2Seq	BiRNN	BiGRU	BiLSTM
1	MSE	5.9E-05	2.6E-05	5.6E-06	7.9E-06	5.6E-06	2.1E-06	1.2E-07	1.8E-07
	MAE	4.8E-03	4.5E-03	2.0E-03	2.5E-03	2.0E-03	1.1E-03	2.1E-04	2.8E-04
	MAPE	6.7E-03	6.6E-03	2.9E-03	3.6E-03	2.9E-03	1.5E-03	2.8E-04	4.6E-04
	SMAPE	6.7E-03	6.6E-03	2.9E-03	3.6E-03	2.9E-03	1.5E-03	2.8E-04	4.6E-04
	FD	3.9E-02	1.9E-02	2.0E-02	8.1E-03	2.0E-02	9.4E-03	7.7E-03	7.1E-03
	AED	7.5E-03	6.7E-03	3.1E-03	3.8E-03	3.1E-03	1.8E-03	3.4E-04	4.4E-04
2	MSE	1.1E-05	9.9E-06	2.4E-06	6.2E-06	2.4E-06	1.1E-05	7.6E-07	1.4E-06
	MAE	2.9E-03	2.8E-03	1.5E-03	2.3E-03	1.5E-03	2.7E-03	5.9E-04	9.1E-04
	MAPE	4.0E-03	4.0E-03	2.2E-03	3.4E-03	2.2E-03	5.3E-03	1.0E-03	1.8E-03
	SMAPE	4.0E-03	4.0E-03	2.2E-03	3.4E-03	2.2E-03	5.3E-03	1.0E-03	1.8E-03
	FD	1.0E-02	1.2E-02	3.8E-02	5.3E-02	3.8E-02	1.1E-02	6.4E-03	6.6E-03
	AED	4.4E-03	4.2E-03	2.2E-03	3.5E-03	2.2E-03	4.4E-03	9.6E-04	1.4E-03
3	MSE	3.6E-05	1.7E-05	4.2E-06	1.1E-05	4.2E-06	2.7E-06	1.5E-07	5.8E-08
	MAE	4.6E-03	3.4E-03	1.8E-03	3.0E-03	1.8E-03	1.4E-03	2.8E-04	1.5E-04
	MAPE	5.8E-03	4.5E-03	2.5E-03	4.2E-03	2.5E-03	2.1E-03	2.9E-04	1.9E-04
	SMAPE	5.8E-03	4.5E-03	2.5E-03	4.2E-03	2.5E-03	2.1E-03	2.9E-04	1.9E-04
	FD	2.3E-02	2.7E-02	1.3E-02	1.4E-02	1.3E-02	4.9E-03	2.6E-03	1.9E-03
	AED	7.4E-03	5.3E-03	2.7E-03	4.6E-03	2.7E-03	2.1E-03	4.9E-04	2.4E-04
4	MSE	4.7E-05	2.0E-05	4.4E-06	6.3E-06	4.4E-06	8.1E-06	8.0E-07	7.8E-07
	MAE	4.3E-03	3.9E-03	1.8E-03	2.2E-03	1.8E-03	2.6E-03	5.4E-04	5.3E-04
	MAPE	5.5E-03	5.5E-03	2.4E-03	3.0E-03	2.4E-03	4.2E-03	8.4E-04	8.4E-04
	SMAPE	5.5E-03	5.5E-03	2.4E-03	3.0E-03	2.4E-03	4.2E-03	8.4E-04	8.4E-04
	FD	3.2E-02	1.5E-02	1.6E-02	7.4E-03	1.6E-02	1.1E-02	8.1E-03	7.7E-03
	AED	7.0E-03	6.0E-03	2.8E-03	3.4E-03	2.8E-03	3.7E-03	7.8E-04	8.1E-04
5	MSE	3.8E-05	4.9E-05	1.6E-05	3.2E-05	1.6E-05	3.4E-06	1.9E-07	6.0E-08
	MAE	5.3E-03	6.5E-03	3.6E-03	5.2E-03	3.6E-03	1.6E-03	3.2E-04	1.7E-04
	MAPE	8.4E-03	1.0E-02	5.7E-03	8.2E-03	5.7E-03	2.5E-03	3.4E-04	2.5E-04
	SMAPE	8.4E-03	1.0E-02	5.7E-03	8.2E-03	5.7E-03	2.5E-03	3.4E-04	2.5E-04
	FD	1.7E-02	2.0E-02	1.5E-02	1.6E-02	1.5E-02	5.0E-03	1.9E-03	1.4E-03
	AED	7.6E-03	9.3E-03	5.2E-03	7.5E-03	5.2E-03	2.1E-03	5.7E-04	2.8E-04
6	MSE	8.1E-05	2.0E-05	6.1E-06	1.0E-05	6.1E-06	1.1E-06	3.1E-08	6.2E-08
	MAE	6.7E-03	3.7E-03	2.2E-03	2.7E-03	2.2E-03	9.0E-04	1.2E-04	2.0E-04
	MAPE	1.0E-02	6.1E-03	4.3E-03	5.2E-03	4.3E-03	1.4E-03	1.8E-04	3.3E-04
	SMAPE	1.0E-02	6.1E-03	4.3E-03	5.2E-03	4.3E-03	1.4E-03	1.8E-04	3.3E-04
	FD	3.4E-02	3.7E-02	8.3E-03	1.0E-02	8.3E-03	2.9E-03	1.3E-03	1.4E-03
	AED	1.1E-02	5.6E-03	3.4E-03	4.5E-03	3.4E-03	1.4E-03	1.8E-04	3.0E-04
7	MSE	9.8E-05	4.7E-05	7.7E-06	1.6E-05	7.7E-06	1.7E-06	2.9E-07	2.2E-07
	MAE	7.6E-03	5.8E-03	2.3E-03	3.1E-03	2.3E-03	9.9E-04	4.2E-04	3.2E-04
	MAPE	1.7E-02	1.2E-02	4.5E-03	6.5E-03	4.5E-03	2.1E-03	8.4E-04	6.6E-04
	SMAPE	1.7E-02	1.2E-02	4.5E-03	6.5E-03	4.5E-03	2.1E-03	8.4E-04	6.6E-04
	FD	3.0E-02	2.5E-02	1.4E-02	1.5E-02	1.4E-02	7.1E-03	6.4E-03	6.5E-03
	AED	1.3E-02	9.2E-03	3.4E-03	4.8E-03	3.4E-03	1.6E-03	6.5E-04	5.4E-04
8	MSE	7.4E-05	4.1E-05	6.9E-06	1.1E-05	6.9E-06	6.5E-06	3.4E-07	5.9E-07
	MAE	6.5E-03	5.4E-03	2.4E-03	2.7E-03	2.4E-03	1.9E-03	3.4E-04	5.5E-04
	MAPE	8.6E-03	8.1E-03	4.3E-03	5.0E-03	4.3E-03	4.2E-03	6.5E-04	1.2E-03
	SMAPE	8.6E-03	8.1E-03	4.3E-03	5.0E-03	4.3E-03	4.2E-03	6.5E-04	1.2E-03
	FD	2.5E-02	2.8E-02	1.0E-02	1.2E-02	1.0E-02	1.2E-02	6.8E-03	6.4E-03
	AED	1.1E-02	8.2E-03	3.5E-03	4.6E-03	3.5E-03	3.1E-03	5.2E-04	8.7E-04
9	MSE	1.5E-04	7.9E-05	1.6E-05	3.3E-05	1.6E-05	2.0E-06	2.8E-07	2.4E-07
	MAE	9.9E-03	7.8E-03	3.5E-03	4.8E-03	3.5E-03	1.2E-03	4.3E-04	3.1E-04
	MAPE	2.0E-02	1.3E-02	6.1E-03	9.4E-03	6.1E-03	2.3E-03	8.0E-04	5.9E-04
	SMAPE	2.0E-02	1.3E-02	6.1E-03	9.4E-03	6.1E-03	2.3E-03	8.0E-04	5.9E-04
	FD	4.3E-02	2.8E-02	1.4E-02	1.6E-02	1.4E-02	7.2E-03	3.5E-03	3.5E-03
	AED	1.5E-02	1.2E-02	5.3E-03	7.6E-03	5.3E-03	1.8E-03	6.6E-04	5.2E-04

Table 18

The results of six indexes for nine selected trajectories across 13 multilayer models in the Chengshan Jiao water area (A denotes BiGRU, and B indicates BiLSTM).

	Criteria	AB	BA	AA	BB	AAA	BBB	AAB	BBA	TBENet	BAB	ABB	BAA	ABAB
1	MSE	1.7E-07	3.1E-07	1.2E-07	1.2E-07	1.2E-07	1.2E-07	1.2E-07	1.1E-07	1.0E-07	2.4E-07	1.6E-07	2.0E-07	2.7E-07
	MAE	2.7E-04	3.6E-04	2.0E-04	1.9E-04	1.9E-04	1.9E-04	2.1E-04	1.6E-04	1.5E-04	3.4E-04	2.5E-04	2.9E-04	3.8E-04
	MAPE	3.5E-04	4.8E-04	3.1E-04	2.6E-04	2.5E-04	2.7E-04	3.0E-04	2.3E-04	2.2E-04	4.5E-04	3.4E-04	4.1E-04	5.4E-04
	SMAPE	3.5E-04	4.8E-04	3.1E-04	2.6E-04	2.5E-04	2.7E-04	3.0E-04	2.3E-04	2.2E-04	4.5E-04	3.4E-04	4.1E-04	5.4E-04
	FD	7.1E-03	7.9E-03	7.1E-03	7.1E-03	7.3E-03	7.1E-03	7.1E-03	7.2E-03	7.0E-03	7.1E-03	7.3E-03	7.2E-03	7.1E-03
	AED	4.4E-04	6.1E-04	3.2E-04	3.0E-04	2.9E-04	2.9E-04	3.3E-04	2.5E-04	2.1E-04	5.5E-04	4.0E-04	4.4E-04	6.1E-04
2	MSE	8.7E-07	1.8E-06	6.4E-07	6.2E-07	6.2E-07	6.8E-07	1.1E-06	6.5E-07	6.0E-07	1.6E-06	7.1E-07	7.1E-07	7.1E-07
	MAE	6.0E-04	9.3E-04	5.4E-04	4.8E-04	4.5E-04	5.3E-04	7.1E-04	5.0E-04	4.4E-04	9.2E-04	5.3E-04	5.7E-04	6.0E-04
	MAPE	1.2E-03	2.1E-03	1.1E-03	9.2E-04	8.8E-04	1.0E-03	1.5E-03	9.9E-04	8.7E-04	2.0E-03	1.0E-03	1.1E-03	1.1E-03
	SMAPE	1.2E-03	2.1E-03	1.1E-03	9.2E-04	8.8E-04	1.0E-03	1.5E-03	9.9E-04	8.7E-04	2.0E-03	1.0E-03	1.1E-03	1.1E-03
	FD	6.9E-03	7.1E-03	6.1E-03	6.3E-03	6.3E-03	6.2E-03	6.04E-03	6.1E-03	6.01E-03	7.0E-03	6.4E-03	6.7E-03	6.1E-03
	AED	9.8E-04	1.6E-03	8.7E-04	7.8E-04	7.4E-04	8.5E-04	1.2E-03	8.2E-04	7.2E-04	1.5E-03	8.4E-04	9.0E-04	9.5E-04
3	MSE	1.5E-07	4.7E-07	9.0E-08	4.9E-08	3.9E-08	7.2E-08	9.5E-08	4.0E-08	3.8E-08	4.0E-07	1.6E-07	9.4E-08	1.6E-07
	MAE	2.8E-04	5.5E-04	2.2E-04	1.4E-04	1.22E-04	1.9E-04	2.1E-04	1.3E-04	1.21E-04	5.1E-04	2.9E-04	2.5E-04	3.1E-04
	MAPE	3.2E-04	7.9E-04	2.6E-04	1.9E-04	1.7E-04	2.6E-04	3.3E-04	1.9E-04	1.6E-04	7.4E-04	3.4E-04	3.4E-04	4.1E-04
	SMAPE	3.2E-04	7.9E-04	2.6E-04	1.9E-04	1.7E-04	2.6E-04	3.3E-04	1.9E-04	1.6E-04	7.4E-04	3.4E-04	3.4E-04	4.1E-04
	FD	2.1E-03	2.7E-03	2.5E-03	2.3E-03	2.1E-03	2.4E-03	2.4E-03	2.2E-03	2.0E-03	2.7E-03	2.8E-03	2.1E-03	2.8E-03
	AED	4.8E-04	8.3E-04	3.7E-04	2.3E-04	2.9E-04	3.0E-04	3.2E-04	2.1E-04	2.0E-04	8.2E-04	5.0E-04	3.9E-04	5.0E-04
4	MSE	7.8E-07	9.5E-07	7.6E-07	7.5E-07	7.23E-07	7.7E-07	8.6E-07	7.6E-07	7.2E-07	1.0E-06	8.5E-07	7.6E-07	7.3E-07
	MAE	5.4E-04	6.8E-04	5.2E-04	5.3E-04	5.1E-04	5.4E-04	6.0E-04	5.2E-04	5.1E-04	6.9E-04	5.9E-04	5.3E-04	5.3E-04
	MAPE	8.3E-04	1.1E-03	8.2E-04	8.3E-04	8.12E-04	8.6E-04	9.5E-04	8.2E-04	8.10E-04	1.1E-03	9.2E-04	8.4E-04	8.3E-04
	SMAPE	8.3E-04	1.1E-03	8.2E-04	8.3E-04	8.12E-04	8.6E-04	9.5E-04	8.2E-04	8.10E-04	1.1E-03	9.2E-04	8.4E-04	8.3E-04
	FD	7.5E-03	7.6E-03	7.8E-03	7.6E-03	7.7E-03	7.7E-03	7.5E-03	7.6E-03	7.1E-03	7.7E-03	7.5E-03	7.3E-03	7.4E-03
	AED	8.0E-04	1.0E-03	7.6E-04	7.8E-04	7.3E-04	7.8E-04	8.9E-04	7.6E-04	7.0E-04	1.0E-03	9.0E-04	7.7E-04	7.9E-04
5	MSE	1.8E-07	6.0E-07	1.1E-07	6.4E-08	3.6E-08	8.2E-08	1.3E-07	3.8E-08	3.1E-08	4.8E-07	1.9E-07	1.1E-07	2.4E-07
	MAE	3.2E-04	6.6E-04	2.6E-04	1.6E-04	1.3E-04	2.1E-04	2.6E-04	1.4E-04	1.1E-04	5.7E-04	3.3E-04	2.8E-04	3.8E-04
	MAPE	3.8E-04	1.0E-03	3.2E-04	2.1E-04	1.9E-04	3.2E-04	4.2E-04	2.1E-04	1.5E-04	8.6E-04	4.3E-04	3.9E-04	5.0E-04
	SMAPE	3.8E-04	1.0E-03	3.2E-04	2.1E-04	1.9E-04	3.2E-04	4.2E-04	2.1E-04	1.5E-04	8.6E-04	4.3E-04	3.9E-04	5.0E-04
	FD	1.5E-03	2.6E-03	1.6E-03	1.8E-03	1.3E-03	1.8E-03	1.9E-03	1.3E-03	1.1E-03	2.4E-03	1.6E-03	1.3E-03	1.4E-03
	AED	5.4E-04	9.9E-04	4.3E-04	2.8E-04	2.1E-04	3.3E-04	3.9E-04	3.2E-04	2.4E-04	9.2E-04	5.6E-04	4.3E-04	6.2E-04
6	MSE	5.3E-08	7.3E-08	3.2E-08	3.4E-08	3.5E-08	3.4E-08	3.7E-08	3.1E-08	3.0E-08	7.2E-08	4.6E-08	6.0E-08	8.0E-08
	MAE	1.6E-04	1.9E-04	1.2E-04	1.2E-04	1.2E-04	1.1E-04	1.3E-04	1.2E-04	1.1E-04	2.0E-04	1.5E-04	1.7E-04	2.2E-04
	MAPE	2.2E-04	2.6E-04	2.0E-04	1.7E-04	1.7E-04	1.7E-04	1.9E-04	1.50E-04	1.46E-04	2.8E-04	2.1E-04	2.6E-04	3.3E-04

(continued on next page)

Table 18 (continued)

	Criteria	AB	BA	AA	BB	AAA	BBB	AAB	BBA	TBENet	BAB	ABB	BAA	ABAB
7	SMAPE	2.2E-04	2.6E-04	2.0E-04	1.7E-04	1.7E-04	1.7E-04	1.9E-04	1.50E-04	1.46E-04	2.8E-04	2.1E-04	2.6E-04	3.3E-04
	FD	1.4E-03	1.4E-03	1.3E-03	1.3E-03	1.3E-03	1.4E-03	1.3E-03	1.3E-03	1.2E-03	1.5E-03	1.4E-03	1.6E-03	1.5E-03
	AED	2.7E-04	3.1E-04	1.8E-04	1.9E-04	1.8E-04	1.7E-04	2.0E-04	1.6E-04	1.5E-04	3.1E-04	2.3E-04	2.6E-04	3.5E-04
	MSE	1.3E-07	5.6E-07	2.6E-07	1.3E-07	1.7E-07	1.9E-07	3.7E-07	1.5E-07	8.6E-08	4.0E-07	2.2E-07	2.1E-07	2.7E-07
	MAE	2.4E-04	5.8E-04	3.6E-04	2.2E-04	2.7E-04	3.0E-04	4.5E-04	2.4E-04	1.5E-04	4.7E-04	3.4E-04	3.2E-04	3.7E-04
	MAPE	5.3E-04	1.2E-03	8.3E-04	4.5E-04	5.9E-04	6.5E-04	9.9E-04	5.3E-04	3.0E-04	9.5E-04	7.0E-04	6.6E-04	8.2E-04
	SMAPE	5.3E-04	1.2E-03	8.3E-04	4.5E-04	5.9E-04	6.5E-04	9.9E-04	5.3E-04	3.0E-04	9.5E-04	7.0E-04	6.6E-04	8.2E-04
	FD	6.7E-03	6.6E-03	6.5E-03	6.1E-03	6.1E-03	6.1E-03	6.1E-03	6.0E-03	6.0E-03	6.2E-03	6.4E-03	6.5E-03	6.5E-03
	AED	4.0E-04	8.9E-04	6.2E-04	3.6E-04	4.5E-04	5.0E-04	7.4E-04	4.1E-04	2.4E-04	7.7E-04	5.4E-04	5.1E-04	6.2E-04
	MSE	4.1E-07	1.1E-06	3.5E-07	3.3E-07	3.2E-07	3.8E-07	6.7E-07	3.7E-07	3.1E-07	1.0E-06	4.5E-07	4.0E-07	4.0E-07
8	MAE	4.0E-04	7.6E-04	3.8E-04	3.2E-04	2.79E-04	3.6E-04	5.4E-04	3.5E-04	2.76E-04	7.6E-04	3.6E-04	4.1E-04	3.9E-04
	MAPE	8.4E-04	1.8E-03	8.2E-04	6.3E-04	5.8E-04	7.0E-04	1.2E-03	7.4E-04	5.7E-04	1.7E-03	7.5E-04	8.0E-04	7.7E-04
	SMAPE	8.4E-04	1.8E-03	8.2E-04	6.3E-04	5.8E-04	7.0E-04	1.2E-03	7.4E-04	5.7E-04	1.7E-03	7.5E-04	8.0E-04	7.7E-04
	FD	6.9E-03	7.0E-03	6.7E-03	6.6E-03	6.6E-03	6.7E-03	6.7E-03	6.9E-03	6.1E-03	6.5E-03	6.7E-03	6.8E-03	6.4E-03
	AED	6.3E-04	1.4E-03	6.2E-04	4.9E-04	4.32E-04	5.5E-04	9.3E-04	5.6E-04	4.28E-04	1.2E-03	5.7E-04	6.1E-04	6.1E-04
	MSE	1.3E-07	5.2E-07	2.2E-07	1.5E-07	1.8E-07	1.9E-07	3.4E-07	1.7E-07	1.1E-07	4.1E-07	2.1E-07	1.9E-07	2.6E-07
	MAE	2.4E-04	5.4E-04	3.4E-04	2.4E-04	2.8E-04	2.9E-04	4.5E-04	2.6E-04	1.7E-04	4.7E-04	3.2E-04	2.9E-04	3.8E-04
	MAPE	4.6E-04	9.5E-04	7.1E-04	4.5E-04	5.8E-04	6.0E-04	8.7E-04	5.1E-04	3.0E-04	8.9E-04	5.9E-04	5.5E-04	7.8E-04
	SMAPE	4.6E-04	9.5E-04	7.1E-04	4.5E-04	5.8E-04	6.0E-04	8.7E-04	5.1E-04	3.0E-04	8.9E-04	5.9E-04	5.5E-04	7.8E-04
	FD	3.8E-03	4.1E-03	3.3E-03	3.2E-03	3.3E-03	3.3E-03	3.8E-03	3.4E-03	3.0E-03	3.8E-03	3.1E-03	3.2E-03	3.6E-03
9	AED	3.9E-04	8.3E-04	5.6E-04	3.9E-04	4.7E-04	4.8E-04	7.2E-04	4.2E-04	2.8E-04	7.6E-04	5.0E-04	4.6E-04	6.1E-04
		04	04	04	04		04				04	04	04	04

companies. Accurate STP can assist them in better planning ship arrivals and departures, improving traffic safety and transportation efficiency.

(2) The novel model has the potential to generate real-time STP, providing a valuable reference for emergency response, involving maritime rescue organisations, coast guards, and maritime regulatory authorities. Accurate prediction results can aid them in making better decisions, such as dispatching rescue vessels during emergencies or responding to potential safety issues.

(3) The new prediction model may offer significant insights for the development of autonomous navigation technology. Ship manufacturers, autonomous driving system developers, and relevant research institutions can leverage these findings to enhance the design and functionality of autonomous navigation systems. Accurate STP is crucial for achieving reliable autonomous navigation, and the introduction of such a model provides guidance and inspiration for various stakeholders involved in this domain.

Ship prediction research offers a plethora of benefits across diverse sectors. In the maritime industry, it optimises operational efficiency by providing accurate trajectory predictions, facilitating route optimisation, fuel conservation, and scheduling. Port authorities benefit from enhanced resource allocation and traffic management, resulting in reduced congestion and improved port efficiency. For shipping companies, these predictions aid in fleet management, route planning, and risk assessment, minimising delays, optimising cargo handling, and reducing accident risks. Navigation service providers integrate ship prediction models into systems to furnish real-time information and alerts to ship captains, enabling informed decisions and hazard avoidance. Environmental monitoring agencies utilise these models to predict ship movements in sensitive areas, preventing accidents like oil spills and mitigating maritime activities' ecological impacts. Additionally, ship prediction aids search and rescue operations by predicting distressed vessel drift patterns, enhancing search efficiency and rescue success rates.

Furthermore, ship prediction research propels advancements in autonomous navigation systems for unmanned ships. By accurately forecasting ship trajectories, these systems autonomously navigate vessels, revolutionising the maritime industry towards fully autonomous operations. Such innovations promise increased operational efficiency, reduced costs, and heightened safety standards. Integrating prediction models into autonomous systems represents a significant leap in maritime technology, potentially transforming

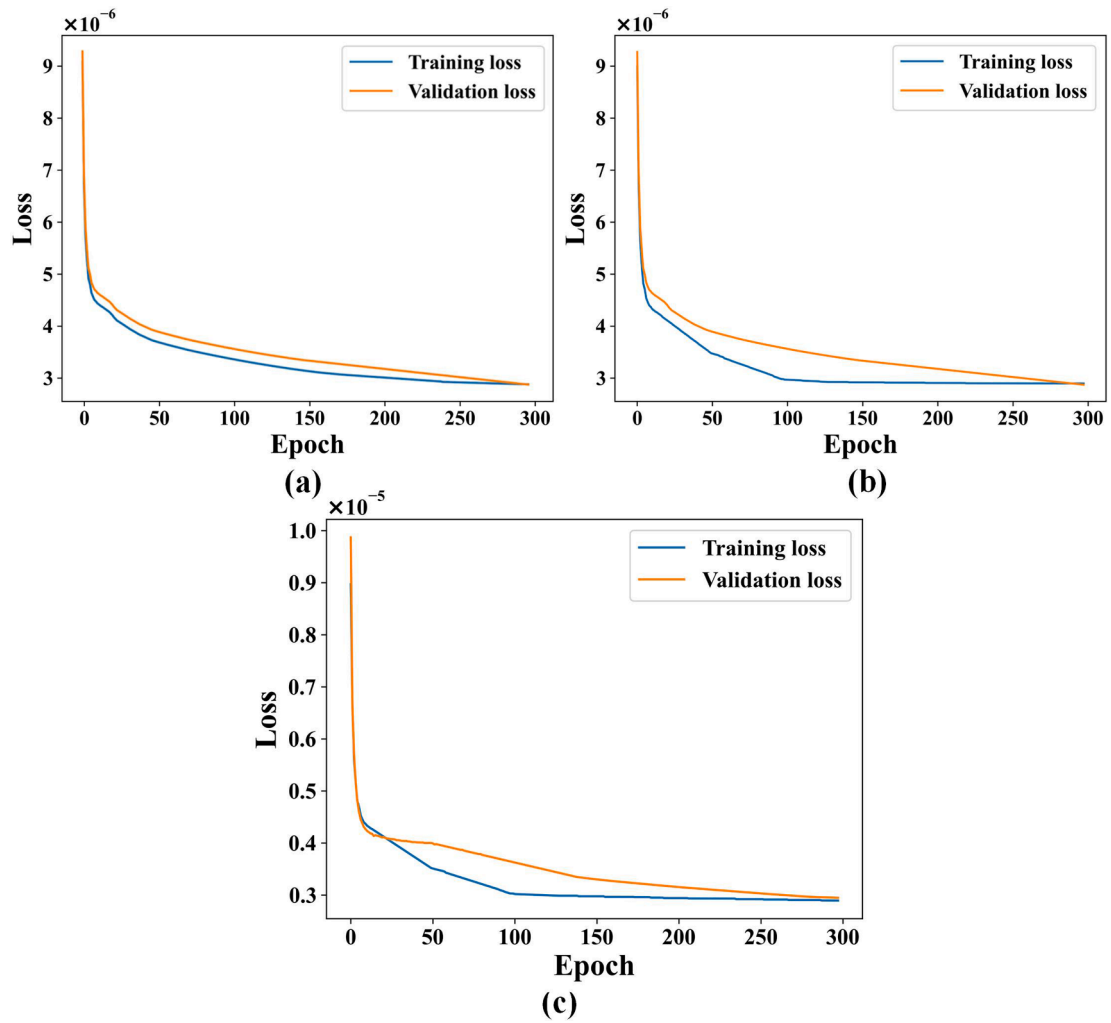
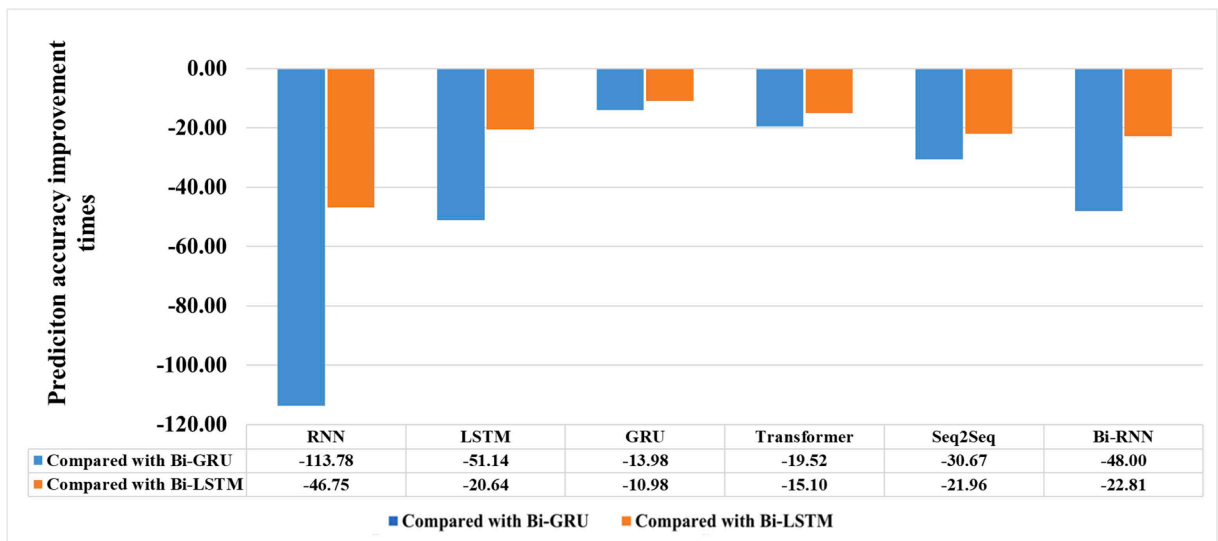
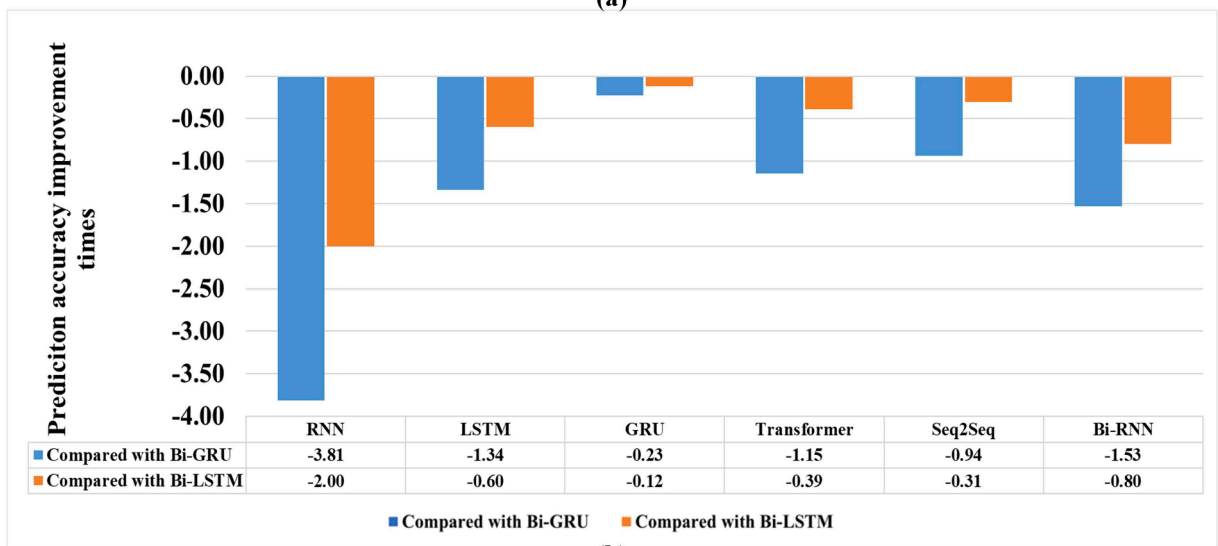


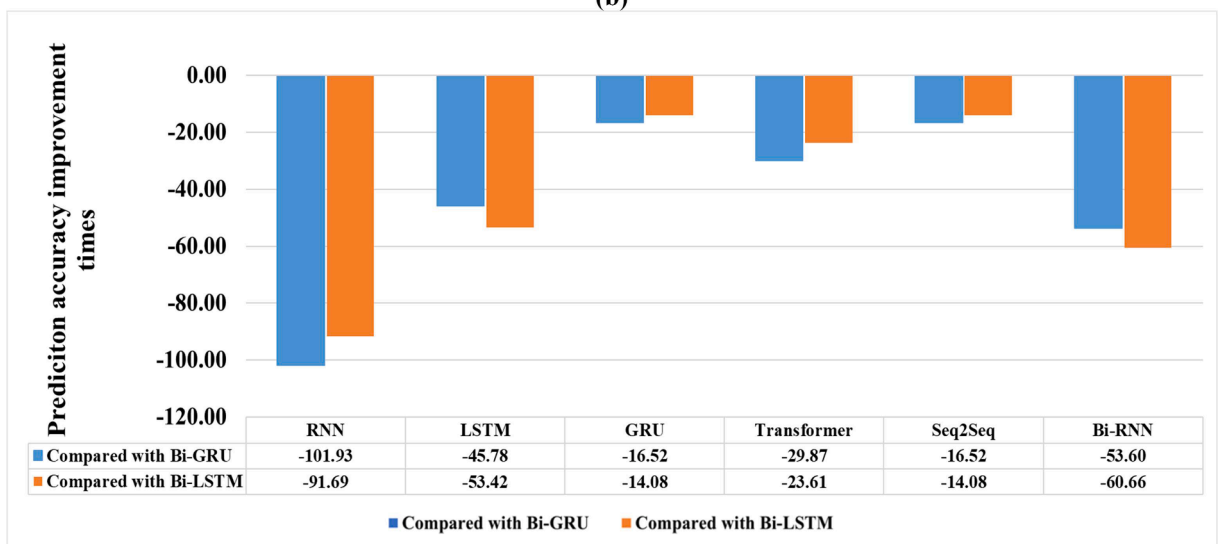
Fig. 11. Visualisation results of loss function descent curve, (a) the result in the Caofeidian water area, (b) the result in the Zhoushan water area, and (c) the result in the Chengshan Jiao water area.



(a)



(b)



(c)

(caption on next page)

Fig. 12. Comparison of the results of all single models for improved prediction accuracy in three water areas, (a) the result in the Caofeidian water area, (b) the result in the Zhoushan water area, (c) the result in the Chengshan Jiao water area (Note: the numbers in this figure denote multiples).

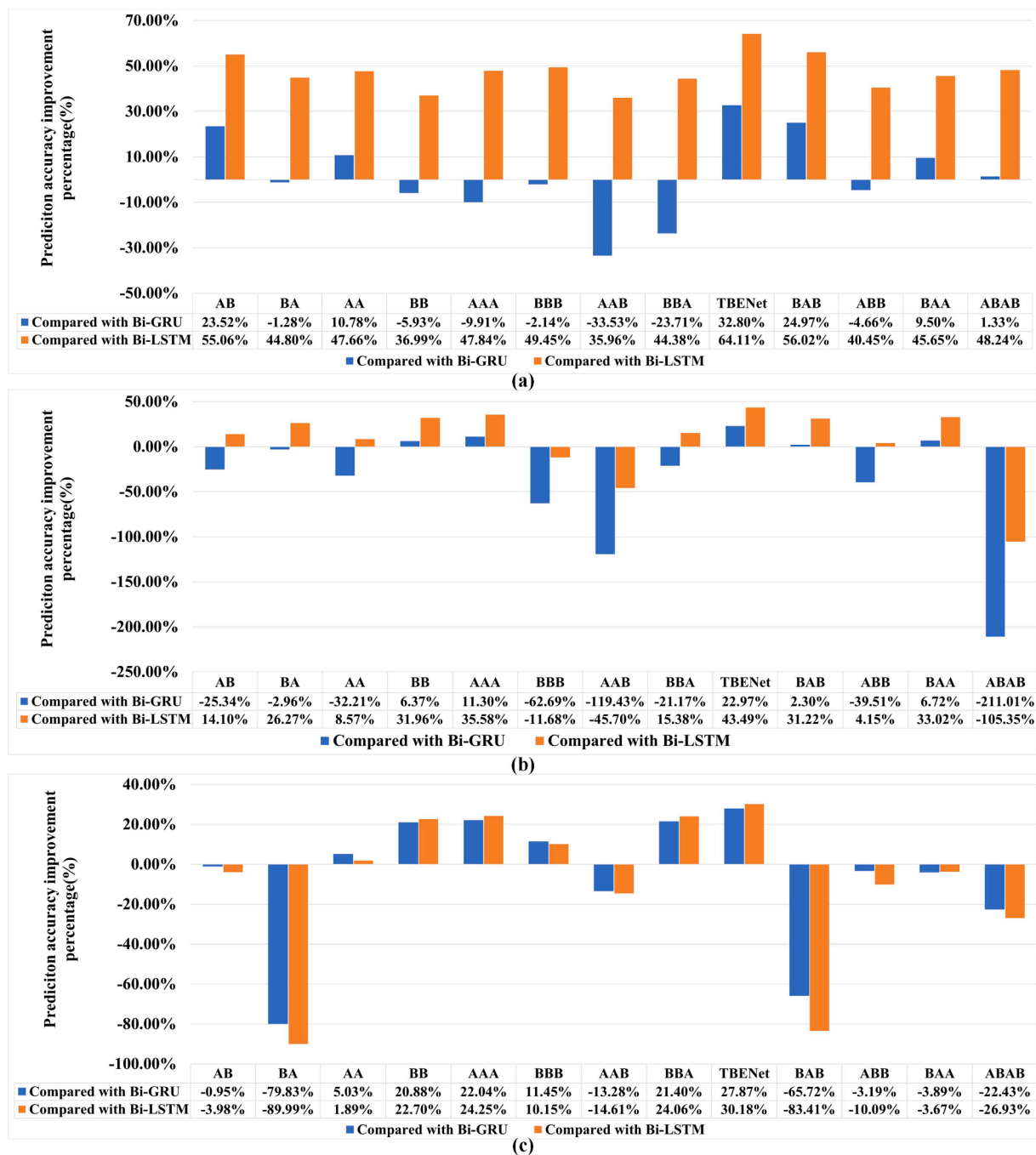


Fig. 13. Comparison of other models' results for improved prediction accuracy in three water areas, (a) the result in the Caofeidian water area, (b) the result in the Zhoushan water area, (c) the result in the Chengshan Jiao water area.

global shipping practices. This underscores the importance of ongoing research in ship prediction, offering not only immediate benefits but also paving the way for future advancements in autonomous shipping technology.

6. Conclusion

STP plays a vital role in enhancing maritime safety and optimising route planning. This paper initiates a comprehensive analysis of the existing literature on STP. Based on this analysis, research gaps and future developmental directions are identified and presented in a targeted manner. Subsequently, the TBENet model is proposed to address the issue of inadequate prediction accuracy in existing methods. It uniquely sequences BiGRU, BiLSTM, and BiGRU to enable accurate short-term prediction of ship trajectories. A thorough comparative experiment is carried out using datasets from three distinct water areas. The effectiveness of the proposed methodology is assessed by comparing it with twenty other prediction models and evaluating it using six distinct metrics. The experimental results demonstrated the superiority of the proposed method in this study. It makes new contributions, including a systematic review, a new prediction model, and a comprehensive experimental analysis. The insights of this study are beneficial for maritime traffic management organisations, port operators, and shipping companies, aiding in better planning and traffic safety enhancement. Additionally, stakeholders in emergency response, such as maritime rescue organisations and coast guards, can leverage real-time STP to make informed decisions and respond effectively. The findings also provide valuable insights for ship manufacturers, autonomous driving system developers, and research institutions to enhance the design and functionality of autonomous navigation systems.

When evaluating various application scenarios, it is crucial to take into account factors such as model complexity, computational resources, time constraints, and the specific requirements of trajectory prediction tasks. Future directions include incorporating supplementary data like speed, course, weather, and sea state into the prediction model alongside geographic information to improve its overall effectiveness. Moreover, techniques like multi-task learning and transfer learning can be explored to enhance the adaptability and generalisation capability of the model, further advancing STP.

CRedit authorship contribution statement

Huanhuan Li: Writing – review & editing, Writing – original draft, Validation, Supervision, Software, Project administration, Methodology, Investigation, Formal analysis, Data curation, Conceptualization. **Wenbin Xing:** Writing – review & editing, Writing – original draft, Visualization, Validation, Software, Investigation, Formal analysis. **Hang Jiao:** Writing – original draft, Visualization, Validation, Investigation, Formal analysis. **Kum Fai Yuen:** Writing – review & editing, Visualization, Validation, Formal analysis. **Ruobin Gao:** Writing – original draft, Visualization, Validation, Formal analysis. **Yan Li:** Visualization, Validation, Investigation, Formal analysis, Data curation. **Christian Matthews:** Writing – review & editing, Visualization, Validation, Formal analysis. **Zaili Yang:** Writing – review & editing, Writing – original draft, Resources, Project administration, Methodology, Funding acquisition.

Declaration of competing interest

The authors declare the following financial interests/personal relationships which may be considered as potential competing interests: Zaili Yang reports financial support was provided by European Research Council.

Acknowledgements

This project has received funding from the European Research Council (ERC) under the European Union's Horizon 2020 research and innovation programme (Grant Agreement No. 864724) and Royal Society International Exchanges 2021 Cost Share (NSFC) (IEC \NSFC\211211).

References

- Abebe, M., Noh, Y., Kang, Y.-J., Seo, C., Kim, D., Seo, J., 2022. Ship trajectory planning for collision avoidance using hybrid ARIMA-LSTM models. *Ocean Eng.* 256, 111527. <https://doi.org/10.1016/j.oceaneng.2022.111527>.
- Alizadeh, D., Alesheikh, A.A., Sharif, M., 2021a. Vessel Trajectory Prediction Using Historical Automatic Identification System Data. *J. Navig.* 74, 156–174. <https://doi.org/10.1017/S0373463320000442>.
- Alizadeh, D., Alesheikh, A.A., Sharif, M., 2021b. Prediction of vessels locations and maritime traffic using similarity measurement of trajectory. *Ann. GIS* 27, 151–162.
- Bai, X., Lam, J.S.L., Jakher, A., 2021. Shipping sentiment and the dry bulk shipping freight market: New evidence from newspaper coverage. *Transport. Res. Part E: Logist. Transport. Rev.* 155, 102490. <https://doi.org/10.1016/j.tre.2021.102490>.
- Bao, K., Bi, J., Gao, M., Sun, Y., Zhang, X., Zhang, W., 2022. An improved ship trajectory prediction based on AIS data using MHA-BiGRU. *J. Mar. Sci. Eng.* 10, 804. <https://doi.org/10.3390/jmse10060804>.
- Billah, M.M., Zhang, J., Zhang, T., 2022. A method for vessel's trajectory prediction based on encoder decoder architecture. *J. Mar. Sci. Eng.* 10, 1529. <https://doi.org/10.3390/jmse10101529>.
- Capobianco, S., Millefiori, L.M., Forti, N., Braca, P., Willett, P., 2021. Deep learning methods for vessel trajectory prediction based on recurrent neural networks. *IEEE Trans. Aerosp. Electron. Syst.* 57, 4329–4346. <https://doi.org/10.1109/TAES.2021.3096873>.
- Chae, C.-J., Kim, M., Kim, H.-J., 2020. A study on identification of development status of MASS technologies and directions of improvement. *Appl. Sci.-Basel* 10, 4564. <https://doi.org/10.3390/app10134564>.
- Chen, R., Chen, M., Li, W., Guo, N., 2020b. Predicting future locations of moving objects by recurrent mixture density network. *ISPRS Int. J. Geo-Inf.* 9, 116. <https://doi.org/10.3390/ijgi9020116>.
- Chen, C.-W., Harrison, C., Huang, H.-H., 2020. The unsupervised method of vessel movement trajectory prediction. *arXiv preprint arXiv:2007.13712*.

- Chen, X., Ling, J., Yang, Y., Zheng, H., Xiong, P., Postolache, O., Xiong, Y., 2020c. Ship Trajectory Reconstruction from AIS Sensory Data via Data Quality Control and Prediction. *Math. Probl. Eng.* 2020, 7191296. <https://doi.org/10.1155/2020/7191296>.
- Chen, G., Wang, W., Xue, Y., 2021a. Identification of Ship Dynamics Model Based on Sparse Gaussian Process Regression with Similarity. *Symmetry-Basel* 13, 1956. <https://doi.org/10.3390/sym13101956>.
- Chen, X., Wei, C., Zhou, G., Wu, H., Wang, Z., Biancardo, S.A., 2022. Automatic Identification System (AIS) Data Supported Ship Trajectory Prediction and Analysis via a Deep Learning Model. *J. Mar. Sci. Eng.* 10, 1314. <https://doi.org/10.3390/jmse10091314>.
- Chen, Y., Yang, S., Suo, Y., Zheng, M., 2021b. Ship Track Prediction Based on DLGWO-SVR. *Sci. Program.* 2021, 9085617. <https://doi.org/10.1155/2021/9085617>.
- Chung, J., Gulcehre, C., Cho, K., Bengio, Y., 2014. Empirical Evaluation of Gated Recurrent Neural Networks on Sequence Modeling. <https://doi.org/10.48550/arXiv.1412.3555>.
- de la Peña Zarzuelo, I., Freire Soane, M.J., López Bermúdez, B., 2020. Industry 4.0 in the port and maritime industry: A literature review. *J. Ind. Inf. Integr.* 20, 100173. <https://doi.org/10.1016/j.jii.2020.100173>.
- Deng, H., Bai, G., Shen, Z., Xia, L., 2022. Digital economy and its spatial effect on green productivity gains in manufacturing: Evidence from China. *J. Clean. Prod.* 378, 134539. <https://doi.org/10.1016/j.jclepro.2022.134539>.
- Ding, X., Bian, H., Ma, H., Wang, R., 2022. Ship Trajectory Generator under the Interference of Wind, Current and Waves. *Sensors* 22, 9395. <https://doi.org/10.3390/s22239395>.
- El Zaar, A., Benaya, N., Bakir, T., Mansouri, A., El Allati, A., 2024. Prediction of US 30-years-treasury-bonds movement and trading entry point using the robust 1DCNN-BiLSTM-XGBoost algorithm. *Expert. Syst.* 41, e13459.
- Elman, J.L., 1990. Finding structure in time. *Cognit. Sci.* 14, 179–211. [https://doi.org/10.1016/0364-0213\(90\)90002-E](https://doi.org/10.1016/0364-0213(90)90002-E).
- Feng, H., Cao, G., Xu, H., Ge, S.S., 2022. IS-STGCNN: An Improved Social spatial-temporal graph convolutional neural network for ship trajectory prediction. *Ocean Eng.* 266, 112960. <https://doi.org/10.1016/j.oceaneng.2022.112960>.
- Filom, S., Amiri, A.M., Razavi, S., 2022. Applications of machine learning methods in port operations – A systematic literature review. *Transport. Res. Part E: Logist. Transport. Rev.* 161, 102722. <https://doi.org/10.1016/j.tre.2022.102722>.
- Fuentes, G., 2021. Generating bunkering statistics from AIS data: A machine learning approach. *Transport. Res. Part E: Logist. Transport. Rev.* 155, 102495. <https://doi.org/10.1016/j.tre.2021.102495>.
- Gao, R., Li, R., Hu, M., Suganthan, P.N., Yuen, K.F., 2023b. Dynamic ensemble deep echo state network for significant wave height forecasting. *Appl. Energy* 329, 120261. <https://doi.org/10.1016/j.apenergy.2022.120261>.
- Gao, M., Shi, G., Li, S., 2018. Online Prediction of Ship Behavior with Automatic Identification System Sensor Data Using Bidirectional Long Short-Term Memory Recurrent Neural Network. *Sensors* 18, 4211. <https://doi.org/10.3390/s18124211>.
- Gao, D.W., Wang, Q., Zhu, Y.S., Xie, L., Zhang, J.F., Yan, K., Zhang, P., 2023. A novel long sequence multi-step ship trajectory prediction method considering historical data. *Proc. Institut. Mech. Eng., Part M: J. Eng. Maritime Environ.* 237, 166–181. <https://doi.org/10.1177/14750902221109718>.
- Gao, D., Zhu, Y., Zhang, J., He, Y., Yan, K., Yan, B., 2021. A novel MP-LSTM method for ship trajectory prediction based on AIS data. *Ocean Eng.* 228, 108956. <https://doi.org/10.1016/j.oceaneng.2021.108956>.
- Gao, D., Zhu, Y., Guedes Soares, C., 2023a. Uncertainty modelling and dynamic risk assessment for long-sequence AIS trajectory based on multivariate Gaussian Process. *Reliab. Eng. Syst. Saf.* 230, 108963. <https://doi.org/10.1016/j.res.2022.108963>.
- Han, P., Zhu, M., Zhang, H., 2023. Interaction-aware short-term marine vessel trajectory prediction with deep generative models. *IEEE Trans. Ind. Inf.* 1–9. <https://doi.org/10.1109/TII.2023.3302304>.
- Hassan, E., Abd El-Hafeez, T., Shams, M.Y., 2024. Optimizing classification of diseases through language model analysis of symptoms. *Sci Rep* 14, 1507. <https://doi.org/10.1038/s41598-024-51615-5>.
- Hochreiter, S., 1998. The Vanishing Gradient Problem During Learning Recurrent Neural Nets and Problem Solutions. *Int. J. Unc. Fuzz. Knowl. Based Syst.* 06, 107–116. <https://doi.org/10.1142/S0218488598000094>.
- Hochreiter, S., Schmidhuber, J., 1997. Long Short-Term Memory. *Neural Comput.* 9, 1735–1780. <https://doi.org/10.1162/neco.1997.9.8.1735>.
- Hu, X., Zhang, B., Tang, G., 2021. Research on Ship Motion Prediction Algorithm Based on Dual-Pass Long Short-Term Memory Neural Network. *IEEE Access* 9, 28429–28438. <https://doi.org/10.1109/ACCESS.2021.3055253>.
- Huang, P., Chen, Q., Wang, D., Wang, M., Wu, X., Huang, X., 2022. TripleConvTransformer: A deep learning vessel trajectory prediction method fusing descretized meteorological data. *Front. Environ. Sci.* 10, 1012547. <https://doi.org/10.3389/fenvs.2022.1012547>.
- Jia, C., Ma, J., 2023. Conditional temporal GAN for intent-aware vessel trajectory prediction in the precautionary area. *Eng. Appl. Artif. Intel.* 126, 106776. <https://doi.org/10.1016/j.engappai.2023.106776>.
- Jia, H., Yang, Y., An, J., Fu, R., 2023. A ship trajectory prediction model based on attention-BiLSTM optimized by the Whale Optimization Algorithm. *Appl. Sci.* 13, 4907. <https://doi.org/10.3390/app13084907>.
- Jiang, D., Shi, G., Li, N., Ma, L., Li, W., Shi, J., 2023. TRFM-LS: transformer-based deep learning method for vessel trajectory prediction. *JMSE* 11, 880. <https://doi.org/10.3390/jmse11040880>.
- Jordan, M.I., Mitchell, T.M., 2015. Machine learning: Trends, perspectives, and prospects. *Science* 349, 255–260. <https://doi.org/10.1126/science.aaa8415>.
- Kanazawa, M., Skulstad, R., Li, G., Hatledal, L.L., Zhang, H., 2021. A Multiple-output hybrid ship trajectory predictor with consideration for future command assumption. *IEEE Sens. J.* 21, 27124–27135. <https://doi.org/10.1109/JSEN.2021.3119069>.
- Karatas, G.B., Karagoz, P., Ayran, O., 2021. Trajectory pattern extraction and anomaly detection for maritime vessels. *Internet Things* 16, 100436. <https://doi.org/10.1016/j.iot.2021.100436>.
- Kharsa, R., Elnagar, A., Yagi, S., 2024. BERT-Based Arabic Diacritization: A state-of-the-art approach for improving text accuracy and pronunciation. *Expert Syst. Appl.* 248, 123416. <https://doi.org/10.1016/j.eswa.2024.123416>.
- Kim, K.-I., Lee, K.M., 2018. Deep Learning-Based Caution Area Traffic Prediction with Automatic Identification System Sensor Data. *Sensors* 18, 3172. <https://doi.org/10.3390/s18093172>.
- Last, P., Bahlke, C., Hering-Bertram, M., Linsen, L., 2014. Comprehensive analysis of automatic identification system (AIS) data in regard to vessel movement prediction. *J. Navigat.* 67, 791–809.
- Last, P., Hering-Bertram, M., Linsen, L., 2019. Interactive History-Based Vessel Movement Prediction. *IEEE Intell. Syst.* 34, 3–13. <https://doi.org/10.1109/MIS.2019.2954509>.
- LeCun, Y., Bengio, Y., Hinton, G., 2015. Deep learning. *Nature* 521, 436–444. <https://doi.org/10.1038/nature14539>.
- Li, Y., Bai, X., Wang, Q., Ma, Z., 2022b. A big data approach to cargo type prediction and its implications for oil trade estimation. *Transport. Res. Part E: Logist. Transport. Rev.* 165, 102831. <https://doi.org/10.1016/j.tre.2022.102831>.
- Li, H., Lam, J.S.L., Yang, Z., Liu, J., Liu, R.W., Liang, M., Li, Y., 2022a. Unsupervised hierarchical methodology of maritime traffic pattern extraction for knowledge discovery. *Transport. Res. Part C: Emerg. Technol.* 143, 103856. <https://doi.org/10.1016/j.tre.2022.103856>.
- Li, H., Jiao, H., Yang, Z., 2023a. AIS data-driven ship trajectory prediction modelling and analysis based on machine learning and deep learning methods. *Transport. Res. Part E: Logist. Transport. Rev.* 175, 103152. <https://doi.org/10.1016/j.tre.2023.103152>.
- Li, Y., Li, H., Zhang, C., Zhao, Y., Yang, Z., 2024. Incorporation of adaptive compression into a GPU parallel computing framework for analyzing large-scale vessel trajectories. *Transport. Res. Part C: Emerg. Technol.* 163, 104648. <https://doi.org/10.1016/j.trc.2024.104648>.
- Li, K.X., Li, M., Zhu, Y., Yuen, K.F., Tong, H., Zhou, H., 2023b. Smart port: A bibliometric review and future research directions. *Transport. Res. Part E: Logist. Transport. Rev.* 174, 103098. <https://doi.org/10.1016/j.tre.2023.103098>.
- Li, H., Xing, W., Jiao, H., Yang, Z., Li, Y., 2024. Deep bi-directional information-empowered ship trajectory prediction for maritime autonomous surface ships. *Transport. Res. Part E: Logist. Transport. Rev.* 181, 103367. <https://doi.org/10.1016/j.tre.2023.103367>.
- Li, H., Yang, Z., 2023. Incorporation of AIS data-based machine learning into unsupervised route planning for maritime autonomous surface ships. *Transport. Res. Part E: Logist. Transport. Rev.* 176, 103171. <https://doi.org/10.1016/j.tre.2023.103171>.

- Lin, Z., Yue, W., Huang, J., Wan, J., 2023. Ship Trajectory Prediction Based on the TTCN-Attention-GRU Model. *Electronics* 12, 2556. <https://doi.org/10.3390/electronics12122556>.
- Liu, J., Shi, G., Zhu, K., 2019. Vessel Trajectory Prediction Model Based on AIS Sensor Data and Adaptive Chaos Differential Evolution Support Vector Regression (ACDE-SVR). *Appl. Sci.-Basel* 9, 2983. <https://doi.org/10.3390/app9152983>.
- Liu, C., Guo, S., Feng, Y., Hong, F., Huang, H., Guo, Z., 2019a. L-VTP: Long-Term Vessel Trajectory Prediction Based on Multi-Source Data Analysis. *Sensors* 19, 4365. <https://doi.org/10.3390/s19204365>.
- Liu, C., Li, Y., Jiang, R., Du, Y., Lu, Q., Guo, Z., 2021. TPR-DTVN: A Routing Algorithm in Delay Tolerant Vessel Network Based on Long-Term Trajectory Prediction. *Wirel. Commun. Mob. Comput.* 2021, 1–15.
- Liu, R.W., Liang, M., Nie, J., Lim, W.Y.B., Zhang, Y., Guizani, M., 2022a. Deep learning-powered vessel trajectory prediction for improving smart traffic services in maritime internet of things. *IEEE Trans. Netw. Sci. Eng.* 9, 3080–3094. <https://doi.org/10.1109/TNSE.2022.3140529>.
- Liu, R.W., Liang, M., Nie, J., Yuan, Y., Xiong, Z., Yu, H., Guizani, N., 2022b. STMGCN: Mobile edge computing-empowered vessel trajectory prediction using spatio-temporal multigraph convolutional network. *IEEE Trans. Ind. Inform.* 18, 7977–7987. <https://doi.org/10.1109/TII.2022.3165886>.
- Liu, T., Ma, J., 2022. Ship navigation behavior prediction based on AIS data. *IEEE Access* 10, 47997–48008. <https://doi.org/10.1109/ACCESS.2022.3172308>.
- Liu, J., Shi, G., Zhu, K., 2020. Online Multiple Outputs Least-Squares Support Vector Regression Model of Ship Trajectory Prediction Based on Automatic Information System Data and Selection Mechanism. *IEEE Access* 8, 154727–154745. <https://doi.org/10.1109/ACCESS.2020.3018749>.
- Luo, W., Zhang, G., 2020. Ship motion trajectory and prediction based on vector analysis. *J. Coast. Res.* 1183–1188. <https://doi.org/10.2112/SI95-230.1>.
- Ma, C., Dai, G., Zhou, J., 2022a. Short-term traffic flow prediction for urban road sections based on time series analysis and LSTM_BILSTM method. *IEEE Trans. Intell. Transp. Syst.* 23, 5615–5624. <https://doi.org/10.1109/TITS.2021.3055258>.
- Ma, H., Zuo, Y., Li, T., 2022b. Vessel navigation behavior analysis and multiple-trajectory prediction model based on AIS data. *J. Adv. Transp.* 2022, 6622862. <https://doi.org/10.1155/2022/6622862>.
- Makhmudov, F., Kultimuratov, A., Cho, Y.-I., 2024. Enhancing Multimodal Emotion Recognition through Attention Mechanisms in BERT and CNN Architectures. *Appl. Sci.* 14, 4199. <https://doi.org/10.3390/app14104199>.
- Maskooki, A., Virjonen, P., Kallio, M., 2021. Assessing the prediction uncertainty in a route optimization model for autonomous maritime logistics. *Int. Trans. Oper. Res.* 28, 1765–1786. <https://doi.org/10.1111/itor.12882>.
- Mehri, S., Alesheikh, A.A., Basiri, A., 2021. A Contextual Hybrid Model for Vessel Movement Prediction. *IEEE Access* 9, 45600–45613. <https://doi.org/10.1109/ACCESS.2021.3066463>.
- Miller, A., Walczak, S., 2020. Maritime Autonomous Surface Ship's Path Approximation Using Bezier Curves. *Symmetry-Basel* 12, 1704. <https://doi.org/10.3390/sym12101704>.
- Muhammad, G., Alshehri, F., Karray, F., Saddik, A.E., Alsulaiman, M., Falk, T.H., 2021. A comprehensive survey on multimodal medical signals fusion for smart healthcare systems. *Information Fusion* 76, 355–375. <https://doi.org/10.1016/j.inffus.2021.06.007>.
- Munim, Z.H., Dushenko, M., Jimenez, V.J., Shakil, M.H., Imset, M., 2020. Big data and artificial intelligence in the maritime industry: a bibliometric review and future research directions. *Marit. Policy Manag.* 47, 577–597. <https://doi.org/10.1080/03088839.2020.1788731>.
- Murray, B., Perera, L.P., 2020. A dual linear autoencoder approach for vessel trajectory prediction using historical AIS data. *Ocean Eng.* 209, 107478. <https://doi.org/10.1016/j.oceaneng.2020.107478>.
- Murray, B., Perera, L.P., 2021. An AIS-based deep learning framework for regional ship behavior prediction. *Reliab. Eng. Syst. Saf.* 215, 107819. <https://doi.org/10.1016/j.res.2021.107819>.
- Murray, B., Perera, L.P., 2022. Ship behavior prediction via trajectory extraction-based clustering for maritime situation awareness. *J. Ocean Eng. Sci.* 7, 1–13. <https://doi.org/10.1016/j.joes.2021.03.001>.
- Negenborn, R.R., Goerlandt, F., Johansen, T.A., Slaets, P., Valdez Banda, O.A., Vanelander, T., Ventikos, N.P., 2023. Autonomous ships are on the horizon: here's what we need to know. *Nature* 615, 30–33. <https://doi.org/10.1038/d41586-023-00557-5>.
- Nguyen, D., Fablet, R., 2021. TraISformer-a generative transformer for ais trajectory prediction. *arXiv preprint arXiv:2109.03958*.
- Nguyen, D.-D., Van, C.L., Ali, M.I., 2018. Demo: Vessel Trajectory Prediction using Sequence-to-Sequence Models over Spatial Grid. In: *Debs'18: Proceedings of the 12th Acm International Conference on Distributed and Event-Based Systems*. Assoc Computing Machinery, New York, pp. 258–261. <https://doi.org/10.1145/3210284.3219775>.
- Pallotta, G., Vespe, M., Bryan, K., 2013. Vessel Pattern Knowledge Discovery from AIS Data: A Framework for Anomaly Detection and Route Prediction. *Entropy* 15, 2218–2245. <https://doi.org/10.3390/e15062218>.
- Papadimitrakis, M., Stogiannos, M., Sarimveis, H., Alexandridis, A., 2021. Multi-Ship Control and Collision Avoidance Using MPC and RBF-Based Trajectory Predictions. *Sensors* 21, 6959. <https://doi.org/10.3390/s21216959>.
- Park, J., Jeong, J., Park, Y., 2021. Ship Trajectory Prediction Based on Bi-LSTM Using Spectral-Clustered AIS Data. *J. Mar. Sci. Eng.* 9, 1037. <https://doi.org/10.3390/jmse9091037>.
- Perera, L.P., Oliveira, P., Soares, C.G., 2012. Maritime Traffic Monitoring Based on Vessel Detection, Tracking, State Estimation, and Trajectory Prediction. *IEEE Trans. Intell. Transp. Syst.* 13, 1188–1200. <https://doi.org/10.1109/TITS.2012.2187282>.
- Qian, L., Zheng, Y., Li, L., Ma, Y., Zhou, C., Zhang, D., 2022. A New Method of Inland Water Ship Trajectory Prediction Based on Long Short-Term Memory Network Optimized by Genetic Algorithm. *Appl. Sci.-Basel* 12, 4073. <https://doi.org/10.3390/app12084073>.
- Qiang, H., Jin, S., Feng, X., Xue, D., Zhang, L., 2020. Model Predictive Control of a Shipborne Hydraulic Parallel Stabilized Platform Based on Ship Motion Prediction. *IEEE Access* 8, 181880–181892. <https://doi.org/10.1109/ACCESS.2020.2992458>.
- Qin, Z., Zhao, P., Zhuang, T., Deng, F., Ding, Y., Chen, D., 2023. A survey of identity recognition via data fusion and feature learning. *Information Fusion* 91, 694–712. <https://doi.org/10.1016/j.inffus.2022.10.032>.
- Qiu, Z., Yang, P., Xiao, C., Wang, S., Xiao, X., Qin, J., Liu, C.-M., Wang, T., Lei, B., 2024. 3D Multimodal Fusion Network with Disease-induced Joint Learning for Early Alzheimer's Disease Diagnosis. *IEEE Trans. Med. Imaging* 1–1. <https://doi.org/10.1109/TMI.2024.3386937>.
- Qu, Z., Li, Y., Tiwari, P., 2023. QNMF: A quantum neural network based multimodal fusion system for intelligent diagnosis. *Information Fusion* 100, 101913. <https://doi.org/10.1016/j.inffus.2023.101913>.
- Rong, H., Teixeira, A.P., Guedes Soares, C., 2019. Ship trajectory uncertainty prediction based on a Gaussian Process model. *Ocean Eng.* 182, 499–511. <https://doi.org/10.1016/j.oceaneng.2019.04.024>.
- Rong, H., Teixeira, A.P., Guedes Soares, C., 2022. Maritime traffic probabilistic prediction based on ship motion pattern extraction. *Reliab. Eng. Syst. Saf.* 217, 108061. <https://doi.org/10.1016/j.res.2021.108061>.
- Sang, L.-Z., Yan, X., Wall, A., Wang, J., Mao, Z., 2016. CPA Calculation Method based on AIS Position Prediction. *J. Navig.* 69, 1409–1426. <https://doi.org/10.1017/S0373463316000229>.
- Scheepens, R., van de Wetering, H., van Wijk, J.J., 2014. Contour based visualization of vessel movement predictions. *Int. J. Geogr. Inf. Sci.* 28, 891–909. <https://doi.org/10.1080/13658816.2013.868466>.
- Schuster, M., Paliwal, K.K., 1997. Bidirectional recurrent neural networks. *IEEE Trans. Signal Process.* 45, 2673–2681. <https://doi.org/10.1109/78.650093>.
- Shaik, T., Tao, X., Li, L., Xie, H., Velásquez, J.D., 2024. A survey of multimodal information fusion for smart healthcare: Mapping the journey from data to wisdom. *Information Fusion* 102, 102040. <https://doi.org/10.1016/j.inffus.2023.102040>.
- Sorensen, K.A., Heiselberg, P., Heiselberg, H., 2022. Probabilistic Maritime Trajectory Prediction in Complex Scenarios Using Deep Learning. *Sensors* 22, 2058. <https://doi.org/10.3390/s22052058>.
- Suo, Y., Chen, W., Claramunt, C., Yang, S., 2020. A Ship Trajectory Prediction Framework Based on a Recurrent Neural Network. *Sensors* 20, 5133. <https://doi.org/10.3390/s20185133>.
- Sutskever, I., Vinyals, O., Le, Q.V., 2014. Sequence to Sequence Learning with Neural Networks. <https://doi.org/10.48550/arXiv.1409.3215>.

- Sutulo, S., Moreira, L., Soares, C.G., 2002. Mathematical models for ship path prediction in manoeuvring simulation systems. *Ocean Eng.* 29, 1–19. [https://doi.org/10.1016/S0029-8018\(01\)00023-3](https://doi.org/10.1016/S0029-8018(01)00023-3).
- Syed, M.A.B., Ahmed, I., 2023. A CNN-LSTM Architecture for marine vessel track association using automatic identification system (AIS) data. *Sensors* 23, 6400. <https://doi.org/10.3390/s23146400>.
- Tan, W., Tiwari, P., Pandey, H.M., Moreira, C., Jaiswal, A.K., 2020. Multimodal medical image fusion algorithm in the era of big data. *Neural Comput. & Applic.* <https://doi.org/10.1007/s00521-020-05173-2>.
- Tang, H., Wei, L., Yin, Y., Shen, H., Qi, Y., 2020. Detection of Abnormal Vessel Behaviour Based on Probabilistic Directed Graph Model. *J. Navig.* 73, 1014–1035. <https://doi.org/10.1017/S0373463320000144>.
- Tang, H., Yin, Y., Shen, H., 2022. A model for vessel trajectory prediction based on long short-term memory neural network. *J. Marine Eng. Technol.* 21, 136–145.
- Tu, E., Zhang, G., Mao, S., Rachmawati, L., Huang, G.-B., 2020. Modeling historical AIS data for vessel path prediction: A comprehensive treatment. *arXiv preprint arXiv:2001.01592*.
- Tzoumpas, K., Estrada, A., Miraglio, P., Zambelli, P., 2024. A Data Filling Methodology for Time Series Based on CNN and (Bi)LSTM Neural Networks. *IEEE Access* 12, 31443–31460. <https://doi.org/10.1109/ACCESS.2024.3369891>.
- Vaswani, A., Shazeer, N., Parmar, N., Uszkoreit, J., Jones, L., Gomez, A.N., Kaiser, L., Polosukhin, I., 2023. Attention Is All You Need. <https://arxiv.org/abs/1706.03762>.
- Venskus, J., Treigys, P., Markeviciute, J., 2021. Unsupervised marine vessel trajectory prediction using LSTM network and wild bootstrapping techniques. *Nonlinear Anal.-Model. Control* 26, 718–737. <https://doi.org/10.15388/namc.2021.26.23056>.
- Volkova, T.A., Balykina, Y.E., Bessalov, A., 2021. Predicting Ship Trajectory Based on Neural Networks Using AIS Data. *J. Mar. Sci. Eng.* 9, 254. <https://doi.org/10.3390/jmse9030254>.
- Wang, S., 2024. Intelligent BiLSTM-Attention-IBPNN Method for Anomaly Detection in Financial Auditing. *IEEE Access* 12, 90005–90015. <https://doi.org/10.1109/ACCESS.2024.3420243>.
- Wang, R., Alazzam, M.B., Alassery, F., Almulihi, A., White, M., 2021. Innovative Research of Trajectory Prediction Algorithm Based on Deep Learning in Car Network Collision Detection and Early Warning System. *Mob. Inf. Syst.* 2021, 3773688. <https://doi.org/10.1155/2021/3773688>.
- Wang, Y., Skerry-Ryan, R.J., Stanton, D., Wu, Y., Weiss, R.J., Jaitly, N., Yang, Z., Xiao, Y., Chen, Z., Bengio, S., Le, Q., Agiomyriannakis, Y., Clark, R., Saurous, R.A., 2017. Tacotron: Towards End-to-End Speech Synthesis.
- Wang, Jijia, Huang, J.X., Tu, X., Wang, Junmei, Huang, A.J., Laskar, M.T.R., Bhuiyan, A., 2024. Utilizing BERT for Information Retrieval: Survey, Applications, Resources, and Challenges. *ACM Comput. Surv.* 56, 185:1–185:33. <https://doi.org/10.1145/3648471>.
- Wang, L., Fan, X., Chen, J., Cheng, J., Tan, J., Ma, X., 2020. 3D object detection based on sparse convolution neural network and feature fusion for autonomous driving in smart cities. *Sustain. Cities Soc.* 54, 102002. <https://doi.org/10.1016/j.scs.2019.102002>.
- Wang, J., Guo, Y., Wang, Y., 2022a. A sequential random forest for short-term vessel speed prediction. *Ocean Eng.* 248, 110691. <https://doi.org/10.1016/j.oceaneng.2022.110691>.
- Wang, S., He, Z., 2021. A prediction model of vessel trajectory based on generative adversarial network. *J. Navig.* 74, 1161–1171. <https://doi.org/10.1017/S0373463321000382>.
- Wang, S., Sun, Z., Yuan, Q., Sun, Z., Wu, Z., Hsieh, T.-H., 2022b. Autonomous piloting and berthing based on Long Short Time Memory neural networks and nonlinear model predictive control algorithm. *Ocean Eng.* 264, 112269. <https://doi.org/10.1016/j.oceaneng.2022.112269>.
- Wang, S., Li, Y., Xing, H., 2023b. A novel method for ship trajectory prediction in complex scenarios based on spatio-temporal features extraction of AIS data. *Ocean Eng.* 281, 114846. <https://doi.org/10.1016/j.oceaneng.2023.114846>.
- Wang, S., Li, Y., Zhang, Z., Xing, H., 2023c. Big data driven vessel trajectory prediction based on sparse multi-graph convolutional hybrid network with spatio-temporal awareness. *Ocean Eng.* 287, 115695. <https://doi.org/10.1016/j.oceaneng.2023.115695>.
- Wang, J., Li, J., Wang, R., Zhou, X., 2024a. VAE-Driven Multimodal Fusion for Early Cardiac Disease Detection. *IEEE Access* 12, 90535–90551. <https://doi.org/10.1109/ACCESS.2024.3420444>.
- Wang, C., Ma, L., Li, R., Durrani, T.S., Zhang, H., 2019a. Exploring Trajectory Prediction Through Machine Learning Methods. *IEEE Access* 7, 101441–101452. <https://doi.org/10.1109/ACCESS.2019.2929430>.
- Wang, M., Wang, Y., Cui, E., Fu, X., 2023a. A novel multi-ship collision probability estimation method considering data-driven quantification of trajectory uncertainty. *Ocean Eng.* 272, 113825. <https://doi.org/10.1016/j.oceaneng.2023.113825>.
- Wang, L., Wu, Q., Liu, J., Li, S., Negenborn, R.R., 2019b. State-of-the-Art Research on Motion Control of Maritime Autonomous Surface Ships. *J. Mar. Sci. Eng.* 7, 438. <https://doi.org/10.3390/jmse7120438>.
- Wang, C., Zhang, X., Gao, H., Bashir, M., Li, H., Yang, Z., 2024. Optimizing anti-collision strategy for MASS: A safe reinforcement learning approach to improve maritime traffic safety. *Ocean Coast. Manage.* 253, 107161. <https://doi.org/10.1016/j.ocecoaman.2024.107161>.
- Wei, Y., 2020. Design of Ship Navigation Trajectory Analysis and Application System Based on Image Processing Technology. *J. Coast. Res.* 211–213. <https://doi.org/10.2112/JCR-S115-066.1>.
- Wong, E.Y.C., Lam, J.S.L., Ng, A.K.Y., Yip, T.L., 2022. Decision analytics and trade ideology: New perspectives of maritime logistics. *Transport. Res. Part E: Logist. Transport. Rev.* 168. <https://doi.org/10.1016/j.tre.2022.102889>.
- Wu, W., Deng, X., Jiang, P., Wan, S., Guo, Y., 2023b. CrossFuser: Multi-Modal Feature Fusion for End-to-End Autonomous Driving Under Unseen Weather Conditions. *IEEE Trans. Intell. Transp. Syst.* 24, 14378–14392. <https://doi.org/10.1109/TITS.2023.3307589>.
- Wu, Q., Li, X., Wang, K., Bilal, H., 2023a. Regional feature fusion for on-road detection of objects using camera and 3D-LiDAR in high-speed autonomous vehicles. *Soft Comput.* 27, 18195–18213. <https://doi.org/10.1007/s00500-023-09278-3>.
- Xia, H., Lu, L., Song, S., 2024. Feature fusion of multi-granularity and multi-scale for facial expression recognition. *Vis Comput* 40, 2035–2047. <https://doi.org/10.1007/s00371-023-02900-3>.
- Xiao, Z., Ponnambalam, L., Fu, X., Zhang, W., 2017. Maritime Traffic Probabilistic Forecasting Based on Vessels' Waterway Patterns and Motion Behaviors. *IEEE Trans. Intell. Transp. Syst.* 18, 3122–3134. <https://doi.org/10.1109/TITS.2017.2681810>.
- Xiao, Z., Fu, X., Zhang, L., Goh, R.S.M., 2020a. Traffic Pattern Mining and Forecasting Technologies in Maritime Traffic Service Networks: A Comprehensive Survey. *IEEE Trans. Intell. Transp. Syst.* 21, 1796–1825. <https://doi.org/10.1109/TITS.2019.2908191>.
- Xiao, Z., Fu, X., Zhang, L., Zhang, W., Liu, R.W., Liu, Z., Goh, R.S.M., 2020b. Big data driven vessel trajectory and navigating state prediction with adaptive learning, motion modeling and particle filtering techniques. *IEEE Trans. Intell. Transp. Syst.* 23, 3696–3709.
- Xiao, J., Gan, C., Zhu, Q., Zhu, Y., Liu, G., 2023a. CFNet: Facial expression recognition via constraint fusion under multi-task joint learning network. *Appl. Soft Comput.* 141, 110312. <https://doi.org/10.1016/j.asoc.2023.110312>.
- Xiao, Y., Li, X., Yao, W., Chen, J., Hu, Y., 2023b. Bidirectional Data-Driven Trajectory Prediction for Intelligent Maritime Traffic. *IEEE Trans. Intell. Transp. Syst.* 24, 1773–1785. <https://doi.org/10.1109/TITS.2022.3219998>.
- Xin, X., Liu, K., Li, H., Yang, Z., 2024. Maritime traffic partitioning: An adaptive semi-supervised spectral regularization approach for leveraging multi-graph evolutionary traffic interactions. *Transport. Res. Part C: Emerg. Technol.* 164, 104670. <https://doi.org/10.1016/j.trc.2024.104670>.
- Xu, X., Liu, C., Li, J., Miao, Y., Zhao, L., 2023. Long-Term Trajectory Prediction for Oil Tankers via Grid-Based Clustering. *JMSE* 11, 1211. <https://doi.org/10.3390/jmse11061211>.
- Xu, Y., Zhang, J., Ren, Y., Zeng, Y., Yuan, J., Liu, Z., Wang, L., Ou, D., 2022. Improved Vessel Trajectory Prediction Model Based on Stacked-BiGRUs. *Secur. Commun. Netw.* 2022, 8696558. <https://doi.org/10.1155/2022/8696558>.
- Yan, L., Shi, Y., Wei, M., Wu, Y., 2023. Multi-feature fusing local directional ternary pattern for facial expressions signal recognition based on video communication system. *Alex. Eng. J.* 63, 307–320. <https://doi.org/10.1016/j.aej.2022.08.003>.
- Yang, M., Lam, J.S.L., 2023. Operational and economic evaluation of ammonia bunkering – Bunkering supply chain perspective. *Transport. Res. Part D: Transport Environ.* 117, 103666. <https://doi.org/10.1016/j.trd.2023.103666>.

- Yang, D., Wu, L., Wang, S., Jia, H., Li, K.X., 2019. How big data enriches maritime research - a critical review of Automatic Identification System (AIS) data applications. *Transp. Rev.* 39, 755–773. <https://doi.org/10.1080/01441647.2019.1649315>.
- You, L., Xiao, S., Peng, Q., Claramunt, C., Han, X., Guan, Z., Zhang, J., 2020. ST-Seq2Seq: A Spatio-Temporal Feature-Optimized Seq2Seq Model for Short-Term Vessel Trajectory Prediction. *IEEE Access* 8, 218565–218574. <https://doi.org/10.1109/ACCESS.2020.3041762>.
- Yuan, Y., Cheng, H., Sester, M., 2022. Keypoints-Based Deep Feature Fusion for Cooperative Vehicle Detection of Autonomous Driving. *IEEE Robotics and Automation Letters* 7, 3054–3061. <https://doi.org/10.1109/LRA.2022.3143299>.
- Zhang, C., Bin, J., Wang, W., Peng, X., Wang, R., Halldearn, R., Liu, Z., 2020. AIS data driven general vessel destination prediction: A random forest based approach. *Transp. Res. Pt. C-Emerg. Technol.* 118, 102729. <https://doi.org/10.1016/j.trc.2020.102729>.
- Zhang, D., Chu, X., Wu, W., He, Z., Wang, Z., Liu, C., 2023a. Model identification of ship turning maneuver and extreme short-term trajectory prediction under the influence of sea currents. *Ocean Eng.* 278, 114367. <https://doi.org/10.1016/j.oceaneng.2023.114367>.
- Zhang, X., Fu, X., Xiao, Z., Xu, H., Qin, Z., 2022c. Vessel Trajectory Prediction in Maritime Transportation: Current Approaches and Beyond. *IEEE Trans. Intell. Transp. Syst.* 23, 19980–19998. <https://doi.org/10.1109/TITS.2022.3192574>.
- Zhang, M., Huang, L., Wen, Y., Zhang, J., Huang, Y., Zhu, M., 2022b. Short-Term Trajectory Prediction of Maritime Vessel Using k-Nearest Neighbor Points. *J. Mar. Sci. Eng.* 10, 1939. <https://doi.org/10.3390/jmse10121939>.
- Zhang, X., Liu, J., Gong, P., Chen, C., Han, B., Wu, Z., 2023b. Trajectory prediction of seagoing ships in dynamic traffic scenes via a gated spatio-temporal graph aggregation network. *Ocean Eng.* 287, 115886. <https://doi.org/10.1016/j.oceaneng.2023.115886>.
- Zhang, X., Ma, Y., Wang, M., 2024b. An attention-based Logistic-CNN-BiLSTM hybrid neural network for credit risk prediction of listed real estate enterprises. *Expert. Syst.* 41, e13299.
- Zhang, C., Sjarif, N.N.A., Ibrahim, R., 2024a. Deep learning models for price forecasting of financial time series: A review of recent advancements: 2020–2022. *WIREs Data Min. Knowl. Discovery* 14, e1519.
- Zhang, L., Zhang, J., Niu, J., Wu, Q.M.J., Li, G., 2021. Track Prediction for HF Radar Vessels Submerged in Strong Clutter Based on MSCNN Fusion with GRU-AM and AR Model. *Remote Sens.* 13, 2164. <https://doi.org/10.3390/rs13112164>.
- Zhang, X., Zhou, Y., Yang, G., Han, T., Chen, T., 2024c. Context-aware code generation with synchronous bidirectional decoder. *J. Syst. Softw.* 214, 112066. <https://doi.org/10.1016/j.jss.2024.112066>.
- Zhang, L., Zhu, Y., Su, J., Lu, W., Li, J., Yao, Y., 2022a. A Hybrid Prediction Model Based on KNN-LSTM for Vessel Trajectory. *Mathematics* 10, 4493. <https://doi.org/10.3390/math10234493>.
- Zhao, J., Lu, J., Chen, X., Yan, Z., Yan, Y., Sun, Y., 2022a. High-fidelity data supported ship trajectory prediction via an ensemble machine learning framework. *Phys. A* 586, 126470. <https://doi.org/10.1016/j.physa.2021.126470>.
- Zhao, J., Yan, Z., Chen, X., Han, B., Wu, S., Ke, R., 2022b. k-GCN-LSTM: A k-hop Graph Convolutional Network and Long-Short-Term Memory for ship speed prediction. *Phys. A* 606, 128107. <https://doi.org/10.1016/j.physa.2022.128107>.
- Zhou, H., Chen, Y., Zhang, S., 2019. Ship trajectory prediction based on BP neural network. *J. Artif. Intell.* 1, 29.
- Zuo, Z., Wang, X., Guo, S., Liu, Z., Li, Z., Wang, Y., 2024. Trajectory prediction network of autonomous vehicles with fusion of historical interactive features. *IEEE Trans. Intell. Veh.* 9, 2171–2183. <https://doi.org/10.1109/TIV.2023.3319024>.